Conservation Laws of a Nonlinear Incompressible Two-Fluid Model

A Thesis Submitted to the
College of Graduate Studies and Research
in Partial Fulfillment of the Requirements
for the degree of Master of Science
in the Department of Mathematics and Statistics
University of Saskatchewan
Saskatoon

By
Abdus Sattar Mia

Permission to Use

In presenting this thesis in partial fulfilment of the requirements for a Postgraduate degree from the University of Saskatchewan, I agree that the Libraries of this University may make it freely available for inspection. I further agree that permission for copying of this thesis in any manner, in whole or in part, for scholarly purposes may be granted by the professor or professors who supervised my thesis work or, in their absence, by the Head of the Department or the Dean of the College in which my thesis work was done. It is understood that any copying or publication or use of this thesis or parts thereof for financial gain shall not be allowed without my written permission. It is also understood that due recognition shall be given to me and to the University of Saskatchewan in any scholarly use which may be made of any material in my thesis.

Requests for permission to copy or to make other use of material in this thesis in whole or part should be addressed to:

Head of the Department of Mathematics and Statistics
University of Saskatchewan
Room 142 McLean Hall
106 Wiggins Road
Saskatoon, Saskatchewan
Canada
S7N 5E6

Abstract

We study the conservation laws of the Choi-Camassa two-fluid model (1999) which is developed by approximating the two-dimensional (2D) Euler equations for incompressible motion of two non-mixing fluids in a channel. As preliminary work of this thesis, we compute the basic local conservation laws and the point symmetries of the 2D Euler equations for the incompressible fluid, and those of the vorticity system of the 2D Euler equations. To serve the main purpose of this thesis, we derive local conservation laws of the Choi-Camassa equations with an explicit expression for each locally conserved density and corresponding spatial flux. Using the direct conservation law construction method, we have constructed seven conservation laws including the conservation of mass, total horizontal momentum, energy, and irrotationality. The conserved quantities of the Choi-Camassa equations are compared with those of the full 2D Euler equations of incompressible fluid.

We review periodic solutions, solitary wave solutions and kink solutions of the Choi-Camassa equations. As a result of the presence of Galilean symmetry for the Choi-Camassa model, the solitary wave solutions, the kink and the anti-kink solutions travel with arbitrary constant wave speed. We plot the local conserved densities of the Choi-Camassa model on the solitary wave and on the kink wave. For the solitary waves, all the densities are finite and decay exponentially, while for the kink wave, all the densities except one are finite and decay exponentially.

Acknowledgements

I would like to thank my supervisor Dr. Alexey F. Shevyakov for his continuous supports and suggestions during this research work. I am grateful to the University of Saskatchewan, the Dept. of Mathematics & Statistics, and head of the department for awarding me Dean's scholarship. I am also grateful to my friend Simon who was only person here to share and discuss my thoughts.

Abdus Sattar Mia
Saskatoon, SK, Canada
May 2016.

This thesis has been dedicated

to

my loving son Aryan Tahseen & to my wife Tania Akter.

Contents

List of Figures

List of Abbreviations

DE	Differential equation
KdV	Korteweg-de Vries
mKdV	Modified Korteweg-de Vries
ODE	Ordinary differential equation
PDE	Partial differential equation
PDEs	Partial differential equations
2D	Two-dimensional
3D	Three-dimensional

Chapter 1

Introduction

1.1 Basic Fluid Properties

Mathematical study of nonlinear problems has received, over the years, significant input from fluid dynamics, in particular, the discoveries of Euler equations (1755), Navier-Stokes equations (1821), turbulence (1877), solitons (1965) has enriched the nonlinear science. In the above developed areas, a special role is played by incompressible fluid flows. The study of such flows has been attached with a wide range of mathematical techniques, and today, this is a stimulating part of the applied mathematics, physics and engineering.

In fluid dynamics, the general motion, deformation, and rate of deformation of fluid particles are the interesting features. Like its solid counterpart, a fluid element normally can undergo four different types of motion or deformation: (1) translation, (2) rotation, (3) extensional strain or dilation, and (4) shear strain.

Fluids undergo motion due to forces. Two types of forces are seen in fluid dynamics:
(i) Long-range force— decrease slowly with distance. For example, gravity, electromagnetic forces, internal forces;
(ii) Short-range force (surface force)— decrease rapidly with distance between interacting elements, acting on the boundary between two fluids.

Suppose that a fluid is contained in a domain $\mathscr{D} \subseteq \mathbb{R}^d$ where $d = 3$ (or 2). A fluid flow at any point $(x, y, z) \in \mathscr{D}$ and at any time $t \in \mathbb{R}$ is defined as $(u_1(x, y, z, t),\ u_2(x, y, z, t),\ u_3(x, y, z, t))$, where $u_1,\ u_2,\ u_3$ are the velocity components of the fluid flow in Cartesian coordinates. The *velocity field* is defined as $\mathbf{u} = (u_1,\ u_2,\ u_3)$. This kind of setting that describes the flow at every fixed point as a function of time is called the *Eulerian formulation* of motion and $\mathbf{u}$ is known as the Eulerian velocity vector field. Let $Q(x, y, z, t)$ represents any parameter of the fluid. Then the total differential change in Q is given by

$$dQ = \frac{\partial Q}{\partial t}dt + \frac{\partial Q}{\partial x}dx + \frac{\partial Q}{\partial y}dy + \frac{\partial Q}{\partial z}dz. \tag{1.1}$$

Suppose the position of a point at time t is recorded by the variables $(x(t), y(t), z(t))$. At any fixed fluid

molecule the velocity components can be expressed as

$$\frac{dx}{dt} = u_1(x(t), y(t), z(t), t), \tag{1.2a}$$

$$\frac{dy}{dt} = u_2(x(t), y(t), z(t), t), \tag{1.2b}$$

$$\frac{dz}{dt} = u_3(x(t), y(t), z(t), t). \tag{1.2c}$$

Substituting the equations (1.2a)–(1.2c) into (1.1) yields

$$\frac{dQ}{dt} = \frac{\partial Q}{\partial t} + u_1\frac{\partial Q}{\partial x} + u_2\frac{\partial Q}{\partial y} + u_3\frac{\partial Q}{\partial z}. \tag{1.3}$$

The quantity dQ/dt is known as *material derivative*. This derivative is also denoted by the symbol DQ/Dt. In the vector notation, (1.3) is

$$\frac{DQ}{Dt} = \frac{\partial Q}{\partial t} + \mathbf{u} \cdot \nabla Q, \tag{1.4}$$

where $\nabla = (\partial_x, \partial_y, \partial_z)$ is the *gradient vector*

$$\mathbf{i}\frac{\partial}{\partial x} + \mathbf{j}\frac{\partial}{\partial y} + \mathbf{k}\frac{\partial}{\partial z}, \tag{1.5}$$

and ∂_x denotes partial derivative with respect to x.

Definition 1.1.1. The *particle path or trajectory* (see Figure 1.1) of a fluid particle is the curve traced out by the particle as time progresses. If the particle starts at position $\mathbf{x}_0 = (x_0, y_0, z_0)$ then its particle path is the solution of the system of differential equations

$$\frac{d}{dt}\mathbf{x} = \mathbf{u}(\mathbf{x}, t) \tag{1.6}$$

with the initial condition $\mathbf{x}(0) = \mathbf{x}_0$.

Definition 1.1.2. If the flow velocity is the same magnitude and direction at every point in the fluid, the flow is said to be *uniform*. If at a given instant, the velocity is not the same at every point, the flow is *non-uniform*.

By this definition, every fluid that flows near a solid boundary with no-slip condition [6, 41] will be non-uniform as the fluid at the boundary must take the speed of the boundary, usually zero. However if the size and the shape of the cross-section of the stream of fluid is constant, the flow is considered *uniform*.

Definition 1.1.3. A *steady flow* is the flow in which the conditions (velocity, pressure, cross-section etc.) may differ from point to point, but do not change in time. Otherwise the flow is called *unsteady*.

Definition 1.1.4. A fluid is said to be *incompressible* if the density of the fluid ρ has the property

$$\frac{d\rho}{dt} = 0 \quad (\implies \nabla \cdot \mathbf{u} = 0). \tag{1.7}$$

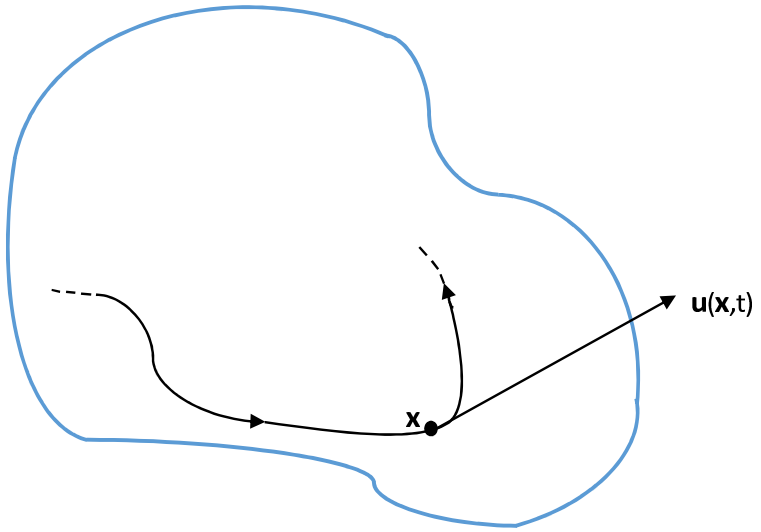

Figure 1.1: Trajectory of the fluid particle moving through $\mathbf{x}$ at time t

Definition 1.1.5. Let $\mathbf{f}(\mathbf{x}) = (f_1, f_2, \cdots, f_m)$ be a vector valued function and $\mathbf{x} = (x_1, x_2, \cdots, x_n)$. Then the *Jacobian matrix* $\mathbf{J}$ of $\mathbf{f}$ is an $m \times n$ matrix, defined as follows:

$$\mathbf{J} = \nabla \mathbf{f} = \left(\frac{\partial \mathbf{f}}{\partial x_1}, \frac{\partial \mathbf{f}}{\partial x_2}, \cdots, \frac{\partial \mathbf{f}}{\partial x_n} \right) = \begin{pmatrix} \frac{\partial f_1}{\partial x_1} & \frac{\partial f_1}{\partial x_2} & \cdots & \frac{\partial f_1}{\partial x_n} \\ \frac{\partial f_2}{\partial x_1} & \frac{\partial f_2}{\partial x_2} & \cdots & \frac{\partial f_2}{\partial x_n} \\ \vdots & \vdots & \ddots & \vdots \\ \frac{\partial f_m}{\partial x_1} & \frac{\partial f_m}{\partial x_2} & \cdots & \frac{\partial f_m}{\partial x_n} \end{pmatrix}. \tag{1.8}$$

If $m = n$, the Jacobian matrix is a square matrix. In this case the determinant of $\mathbf{J}$ is called the *Jacobian determinant* of $\mathbf{J}$ and is denoted by J.

Proposition 1.1.1. *Let* $\mathbf{u}$ *be the fluid velocity and* $\mathbf{X}$ *be the trajectory of a fluid particle* $\mathbf{x}$ *at time* $t = 0$*, then the following statements are equivalent:*

i) Fluid flow is incompressible;

ii) Jacobian determinant J *of* $\mathbf{X}(\mathbf{x}, t)$ *satisfies* $J(\mathbf{x}, t) \equiv 1$*;*

iii) The velocity field $\mathbf{u}$ *is divergence free, i.e.,* $\nabla \cdot \mathbf{u} = 0$*.*

Proof. See [7].

Definition 1.1.6. A fluid is said to be *homogeneous* if its mass density ρ is constant in space.

Definition 1.1.7. Let $\mathbf{u}$ be any velocity field of the fluid flow. Then the *vorticity* is defined as curl of the velocity field:

$$\boldsymbol{\omega} = \nabla \times \mathbf{u}. \tag{1.9}$$

Definition 1.1.8. The flow is called *irrotational* if the vorticity of the velocity field $\mathbf{u}$ is zero everywhere:

$$\boldsymbol{\omega} \equiv 0. \tag{1.10}$$

The definition (1.10) is called the *irrotationality condition* of the fluid. For an irrotational flow, we get

$$\nabla \times \mathbf{u} = \left(\frac{\partial u_3}{\partial y} - \frac{\partial u_2}{\partial z}\right)\mathbf{i} + \left(\frac{\partial u_1}{\partial z} - \frac{\partial u_3}{\partial x}\right)\mathbf{j} + \left(\frac{\partial u_2}{\partial x} - \frac{\partial u_1}{\partial y}\right)\mathbf{k} = 0. \tag{1.11}$$

It is obvious that

$$\frac{\partial u_3}{\partial y} = \frac{\partial u_2}{\partial z}, \quad \frac{\partial u_1}{\partial z} = \frac{\partial u_3}{\partial x}, \quad \frac{\partial u_2}{\partial x} = \frac{\partial u_1}{\partial y}. \tag{1.12}$$

Then it follows from (1.12) that the velocity components can be locally expressed in terms of a scalar function $\phi(x, y, z, t)$ as

$$u_1 = \frac{\partial \phi}{\partial x}, \quad u_2 = \frac{\partial \phi}{\partial y}, \quad u_3 = \frac{\partial \phi}{\partial z}, \tag{1.13}$$

where ϕ is called the *velocity potential*. In the vector form, (1.13) becomes

$$\mathbf{u} = \nabla \phi. \tag{1.14}$$

The local existence of velocity potential is a consequence of the irrotationality of the fluid flow field. This can also be defined for the two-dimensional flows.

A fluid is incompressible [7] if and only if

$$\nabla \cdot \mathbf{u} = 0 \tag{1.15}$$

which is also known as *solenoidality* condition. The equation (1.15) for a potential flow (1.14) implies $\nabla^2 \phi = 0$. Thus, velocity potential of the velocity field of the incompressible irrotational fluid satisfies the Laplace equation.

Definition 1.1.9. A line whose tangent at point $\mathbf{x}$ is everywhere parallel to the velocity $\mathbf{u}(\mathbf{x}, t)$ is called a *streamline*. If the velocity field $\mathbf{u} = (u, v, w)$ is known, the family of streamlines at instant t are solutions of the ODE system

$$\frac{dx}{u_1(\mathbf{x}, t)} = \frac{dy}{u_2(\mathbf{x}, t)} = \frac{dz}{u_3(\mathbf{x}, t)} = dt. \tag{1.16}$$

For a *steady flow* (i.e., when the fluid velocity $\mathbf{u}$ is time independent), the path of a fluid element (trajectory) coincides with a streamline [7]. If the flow is not steady, the streamlines can be still defined in the same way, but they are not the trajectories of fluid elements.

Definition 1.1.10. Let $\mathbf{u}$ be the fluid velocity which is *solenoidal*, i.e., $\nabla \cdot \mathbf{u} = 0$. The *stream function* (vector potential) $\boldsymbol{\psi}$ for an incompressible fluid with velocity field $\mathbf{u}$ is defined by

$$\mathbf{u} = \nabla \times \boldsymbol{\psi}. \tag{1.17}$$

Stream functions are particularly useful for two-dimensional (2D) and axisymmetric flows. The 2D incompressible fluid flow is solenoidal. In the two-dimensional flow, the velocity vector is

$$\mathbf{u} = (u_1, u_2, 0), \quad \partial_z = 0, \quad \boldsymbol{\psi} = (0, 0, \psi). \tag{1.18}$$

Then by the definition (1.17), we have

$$u_1 = \frac{\partial \psi}{\partial y}, \quad u_2 = -\frac{\partial \psi}{\partial x}. \tag{1.19}$$

Thus, the velocity field and vector potential of a two-dimensional flow can be expressed in terms of a single scalar function, the stream function, ψ. It is evident from $\nabla \cdot \mathbf{u} = 0$ that the gradient $\nabla\psi$ is perpendicular to the streamlines. Hence, the stream function is constant along the streamlines of a steady or unsteady flow. A stream function is always defined up to any arbitrary constant.

Also for the 2D case, by the condition (1.18),

$$\nabla \cdot \boldsymbol{\psi} = 0. \tag{1.20}$$

For irrotational fluids, from the definition of irrotationalty given by (1.10), we see that

$$\nabla \times (\nabla \times \boldsymbol{\psi}) = \nabla(\nabla \cdot \boldsymbol{\psi}) - \nabla^2 \boldsymbol{\psi} = 0. \tag{1.21}$$

Then using (1.20) into (1.21), for two spatial dimensions, we get

$$\nabla^2 \psi = 0, \tag{1.22}$$

which shows that ψ satisfies the Laplace equation. Moreover, ψ is a harmonic conjugate of ϕ.

Now consider a planar flow with polar coordinates $\mathbf{u} = \mathbf{u}(r, \theta, t)$, where $\mathbf{u} = u^{(r)}\mathbf{e}_r + u^{(\theta)}\mathbf{e}_\theta$. Then the solenoidal condition $\nabla \cdot \mathbf{u} = 0$ implies

$$\frac{1}{r}\frac{\partial}{\partial r}(r u^{(r)}) + \frac{1}{r}\frac{\partial}{\partial \theta} u^{(\theta)} = 0. \tag{1.23}$$

This is satisfied if and only if there exists a function $\psi(r, \theta, t)$ such that

$$\frac{1}{r}\frac{\partial \psi}{\partial \theta} = u^{(r)}, \qquad -\frac{\partial \psi}{\partial r} = u^{(\theta)}. \tag{1.24}$$

Example 1.1.1. Consider the two-dimensional flow in the Cartesian coordinates given by

$$\mathbf{u} = (2x, \ -2y). \tag{1.25}$$

Obviously $\nabla \cdot \mathbf{u} = 0$, so there exist a stream function satisfying

$$\frac{\partial \psi}{\partial y} = 2x \quad \text{and} \quad -\frac{\partial \psi}{\partial x} = -2y. \tag{1.26}$$

Integrating the first partial differential equation with respect to y we get

$$\psi = 2xy + f(x), \tag{1.27}$$

where $f(x)$ is an arbitrary function of x. However, we know that ψ must satisfy the second partial differential equation in (1.26). Therefore the second partial differential equation in (1.26) gives

$$f'(x) = 0. \tag{1.28}$$

Thus f is an arbitrary constant. Taking $f = 0$ for simplicity yields the stream function is given by

$$\psi = 2xy. \tag{1.29}$$

Next consider the plane polar coordinates such that $\mathbf{u} = \mathbf{u}(r, \theta, t)$, and the corresponding flow be

$$\mathbf{u} = (2r\cos(2\theta),\ -2r\sin(2\theta)) \tag{1.30}$$

which satisfies the solenoidal condition (1.15). Then by (1.24), we have

$$\frac{1}{r}\frac{\partial \psi}{\partial \theta} = 2r\cos(2\theta), \qquad -\frac{\partial \psi}{\partial r} = -2r\sin(2\theta). \tag{1.31}$$

Applying a similar procedure as above, the stream function is given by

$$\psi = r^2\sin(2\theta) + \text{const.} \tag{1.32}$$

1.2 The Euler Equations

In fluid dynamics, the Euler equations are a set of nonlinear partial differential equations formulated by a Swiss mathematician, Leonhard Euler, in 1755 to describe the flow of incompressible and frictionless (ideal) fluids. These equations have been used to describe and explain many physical phenomena in nature. The equations can be derived based on the following assumptions:

(1) For all times $t > 0$, there exists a well-defined mass density $\rho(\mathbf{x}, t)$ such that the total mass $m(\Omega, t)$ in the domain Ω at time t is given by

$$m = \int_\Omega \rho \, d\mathbf{x}. \tag{1.33}$$

(2) Mass is neither produced nor disappeared.

(3) The rate of change of the momentum of a fluid region is equal to the total applied force (Newton's second law).

These assumptions are equivalent to saying that the mass and momentum are conserved in Ω [7].

Continuity equation

First, we derive the equation of conservation of mass, i.e., the continuity equation. For this, we fix a volume $V \subset \Omega$. Recall the fluid velocity $\mathbf{u}$ for an incompressible fluid of density ρ. The rate of change of mass in V is given by

$$\begin{aligned} \frac{d}{dt} m(V,t) &= \frac{d}{dt} \int_V \rho \, d\mathbf{x} \\ &= \int_V \frac{\partial}{\partial t} \rho \, d\mathbf{x}. \end{aligned} \tag{1.34}$$

Assume that ∂V denotes the boundary of V and $\mathbf{n}$ is the unit outer normal, dA is the area element on ∂V.

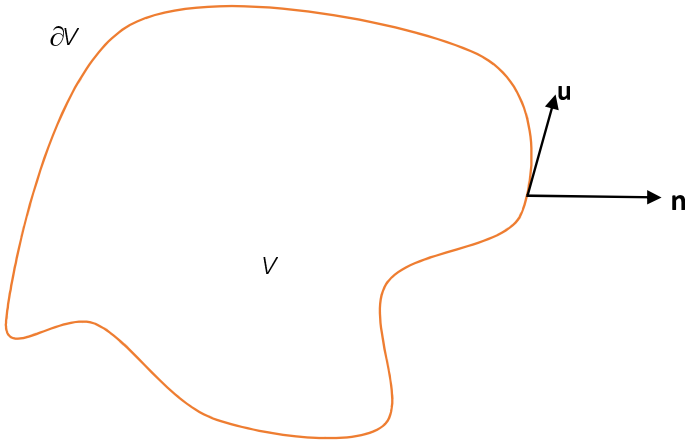

Figure 1.2: A region V bounded by the surface ∂V.

The fluid flow of the volume through ∂V per unit area is given by $\mathbf{u} \cdot \mathbf{n}$ and the corresponding flow of mass by $\rho(\mathbf{u} \cdot \mathbf{n})$. Hence, the total flow of mass through ∂V is

$$\int_{\partial V} \rho \mathbf{u} \cdot \mathbf{n} \, dA. \tag{1.35}$$

Then by the principle of mass conservation,

"*The change of mass in V is equal to the flow of mass over the boundary ∂V into V*"

we have

$$\frac{d}{dt} \int_V \rho \, d\mathbf{x} = \int_{\partial V} \rho \mathbf{u} \cdot (-\mathbf{n}) \, dA. \tag{1.36}$$

Then, using the divergence Theorem, we get

$$\int_V \left(\frac{\partial \rho}{\partial t} + \nabla \cdot (\rho \mathbf{u}) \right) d\mathbf{x} = 0. \tag{1.37}$$

Since the equation (1.37) holds for any subdomain V, one concludes by the *Du Bois-Reymond lemma* [6] that

$$\frac{\partial \rho}{\partial t} + \nabla \cdot (\rho \mathbf{u}) = 0. \tag{1.38}$$

If the medium is homogeneous, i.e., the density of the fluid is constant, the conservation of mass reduces to the equation

$$\nabla \cdot \mathbf{u} = 0. \tag{1.39}$$

Momentum equations

Consider an incompressible flow and fix a volume V. We derive the momentum balance equations by the conservation of momentum. The total momentum of the volume V is

$$\int_V \rho \mathbf{u}\, d\mathbf{x}. \tag{1.40}$$

Then by virtue of the assumption (3) (Newton's second law), one has

$$\frac{d}{dt}\int_V \rho \mathbf{u}\, d\mathbf{x} = \mathbf{F}(V), \tag{1.41}$$

where $\mathbf{F}(V)$ is the force acting on the fluid inside V. Let the pressure force acting on the surface of the volume V in the inward normal direction be p (scalar quantity) and the body force (external force) per unit mass be f. Hence, the total force exerted on the fluid inside V is

$$\begin{aligned} \mathbf{F}(V) &= \int_{\partial V} -p\mathbf{n}\, dS + \int_V \rho f\, d\mathbf{x} \\ &= \int_V -\nabla p\, d\mathbf{x} + \int_V \rho f\, d\mathbf{x}. \end{aligned} \tag{1.42}$$

Applying the Transport Theorem, one can write

$$\frac{d}{dt}\int_V \rho \mathbf{u}\, d\mathbf{x} = \int_V \rho(\mathbf{u}_t + (\mathbf{u}\cdot\nabla)\mathbf{u})\, d\mathbf{x}. \tag{1.43}$$

Hence, substituting (1.42) and (1.43) into (1.41), one gets

$$\int_V \rho(\mathbf{u}_t + (\mathbf{u}\cdot\nabla)\mathbf{u})\, d\mathbf{x} = -\int_V \nabla p\, d\mathbf{x} + \int_V \rho f\, d\mathbf{x}. \tag{1.44}$$

Since (1.44) holds for arbitrary V, one concludes by the *Du Bois-Reymond lemma* [6] that

$$\mathbf{u}_t + (\mathbf{u}\cdot\nabla)\mathbf{u} = -\frac{1}{\rho}\nabla p + f. \tag{1.45}$$

The equations (1.38) and (1.45) are known as the Euler system of fluid motion.

The Euler equations include the conservation of mass (1.38) and the conservation of momentum (1.45). To close the system of these conservation laws we need to impose two boundary conditions and two initial conditions. There are two kinds of boundary condition for a free surface: the kinematic and the dynamic boundary conditions. If the fluid is compressible, an equation of state must be added to the Euler system.

Consider the Euler system with free-surface flow for an incompressible fluid. Let the surface of the fluid be given by $z = \zeta(x,t)$. Assume that $z = 0$ coincides with the undisturbed free surface, and the bottom of the fluid is given by $z = -h$. Then the kinematic boundary condition [51] can be written as

$$\zeta_t + \mathbf{u} \cdot \nabla\zeta = 0, \qquad \text{at} \quad z = \zeta(x,t), \tag{1.46}$$

where now x denotes only the horizontal independent variable and z the vertical one.

At a rigid boundary the fluid velocity and the boundary velocity are identical. The normal components are the same because fluid does not cross the rigid boundary. The tangential components of the fluid velocity and the rigid boundary are the same. This is known as *no-slip* boundary condition [6, 41] (introduced by Prandtl 1904). The Euler equations in a closed channel with rough walls have a no-slip boundary condition

$$\mathbf{u} = 0 \tag{1.47}$$

on rigid walls at rest.

The dynamic condition on a free surface is that the stresses on top and bottom of the surface are equal. For inviscid fluids, this means that the pressure is continuous across the free surface. Consider there is no surface tension. Then, we have $[p] = 0$, where $[p]$ denotes the jump in p across the surface. In the case of an air-water interface, we can often neglect the motion of the air because of its much smaller density, and treat it as a fluid with constant pressure p_0. The dynamic boundary condition for the water is then

$$p = p_0. \tag{1.48}$$

The initial condition is given by

$$\mathbf{u}\big|_{t=0} = \mathbf{u}_0. \tag{1.49}$$

Vorticity formulation

We find the vorticity equation for incompressible fluid. By taking the curl of the Euler equation (1.45) and using the identity $\nabla \times \nabla f = 0$, we obtain

$$\nabla \times \mathbf{u}_t + \nabla \times [(\mathbf{u} \cdot \nabla)\mathbf{u}] = 0. \tag{1.50}$$

The first term on the left side, for fixed reference frames, becomes

$$\nabla \times \frac{\partial \mathbf{u}}{\partial t} = \frac{\partial}{\partial t}(\nabla \times \mathbf{u}) = \boldsymbol{\omega}_t. \tag{1.51}$$

Now using the identity $\frac{1}{2}\nabla(\mathbf{u} \cdot \mathbf{u}) = \mathbf{u} \times (\nabla \times \mathbf{u}) + \mathbf{u} \cdot \nabla\mathbf{u}$, the convective term can be written as

$$\begin{aligned} \nabla \times (\mathbf{u} \cdot \nabla)\mathbf{u} &= \nabla \times \nabla(|\mathbf{u}|^2/2) - \nabla \times [\mathbf{u} \times (\nabla \times \mathbf{u})] \\ &= \nabla \times (\boldsymbol{\omega} \times \mathbf{u}). \end{aligned} \tag{1.52}$$

Thus, in the three-dimensional (3D) case, we obtain the vorticity equation

$$\boldsymbol{\omega}_t + \nabla \times (\boldsymbol{\omega} \times \mathbf{u}) = 0. \tag{1.53}$$

In the two spatial dimension (2D), one has

$$\mathbf{u} = (u_1, u_2, 0), \quad \text{and} \quad \frac{\partial}{\partial z} \equiv 0. \tag{1.54}$$

So, for the 2D case, vorticity vector is

$$\boldsymbol{\omega} = \nabla \times \mathbf{u} = (0,\ 0,\ u_{2x} - u_{1y}). \tag{1.55}$$

Hence, $(\boldsymbol{\omega} \cdot \nabla)\mathbf{u} = 0$, and the vorticity equation reduces to

$$\boldsymbol{\omega}_t + (\mathbf{u} \cdot \nabla)\boldsymbol{\omega} = 0. \tag{1.56}$$

Remark 1.2.1. In 2D space, $\boldsymbol{\omega}$ is parallel to the z-axis and perpendicular to the velocity field $\mathbf{u}$.

Definition 1.2.1. The *helicity* of a fluid flow confined to a domain $\mathscr{D}$ (bounded or unbounded) of three-dimensional Euclidian space $\mathbb{R}^3$ is the integrated scalar product of a velocity field and the vorticity field over the volume of the flow, i.e.,

$$\mathcal{H}(t) = \int_{\mathscr{D}} \mathbf{u} \cdot \boldsymbol{\omega}\, dV. \tag{1.57}$$

Here, the quantity $h = \mathbf{u} \cdot \boldsymbol{\omega}$ is the *helicity density* of the flow [29]. Both h and $\mathcal{H}$ are pseudoscalar quantities, i.e., they change sign under change from a right-handed to a left-handed frame of reference. Helicity is important at a fundamental level in relation to flow kinematics because it admits topological interpretation in relation to the linkage or linkages of vortex lines of the flow [29].

Definition 1.2.2. A flow in which velocity field $\mathbf{u}$ and vorticity field $\boldsymbol{\omega}$ are parallel to each other is known as *Beltrami flow*, i.e., the Beltrami flow is given by

$$\boldsymbol{\omega} = \alpha \mathbf{u}, \quad \nabla \cdot \mathbf{u} = 0 \tag{1.58}$$

for some α.

The Beltrami flow (1.58) can be studied by distinguishing following three categories [74]:
(i) *Potential fields*: when $\alpha = 0$. In this case $\mathbf{u}$ is irrotational and one has $\mathbf{u} = \nabla\phi$, where ϕ is a scalar function.
(ii) *Linear Beltrami fields*: when α is constant. In the literature, most of the papers (see, e.g., [1, 82, 80]) dealing the Beltrami fields concern with the linear Beltrami fields. Among the several examples in the literature of linear Beltrami fields, the ABC flows (after V. Arnold, E. Beltrami, and S. Childress) have significant features.

(iii) *Nonlinear Beltrami fields*: when α is a function of $\boldsymbol{x}$. There are few examples of Beltrami fields are available with non-constant α. However, the existence of nonlinear Beltrami fields can be seen in [43, 83].

Linear Beltrami fields play a prominent role in the fluid mechanics. They give the special exact solutions to the steady 3D Euler equations (see, e.g., [19, 20]) as well as steady-state Navier-Stokes equations [18] for the incompressible fluid flow.

Besides, linear Beltrami fields produce steady solutions with the stream or vortex lines of arbitrary link type, where the function $B = p + |\mathbf{u}|^2/2$ is analytic and non-constant (see, e.g., [1, 30]). Indeed, the time independent 3D Euler equation (1.45) can be written as

$$\omega \times \mathbf{u} + \nabla(p + |\mathbf{u}|^2/2) = 0. \tag{1.59}$$

For the Beltrami flow, $p = -|\mathbf{u}|^2/2$ is obviously solution to (1.59).

Moreover, Beltrami fields have a vast application in electromechanics and plasma physics. In physics, the Beltrami fields are know as *force-free* fields.

1.2.1 Conserved quantities for incompressible Euler equations

The mass and momentum are conserved locally in the Euler system (1.38) and (1.45). These two quantities are conserved globally on the solutions of the Euler equations for zero boundary conditions at infinity ($\mathbf{u} \to \mathbf{0},\ p \to \text{const as } \mathbf{x} \to \pm\infty$) and are given by

$$\text{total mass, } M = \int_{\mathbb{R}^n} \rho \, d\mathbf{x}, \tag{1.60}$$

$$\text{total momentum, } P = \int_{\mathbb{R}^n} \rho \mathbf{u} \, d\mathbf{x}. \tag{1.61}$$

Here usually $n = 2, 3$. The third physical quantity [8, 14, 52], kinetic energy, is given by

$$E = \int_{\mathbb{R}^n} \frac{1}{2} |\mathbf{u}|^2 \, d\mathbf{x} \tag{1.62}$$

which is conserved because there is no dissipation in the Euler system. However, there are also a number of quantities conserved globally in time on the solutions to the Euler equations. The following conserved quantities can be seen in [8, 14] for smooth solutions to Euler equations with zero boundary conditions at infinity. In the two spatial dimension, the physical quantities are given by

(1) Angular momentum [52],

$$\int_{\mathbb{R}^2} \mathbf{x} \times \mathbf{u} \, d\mathbf{x}, \tag{1.63}$$

(2) Generalized momentum [52],

$$\int_{\mathbb{R}^2} \boldsymbol{\alpha} \cdot \mathbf{u} \, d\mathbf{x}, \tag{1.64}$$

where $\boldsymbol{\alpha} = (\alpha_1(t),\ \alpha_2(t))$.

(3) Center of vorticity [14],

$$\int_{\mathbb{R}^2} \mathbf{x}\omega \, d\mathbf{x}, \tag{1.65}$$

(4) Moment of inertia [14],

$$\int_{\mathbb{R}^2} |\mathbf{x}|^2 \omega \, d\mathbf{x}, \tag{1.66}$$

(5) Total vorticity [14],

$$\int_{\mathbb{R}^2} \omega \, d\mathbf{x}, \tag{1.67}$$

where $\omega = u_{2x} - u_{1y}$. Next we list the physical quantities for the 3D case:

(1) Helicity [8],

$$\int_{\mathbb{R}^3} \mathbf{u} \cdot \boldsymbol{\omega} \, d\mathbf{x}, \tag{1.68}$$

(2) The fluid impulse [8],

$$\int_{\mathbb{R}^3} \mathbf{x} \times \boldsymbol{\omega} \, d\mathbf{x}, \tag{1.69}$$

(3) The moment of fluid impulse [8],

$$\int_{\mathbb{R}^3} \mathbf{x} \times (\mathbf{x} \times \boldsymbol{\omega}) \, d\mathbf{x}. \tag{1.70}$$

(4) Total vorticity [8],

$$\int_{\mathbb{R}^3} \boldsymbol{\omega} \, d\mathbf{x}, \tag{1.71}$$

where the vorticity field $\boldsymbol{\omega}$ is given by (1.9). The *fluid impulse* and the *moment of fluid impulse* have dynamical significance as these are required for a generation of a flow from rest [8].

These quantities for both 2D and 3D cases are constants of motion, i.e., are conserved in time. The conservation can be verified by taking a time derivative of the above quantities, and then using the Euler equations (1.38), (1.45), and the vorticity equation (1.53) to find a divergence expression. We will only verify the conservation of helicity here. Let V be a fixed volume bounded by a surface S. Then, time derivative of the helicity:

$$\begin{aligned} \frac{d}{dt}\int_V \mathbf{u} \cdot \boldsymbol{\omega} \, dV &= \frac{d}{dt}\int_V (\mathbf{u}_t \cdot \boldsymbol{\omega} + \mathbf{u} \cdot \boldsymbol{\omega}_t) dV \\ &= \int_V \left[\big(\mathbf{u} \times (\nabla \times \mathbf{u}) - \nabla(|\mathbf{u}|^2/2) \big) \cdot \boldsymbol{\omega} + \mathbf{u} \cdot (\nabla \times (\boldsymbol{\omega} \times \mathbf{u})) \right] dV \end{aligned} \tag{1.72}$$

We observe that

$$\nabla \cdot \boldsymbol{\omega} = \nabla \cdot (\nabla \times \mathbf{u}) = 0. \tag{1.73}$$

First term in (1.72) $= (\mathbf{u} \times \boldsymbol{\omega}) \cdot \boldsymbol{\omega} \;=\; -(\boldsymbol{\omega} \times \boldsymbol{\omega}) \cdot \mathbf{u} = 0.$

Second term in (1.72), by using identity $\nabla \cdot fA = \nabla f \cdot A + f \nabla \cdot A$,

$$\begin{aligned} \int_V \nabla(|\mathbf{u}|^2/2) \cdot \boldsymbol{\omega}\, dV &= \frac{1}{2} \int_V \nabla \cdot (|\mathbf{u}|^2 \boldsymbol{\omega})\, dV \\ &= \int_S |\mathbf{u}|^2 \boldsymbol{\omega} \cdot \mathbf{n}\, dS = 0. \end{aligned} \tag{1.74}$$

Third term in (1.72) $=(\boldsymbol{\omega} \times \mathbf{u}) \cdot \boldsymbol{\omega} = (\boldsymbol{\omega} \times \boldsymbol{\omega}) \cdot \mathbf{u} = 0.$

Plugging these results back into the equation (1.72), one obtains

$$\frac{d}{dt} \int_V \mathbf{u} \cdot \boldsymbol{\omega}\, dV = 0. \tag{1.75}$$

So, the helicity is a constant of motion for the Euler equations. The conservations of other physical quantities listed above are verified in [8].

1.3 The Navier-Stokes Equations

The Navier-Stokes equations are partial differential equations that describe the motion of gases and viscous fluids. These equations were originally derived in the 1840s on the basis of conservation laws and first-order approximations. The equations are the generalization of the Euler equations. In 1821 French engineer Claude-Louis Navier introduced the element of viscosity (friction) for the more realistic and vastly more difficult problem of viscous fluids. Throughout the middle of the 19th century, British physicist and mathematician Stokes improved on this work, though complete solutions of Navier's problem were obtained only for the case of two-dimensional flows.

Derivation of navier-Stokes equation can be from an application of Newton's law for fluid:
"the rate of change of momentum of the fluid in a material volume equals the total force acting on this volume of fluid", i.e.,

$$\frac{d}{dt}(\text{momentum}) = \text{applied forces}. \tag{1.76}$$

If $\mathbf{u}(x, y, z, t)$ is the fluid velocity for incompressible fluid, the rate of change of momentum is given by

$$\frac{d}{dt}(\rho \mathbf{u}) = \rho \mathbf{u}_t + \rho(\mathbf{u} \cdot \nabla)\mathbf{u}. \tag{1.77}$$

There are three forces acting on the fluid body. The force due to pressure acting on the fluid particle is given by $-\nabla p$, where $p(x, y, z, t)$ is the fluid pressure. The shear stress divergence has simply reduces to the vector Laplacian term $\mu \nabla^2 \mathbf{u}$, $\mu = \text{const}$, which is the internal viscous forces, μ is called viscosity. The so-called body forces are those which apply to the entire mass of the fluid element. Such forces are usually due to external fields such as gravity. We consider only the gravitational body force given by $\rho \mathbf{g}$,

where $\mathbf{g}$ is the gravitational acceleration. Then, total exerted force on the fluid is $(-\nabla p + \mu\nabla^2\mathbf{u} + \rho\mathbf{g})$. One can now substitute this force and (1.77) into (1.76) in order to derive the equation of momentum balance. We also consider the continuity equation (1.38) given by the conservation of the mass of fluids. Then, the 3D Navier-Stokes equations for the viscous flow with fluid density $\rho(\mathbf{x}, t)$ and the coefficient of kinematic viscosity μ are given by

$$\mathbf{u}_t + \mathbf{u} \cdot \nabla\mathbf{u} = -\frac{1}{\rho}\nabla p + \nu\nabla^2\mathbf{u} + \mathbf{g}, \quad \nu = \mu/\rho \tag{1.78}$$

$$\rho_t + \nabla \cdot (\rho\mathbf{u}) = 0, \tag{1.79}$$

where $\mathbf{x} = (x, y, z)$ is spatial variable and t is time variable, and where the scalar-valued function $p(\mathbf{x}, t)$ is the fluid pressure, $\mathbf{u} = (u_1, u_2, u_3)$ is the fluid velocity in Cartesian coordinates, $u_i = u_i(\mathbf{x}, t),\ i = 1, 2, 3,$ and ∇ is the gradient operator (1.5).

For the compressible case an appropriate equation of state must be chosen. For example, it can be the ideal gas equation of state coupled to the adiabatic process:

$$\frac{\partial p}{\partial t} + \mathbf{u} \cdot \nabla p + \gamma p \nabla \cdot \mathbf{u} = 0 \tag{1.80}$$

where γ is the ratio of specific heats.

For an incompressible fluid, the density ρ remains constant in time i.e.

$$\frac{d\rho}{dt} = 0, \quad \rho = \rho(\mathbf{x}). \tag{1.81}$$

Remark 1.3.1. An ideal fluid corresponds to the case $\nu = 0$, when the equations (1.78)–(1.79) reduce to the original Euler system for the inviscid fluid.

Now we demonstrate an important scaling property of the Navier-Stokes equations for a homogeneous constant-density fluid without body force. Suppose we consider such a flow which is characterized by a typical length scale L and speed U. Introduce the dimensionless variables $\tilde{\mathbf{x}},\ \tilde{t},\ \tilde{\mathbf{u}},\ \tilde{p}$ by a scaling transformation

$$\tilde{\mathbf{x}} = \frac{\mathbf{x}}{L}, \quad \tilde{t} = \frac{U}{L}t, \quad \tilde{\mathbf{u}} = \frac{\mathbf{u}}{U}, \quad \tilde{p} = \frac{p}{\rho U^2}. \tag{1.82}$$

Now directly substituting $\tilde{\mathbf{u}}$ into the equation (1.78) with $g = 0$ and then using the chain rule of derivatives, we get (after neglecting the tilde)

$$\mathbf{u}_t + \mathbf{u} \cdot \nabla\mathbf{u} = -\nabla p + \frac{1}{\mathrm{Re}}\nabla^2\mathbf{u} \tag{1.83}$$

which is the Navier-Stokes equations in the dimensionless variables. Here the dimensionless quantity

$$\mathrm{Re} := \frac{UL}{\nu} \tag{1.84}$$

is the *Reynolds number* which provides a dimensionless measure for the viscosity of the flow. This shows that the Reynolds number is inversely proportional to the kinematic viscosity ν, and one can neglect the viscous

term $\nu\nabla^2\mathbf{u}$ in the Navier-Stokes equations in comparison with the inertial term $\mathbf{u}\cdot\nabla\mathbf{u}$ when the Reynolds number is sufficiently large. The Navier-Stokes equations are, however, a singular perturbation of the Euler equations, since the viscosity ν multiplies the term that contains the highest-order spatial derivatives.

Vorticity formulation

Similarly to the Euler equation, the vorticity equation of the Navier-Stokes equation is found by taking the curl of (1.78) and using the identity

$$\nabla\times(\nu\nabla^2\mathbf{u}) = \nu\nabla^2\boldsymbol{\omega}. \tag{1.85}$$

Then, in the 3D case, the vorticity equation of the Navier-Stokes equation for incompressible fluid is given by

$$\boldsymbol{\omega}_t + \mathbf{u}\cdot\nabla\boldsymbol{\omega} = \boldsymbol{\omega}\cdot\nabla\mathbf{u} + \nu\nabla^2\boldsymbol{\omega}. \tag{1.86}$$

For the 2D case, the vorticity equation is of the form

$$\omega_t + \mathbf{u}\cdot\nabla\omega = \nu\nabla^2\omega. \tag{1.87}$$

1.4 Sample Exact Solutions

Due to the complex nature of the equations, the generally exact solutions for the Euler equations and Navier-Stokes equations are not available in the literature. However, there exist some special exact solutions for the Euler equations as well as the Navier-Stokes equations. We now list some sample exact solutions for both systems.

1.4.1 Euler equations

(1) **Taylor-Green vortex flow**

Taylor and Green [3] derive a singular solution for the unsteady, incompressible 3D Euler equations in Cartesian coordinates. In the paper [3], the authors analyze a particular vortex flow with velocity $\mathbf{u} = (u, v, w)$ at time $t = 0$, where

$$u = A\cos(ax)\sin(by)\sin(cz), \tag{1.88a}$$

$$v = B\sin(ax)\cos(by)\sin(cz), \tag{1.88b}$$

$$w = C\sin(ax)\sin(by)\cos(cz), \tag{1.88c}$$

where $A,\ B,\ C,\ a,\ b,\ c$ are real numbers. Inserting the velocity components in (1.88) into the continuity equation (1.39) for incompressible fluid, one gets an algebraic equation

$$Aa + Bb + Cc = 0, \tag{1.89}$$

which has to be satisfied to hold the solution of the form (1.88). One possibility to satisfy (1.89) is

$$A = -B = \beta, \quad a = b = c = k, \quad C = 0, \tag{1.90}$$

where $-\infty < \beta, k < +\infty$. The case (1.90) yields the exact solutions to the 2D Euler equations for incompressible flow.

$$u = \beta \sin(kx) \cos(ky), \tag{1.91a}$$

$$v = -\beta \cos(kx) \sin(ky), \tag{1.91b}$$

$$p = \frac{\rho}{4} \beta (\cos(2kx) + \sin(2ky)), \tag{1.91c}$$

where $0 \leq x, y \leq 2\pi$.

Under the Taylor-Green vortex solution (1.97), the vorticity $\boldsymbol{\omega} = (0, 0, \omega)$ is given by

$$\omega = v_x - u_y = 2k\beta \sin(kx) \sin(ky). \tag{1.92}$$

Next we compute the stream function $\boldsymbol{\psi} = (0, 0, \psi)$ such that

$$\frac{\partial \psi}{\partial y} = u = \beta \sin(kx) \cos(ky), \tag{1.93}$$

$$\frac{\partial \psi}{\partial x} = -v = \beta \cos(kx) \sin(ky). \tag{1.94}$$

Solving (1.93)–(1.94), we get

$$\psi = \frac{\beta}{k} \sin(kx) \sin(ky). \tag{1.95}$$

1.4.2 Navier-Stokes equations

Some examples of exact solutions of the Navier-Stokes equations are given below.

(1) **Taylor-Green vortex flow**

For the Taylor-Green vortex flow, the time-dependent Navier-Stokes equations have the exact solutions in Cartesian coordinates. The setup for the exact solutions is again given by (1.88), and the same condition (1.89) need to be satisfied. Consider the following case to satisfy the condition (1.89):

$$A = -B = 1, \quad a = b = c = 1, \quad C = 0. \tag{1.96}$$

For the case (1.96), the exact solution for the time dependent 2D Navier-Stokes equations is known. The solution is given by

$$u = e^{-2\nu t} \sin(x) \cos(y), \tag{1.97a}$$

$$v = -e^{-2\nu t} \cos(x) \sin(y), \tag{1.97b}$$

$$p = \frac{\rho}{4} e^{-4\nu t} (\cos(2x) + \sin(2y)), \tag{1.97c}$$

where $0 \leq x, y \leq 2\pi$.

Under the Taylor-Green vortex solution (1.97), the vorticity $\boldsymbol{\omega} = (0, 0, \omega)$ is given by

$$\omega = v_x - u_y = 2e^{-2\nu t} \sin(x) \sin(y). \tag{1.98}$$

Next we reproduce stream-function $\boldsymbol{\psi} = (0, 0, \psi)$:

$$\frac{\partial \psi}{\partial y} = u = e^{-2\nu t} \sin(x) \cos(y). \tag{1.99}$$

$$\frac{\partial \psi}{\partial x} = -v = e^{-2\nu t} \cos(x) \sin(y). \tag{1.100}$$

These imply that

$$\psi = e^{-2\nu t} \sin(x) \sin(y). \tag{1.101}$$

(2) **Hagen-Poiseuille flow**

Consider fully developed steady flow in a long circular smooth pipe of radius R, with a constant pressure gradient along the pipe. Take a cross section of the pipe as shown in the Figure 1.3. One can adopt the cylindrical polar coordinates system such that r is the distance from the z-axis, and θ an angle around the pipe. Let all the fluid particles travel along z-axis. Then the fluid velocity field has the form

$$\mathbf{u} = (0,\ 0,\ u^z(r)). \tag{1.102}$$

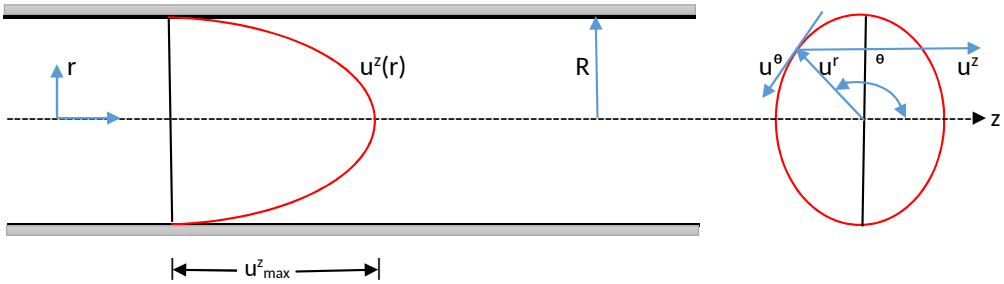

Figure 1.3: Hagen-Poiseuille flow through a pipe

The expressions for the gradient, divergence and Laplacian, in cylindrical polar coordinates are given by

$$\nabla = \left(\frac{\partial}{\partial r},\ \frac{1}{r}\frac{\partial}{\partial \theta},\ \frac{\partial}{\partial z} \right), \tag{1.103}$$

$$\nabla \cdot \mathbf{a} = \frac{1}{r}\frac{\partial}{\partial r}(r a^{(r)}) + \frac{1}{r}\frac{\partial a^{(\theta)}}{\partial \theta} + \frac{\partial a^{(z)}}{\partial z}, \tag{1.104}$$

$$\nabla^2 f = \frac{\partial^2 f}{\partial r^2} + \frac{1}{r}\frac{\partial f}{\partial r} + \frac{1}{r^2}\frac{\partial^2 f}{\partial \theta^2} + \frac{\partial^2 f}{\partial z^2}, \tag{1.105}$$

where $\mathbf{a} = \left(a^{(r)},\ a^{(\theta)},\ a^{(z)}\right)$ and f is any scalar function. Here we only have u^z component in the velocity field (1.102). We also have

$$\frac{\partial p}{\partial r} = \frac{\partial p}{\partial \theta} = 0. \tag{1.106}$$

Recall the Navier-Stokes equation for the velocity field (1.102) so that we get

$$\rho\left(\frac{\partial u^z}{\partial t} + u^r\frac{\partial u^z}{\partial r} + \frac{u^\theta}{r}\frac{\partial u^z}{\partial \theta} + u^z\frac{\partial u^z}{\partial z}\right) = -\frac{\partial p}{\partial z} + \mu\left(\frac{\partial^2 u^z}{\partial r^2} + \frac{1}{r}\frac{\partial u^z}{\partial r} + \frac{1}{r^2}\frac{\partial^2 u^z}{\partial \theta^2} + \frac{\partial^2 u^z}{\partial z^2}\right). \tag{1.107}$$

To construct exact solutions, the following assumptions are considered:

(i) The flow is steady i.e. time-derivative is zero,

(ii) The radial and swirl components of the fluid velocity are zero i.e. $u^r = u^\theta = 0$,

(iii) The flow is axisymmetric ($\partial u^z/\partial\theta = 0$) and fully developed ($\partial u^z/\partial z = 0$).

Under the assumptions $(i) - (iii)$, the equation (1.107) reduces to

$$-\frac{\partial p}{\partial z} + \mu\left(\frac{\partial^2 u^z}{\partial r^2} + \frac{1}{r}\frac{\partial u^z}{\partial r}\right) = 0, \tag{1.108}$$

which can be written as

$$\frac{d}{dr}\left(r\frac{du^z}{dr}\right) = \frac{\partial p}{\partial z}\frac{r}{\mu}. \tag{1.109}$$

Since p is a function of the axial coordinate z only, one has, by integrating twice,

$$u^z = \frac{1}{4\mu}\frac{\partial p}{\partial z}r^2 + C_1\ln r + C_2, \tag{1.110}$$

where $C_1,\ C_2$ are arbitrary constants. Now for $r = 0$, there is a singularity. u^z to be finite we must set $C_1 = 0$. The no slip boundary condition at the pipe wall requires that $u^z = 0$ at $r = R$ (radius of the pipe), which yields

$$C_2 = -\frac{1}{4\mu}\frac{\partial p}{\partial z}R^2. \tag{1.111}$$

Hence the solution becomes

$$u^z = \frac{1}{4\mu}\frac{\partial p}{\partial z}(r^2 - R^2). \tag{1.112}$$

This is a parabolic velocity profile. This exact solution can be seen in (e.g., [24, 46]. The maximum velocity occurs at the pipe centreline when $r = 0$:

$$u^z_{max} = -\frac{R^2}{4\mu}\frac{\partial p}{\partial z}. \tag{1.113}$$

Two important consequences [24] of the Hagen-Poiseuille's solution are as follows:

(i) The discharge (volume flow rate) Q through the cross section of the pipe is given by

$$\begin{aligned} Q &= \int_0^R 2\pi r u^z \, dr \\ &= 2\pi \int_0^R \frac{r}{4\mu} \frac{\partial p}{\partial z} (r^2 - R^2) \, dr \\ &= \frac{\pi R^4}{8\mu} \left(-\frac{\partial p}{\partial z} \right). \end{aligned} \tag{1.114}$$

Let p_0 and p_1 be the pressures at the beginning and end of the pipe of length l. Then pressure gradient is $\partial p/\partial z = (p_0 - p_1)/l$, and the volume flow rate (1.114) is

$$Q = \frac{\pi R^4}{8\mu} \frac{(p_0 - p_1)}{l}. \tag{1.115}$$

It is obvious from (1.115) that the quantity Q/R^4 is directly proportional to the effective pressure gradient along the pipe.

(ii) The average velocity through the cross section of the pipe is

$$\begin{aligned} u^z_{avrg} &= \frac{Q}{\pi R^2} \\ &= \frac{R^2}{8\mu} \left(-\frac{\partial p}{\partial z} \right) \\ &= \frac{1}{2} u^z_{max}. \end{aligned}$$

(3) **Time-dependent Navier-Stokes equations**

Let us consider the transformation

$$\mathbf{x}^* = \mathbf{x}/L, \quad t^* = t\nu/L^2, \quad \mathbf{u}^* = \mathbf{u}/U, \quad p^* = p/(\rho U^2) \tag{1.116}$$

where L is the characteristic length and U is the characteristic velocity. Under this transformation the Navier-Stokes equations for incompressible fluid can be written in the dimensionless form:

$$\mathbf{u}_t + \gamma \, (\mathbf{u} \cdot \nabla)\mathbf{u} = -\gamma \, \nabla p + \nabla^2 \mathbf{u} \tag{1.117}$$

where $\gamma = UL/\nu$ is the only dimensionless parameter.

To construct sample exact solutions of the dimensionless full N-S equations, the following assumptions are considered:

(1) unsteady terms balance viscous terms in the momentum equations,

(2) the velocity field is divergence-free,

(3) the convective terms $(\mathbf{u} \cdot \nabla)\mathbf{u}$ can be expressed as the gradient of a scalar function (the negative of the pressure).

By virtue of the assumption (1), the separable solution can be written in the form

$$\mathbf{u} = \mathbf{V}(\mathbf{x})T(t) \tag{1.118}$$

which implies that

$$\frac{dT}{dt} = \lambda^2 T \tag{1.119}$$

$$\nabla^2 \mathbf{V} = \lambda^2 \mathbf{V}, \quad \lambda = \text{constant}. \tag{1.120}$$

The solution of the (1.119) is given by

$$T(t) = e^{\lambda^2 t} \tag{1.121}$$

Consider a vector valued stream-function $\mathbf{\Psi}$. Due to assumption (2) we can write $\mathbf{V} = \nabla \times \mathbf{\Psi}$. Then (1.120) must satisfy

$$\nabla^2 \mathbf{\Psi} = \lambda^2 \mathbf{\Psi}. \tag{1.122}$$

We construct the stream-function field

$$\mathbf{\Psi} = \mathbf{i}\Psi_1 + \mathbf{j}\Psi_2 + \mathbf{k}\Psi_3 \tag{1.123}$$

with scalar functions $\Psi_1,\ \Psi_2,\ \Psi_3$ given by

$$\Psi_1 = f(y)g(z)h(x) \tag{1.124a}$$

$$\Psi_2 = f(z)g(x)h(y) \tag{1.124b}$$

$$\Psi_3 = f(x)g(y)h(z) \tag{1.124c}$$

where $f,\ g,\ h$ are arbitrary functions. Evaluating (1.122) and separating the variables, we have the following three equations

$$f'' = a^2 f \tag{1.125a}$$

$$g'' = b^2 g \tag{1.125b}$$

$$h'' = c^2 h \tag{1.125c}$$

with $\lambda^2 = a^2 + b^2 + c^2$.

From the assumption (3), since *curl* of a scalar function is equal to zero, we have

$$\nabla \times (\mathbf{u} \cdot \nabla \mathbf{u}) = 0 \tag{1.126}$$

Using (1.118) and a standard vector identity

$$\frac{1}{2}\nabla(|\mathbf{u}|^2) = \mathbf{u} \times (\nabla \times \mathbf{u}) + \mathbf{u} \cdot \nabla \mathbf{u} \tag{1.127}$$

in (1.126), one finds

$$\nabla \times [\mathbf{V} \times (\nabla \times \mathbf{V})] = 0. \tag{1.128}$$

It is noted here that the flows which satisfy the condition (1.128) are known as Beltrami flows. In order to construct solutions one must choose $f,\ g,\ h$ such that (1.128) is satisfied. To satisfy the conditions (1.125a)–(1.125c), $f,\ g,\ h$ must be either sine, cosine, exponential or linear combinations thereof. Let us consider a simple solution set of (1.125a)–(1.125c):

$$f(x) = e^{ax}, \quad g(x) = e^{bx}, \quad h(x) = e^{cx}, \tag{1.129}$$

Now the following two cases arise.
(I) When $a+b+c=0$ and $a,\ b,\ c$ are real. The exact solutions [15] for the full 3D Navier-Stokes equations are given by

$$u_1 = [be^{a(x-z)+b(y-z)} - ae^{a(z-y)+b(x-y)}]e^{2(a^2+ab+b^2)t} \tag{1.130a}$$

$$u_2 = [be^{a(y-x)+b(z-x)} - ae^{a(x-z)+b(y-z)}]e^{2(a^2+ab+b^2)t} \tag{1.130b}$$

$$u_3 = [be^{a(z-y)+b(x-y)} - ae^{a(y-x)+b(z-x)}]e^{2(a^2+ab+b^2)t} \tag{1.130c}$$

$$p = (a^2+ab+b^2)(e^{a(x-y)+b(x-z)} + e^{a(y-z)+b(y-x)+e^{a(z-x)+b(z-y)}})e^{4(a^2+ab+b^2)t} \tag{1.130d}$$

(II) When $a^2+b^2=0$ and c is pure imaginary. This case is also the Beltrami flow and produces a family of velocity fields and pressure depending of the values of $a,\ b$. Choose a is real so that $b=\pm ia$ and assume that $c=\pm ir$, where r is arbitrary real number. Then the obtained exact solutions [15] are

$$u_1 = -a[e^{ax}\sin(ay \pm rz) + e^{az}\cos(ax \pm ry)]e^{-r^2t} \tag{1.131a}$$

$$u_2 = -a[e^{ay}\sin(az \pm rx) + e^{ax}\cos(ay \pm rz)]e^{-r^2t} \tag{1.131b}$$

$$u_3 = -a[e^{az}\sin(ax \pm ry) + e^{ay}\cos(az \pm rx)]e^{-r^2t} \tag{1.131c}$$

$$p = -\frac{a^2}{2}[e^{2ax} + e^{2ay} + e^{2az} + 2e^{a(x+y)}\sin(az \pm rx)\cos(ay \pm rz) + 2e^{a(y+z)}\sin(ax \pm ry)$$
$$\cos(az \pm rx) + 2e^{a(z+x)}\sin(ay \pm rz)\cos(ax \pm ry)]e^{-2r^2t} \tag{1.131d}$$

This solution has an exponentially decaying behaviour in time. Another solution which can be found by taking the imaginary part of $\mathbf{V}$ has a form identical to (1.131a)–(1.131d), except that (i) for the case $b=ia$ cosines are replaced by sines and sines are replaced by negative cosines and (ii) for the case $b=-ia$ cosines are replaced by negative sines and sines are replaced by cosines.

With a similar procedure, the solutions for the 2D case can be constructed by setting $\Psi_1 = \Psi_2 = 0$ and considering $\Psi_3 = f(x)g(y)$. In this case, the flows satisfy (1.128), and are the Beltrami flows.

1.5 Outline of the Thesis

This thesis is based on a two-fluid model which derived by Choi and Camassa [86] through the consideration of layer-averaged horizontal velocities. We herein called it the Choi-Camassa model. The model is an approximation of the 2D Euler system for incompressible fluids in a closed channel. This is a simple two-layer system described by four nonlinear partial differential equations with four dependent variables and two independent variables. The model describes the evolution of finite-amplitude internal waves at the interface of two fluids for both shallow and deep fluid configurations.

The Choi-Camassa model in interesting both mathematically and physically having solitary wave solutions with a zero boundary conditions at the infinity, and periodic solutions for the non-zero boundary conditions. Although the solitary wave solutions of the model have an good agreement with the numerical solutions of the Euler equations and experimental data [61], little is known about its dynamical properties, no closed form exact solutions appear in the literature for this model. Since the 2D Euler system acknowledges many physically important conserved quantities including mass, momentum, energy, etc. as shown in Section 1.2.1, it is natural to ask what conserved quantities are admitted by the Choi-Camassa model, and to make a comparison. Basic conserved quantities of the Choi-Camassa model including mass, momentum and energy have been appeared in [86]. However, due to complex structure of the momentum balance equations, no conserved flux appears in the literature. No systematic method for constructing conservation laws has been used in [86]. But constructing conservation laws can extend the understanding of the model as conservation laws are important in studying the physical properties of a mathematical system.

In Chapter 2, we review the conservation law and the Lie point symmetry method of the PDE system. Related definitions, examples, and theorems are listed. More specifically, we outline the Noether's formulation and the Direct Method for constructing conservations laws of a PDE system. In particular we compute symmetries and conservation laws for the 2D Euler system as well as its vorticity system.

Chapter 3 represents a brief description of the Choi-Camassa model and some of its interesting properties. Besides some significant results of Choi-Camassa model have been summarised and some related fluid models are defined.

The main results of this thesis are formulated in Chapter 4. We systematically derive conservation laws of the Choi-Camassa model using direct method [68, 69]. First we derive the local conservation law multipliers, and then employ them to the model equations in order to construct local conservation laws. In this Chapter, there is a comparison of these conservation laws with the conservation laws of the Euler system. We also provide a discussion on the conservation law computation.

Chapter 5 contains an overview of solutions of the Choi-Camassa model. Due to the nonlinearity and complex nature of the Choi-Camassa model equations, a numerical scheme is used under MAPLE software

to reproduce the solitary wave solutions as well as kink solutions. This chapter also represents the plots of the conserved quantities on the solutions of the Choi-Camassa model.

Finally in Chapter 6, we discuss the results and some open problems related to the Choi-Camassa model.

Chapter 2

Conservation Law: Theory and Examples

A symmetry of a system of partial differential equations (PDEs) is a group transformation which maps solutions of the system into other solutions of the same system. In general, symmetry methods are important for finding exact solutions, to construct new solutions from known solutions of the system of differential equations, and more. A particular class of symmetries, named Lie point symmetries after Sophus Lie [70, 71, 72], plays a vital role in the differential equations. Lie point symmetry of an ODE can be used to reduce the order of the differential equation. Interestingly, for a variational system of differential equations, Lie group [25] of point transformations that leaves invariant the action functional can be employed to find the local conservation laws of the given variational system (see, e.g., [25, 28, 55]).

A local conservation law of a given system of differential equations is a divergence expression that vanishes on solutions of the given system. Conservation laws of a physical system are important for various purposes including (i) to find local and global conserved quantities, (ii) for constructing numerical methods, (iii) to study existence and uniqueness of solutions, and (iv) to construct nonlocally related PDE systems of the given PDE system. The study of conservation laws are related to that of the Lie symmetries due to Emmy Noether's method in finding conservation laws. Emmy Noether (e.g., [28, 55]), in 1918, introduced the notion of a one-parameter transformation in finding conservation laws. She showed that if a system of differential equations admits a variational principle, then any one-parameter Lie group of point transformations (variational symmetry) that leaves invariant the action functional yields a local conservation law [28, 55]. In particular, she gave an explicit formula for the fluxes of the conservation law.

Another standard method in constructing conservation laws of PDE systems is the 'direct conservation law construction method' (Olver [55], Anco and Bluman [68, 69]). This method supersedes the Noether's method since it is applicable to both variational and non-variational systems, and produces all the conservation laws of Noether's method [27, 28].

2.1 Lie Symmetries of PDEs

Definition 2.1.1. A group (G, Π) is a set G with an operation $\Pi : G \times G \to G$ such that for all $a, b, c \in G$:

(i) The group is closed: $\Pi(a,b) \in G$;

(ii) The operation Π is associative: $\Pi(\Pi(a,b),c) = \Pi(a,\Pi(b,c))$;

(iii) There exists an identity element $e \in G$ such that $\Pi(e,a) = \Pi(a,e) = a$;

(iv) There exists an inverse element $a^{-1} \in G$ such that $\Pi(a^{-1},a) = \Pi(a,a^{-1}) = e$.

Definition 2.1.2. Let (S,Π) be a group on $S \subset \mathbb{R}$ with operation Π. Consider some $\boldsymbol{x} \in \mathscr{D} \subset \mathbb{R}^n$ acted on by a continuous point transformation $\mathbf{X} : \mathscr{D} \times S \to \mathscr{D}$ such that

$$\boldsymbol{x}^* = \mathbf{X}(\boldsymbol{x},\epsilon), \tag{2.1}$$

where ϵ is the transformation parameter. Then, $\mathbf{X}$ forms a group of transformations on $\mathscr{D}$ if for every $\epsilon,\delta \in S$:

- $\mathbf{X}(\boldsymbol{x},\epsilon)$ is bijective (one to one and onto) on $\mathscr{D}$;
- $\mathbf{X}(\boldsymbol{x},\epsilon_0) = \boldsymbol{x}$, where ϵ_0 is the identity element; and
- If $\boldsymbol{x}^* = \mathbf{X}(\boldsymbol{x},\epsilon)$ and $\boldsymbol{x}^{**} = \mathbf{X}(\boldsymbol{x}^*,\delta)$, then $\boldsymbol{x}^{**} = \mathbf{X}(\boldsymbol{x},\Pi(\epsilon,\delta))$.

Definition 2.1.3. A group of transformations is a *one-parameter Lie group* of point transformations if:

(i) $\epsilon \in S$ is a parameter (S is an interval in $\mathbb{R}$). Without loss of generality $\epsilon = 0$ corresponds to the identity element e;

(ii) the transformation $\mathbf{X}$ is infinitely differentiable with respect to $\boldsymbol{x} \in \mathscr{D}$ and is an analytic function of ϵ in S;

(iii) $\Pi(\epsilon,\delta)$ is analytic in ϵ and δ, where $\epsilon,\delta \in S$.

A continuous symmetry of a system of partial differential equations (PDEs) is a transformation that leaves invariant the solution manifold of the system, i.e., a symmetry group of a system of PDEs is a group of transformations which maps (deforms) any solution of the system into a solution of the same system [28]. In applications, Lie groups of transformations acting on the solution manifold of the given PDE are considered as a special class of symmetries.

Consider the situation of n independent variables $\boldsymbol{x} = (x^1,...,x^n)$ and m dependent variables $\mathbf{u}(\boldsymbol{x}) = (u^1(\boldsymbol{x}),...,u^m(\boldsymbol{x}))$. Let the partial derivatives be denoted by $u^\mu_i = \partial u^\mu(\boldsymbol{x})/\partial x^i$. The notation

$$\partial\mathbf{u} \equiv \partial^1\mathbf{u} = (u^1_1(\boldsymbol{x}),...,u^1_n(\boldsymbol{x}),...,u^m_1(\boldsymbol{x}),...,u^m_n(\boldsymbol{x})) \tag{2.2}$$

denotes the set of all first-order partial derivatives and

$$\partial^p\mathbf{u} = \left\{ u^\mu_{i_1,...,i_p} \quad | \ \mu = 1,...,m;\ i_1,...,i_p = 1,...,n \right\} \tag{2.3a}$$

$$= \left\{ \frac{\partial^p\mathbf{u}}{\partial x^{i_1}\cdots\partial x^{i_p}} \quad \Big| \ \mu = 1,...,m;\ i_1,...,i_p = 1,...,n \right\} \tag{2.3b}$$

the set of all partial derivatives of order p.

A point transformation is a one-to-one transformation acting on the $(n+m)$-dimensional space $(\boldsymbol{x}, u)$. In particular, a point transformation is of the form

$$(x^i)^* = f^i(\boldsymbol{x}, \mathbf{u}), \tag{2.4a}$$

$$(u^\mu)^* = g^\mu(\boldsymbol{x}, \mathbf{u}). \tag{2.4b}$$

Through invariance of contact conditions, a point transformation (assuming that (2.4a)–(2.4b) is differentiable as needed) naturally extends to a one-to-one transformation acting on $(\boldsymbol{x}, \mathbf{u}, \partial\mathbf{u}, ..., \partial^p\mathbf{u})$-space for p any integer.

Definition 2.1.4. A one-parameter Lie group [25, 28, 55] of point transformations is given by

$$(x^i)^* = f^i(\boldsymbol{x}, \mathbf{u}; \varepsilon) = x^i + \varepsilon\xi^i(\boldsymbol{x}, \mathbf{u}) + O(\varepsilon^2), \tag{2.5a}$$

$$(u^\mu)^* = g^\mu(\boldsymbol{x}, \mathbf{u}; \varepsilon) = u^\mu + \varepsilon\eta^\mu(\boldsymbol{x}, \mathbf{u}) + O(\varepsilon^2), \tag{2.5b}$$

in terms of infinitesimals

$$\xi^i = \frac{d(x^i)^*}{d\varepsilon}\Big|_{\varepsilon=0}, \qquad \eta^\mu = \frac{d(u^\mu)^*}{d\varepsilon}\Big|_{\varepsilon=0} \tag{2.6}$$

with the corresponding infinitesimal generator

$$Y = \sum_{i=1}^{n} \xi^i(\boldsymbol{x}, \mathbf{u})\frac{\partial}{\partial x^i} + \sum_{\mu=1}^{m} \eta^\mu(\boldsymbol{x}, \mathbf{u})\frac{\partial}{\partial u^\mu}. \tag{2.7}$$

A one-parameter group of transformations can be determined locally from its infinitesimal generator, which comes from the following theorem.

Theorem 2.1.5. *A one parameter Lie group of transformations* (2.5a)–(2.5b) *is equivalent to the solutions of the initial value problems*

$$\frac{d(x^i)^*}{d\varepsilon} = \xi^i(\boldsymbol{x}, \mathbf{u}), \quad (x^i)^*\Big|_{\varepsilon=0} = x^i \tag{2.8}$$

$$\frac{d(u^\mu)^*}{d\varepsilon} = \eta^\mu(\boldsymbol{x}, \mathbf{u}), \quad (u^\mu)^*\Big|_{\varepsilon=0} = u^\mu. \tag{2.9}$$

Proof of this theorem can be seen in [25, 26, 55].

Definition 2.1.6. The total derivative operator is given by

$$D_i = D_{x^i} = \frac{\partial}{\partial x^i} + u^\mu_i\frac{\partial}{\partial u^\mu} + u^\mu_{ii_1}\frac{\partial}{\partial u^\mu_{i_1}} + u^\mu_{ii_1i_2}\frac{\partial}{\partial u^\mu_{i_1i_2}} + \cdots \ \cdots \tag{2.10}$$

A one-parameter Lie group of point transformations (2.5a)–(2.5b) induces one-parameter Lie groups of point transformations acting on $(\boldsymbol{x}, \mathbf{u}, \partial\mathbf{u})$-space, ..., $(\boldsymbol{x}, \mathbf{u}, \partial\mathbf{u}, ..., \partial^k\mathbf{u})$-space, as follows.

$$(u^\mu)^*_i = u^\mu_i + \varepsilon\eta^{(1)\mu}_i(\boldsymbol{x}, \mathbf{u}, \partial\mathbf{u}) + O(\varepsilon^2), \tag{2.11}$$

... ...

$$(u^{\mu})^{*}_{i_1\ldots i_k} = u^{\mu}_{i_1\ldots i_k} + \varepsilon\eta^{(k)\mu}_{i_1\ldots i_k}(\boldsymbol{x},\mathbf{u},\partial\mathbf{u},...,\partial^k\mathbf{u}) + O(\varepsilon^2) \tag{2.12}$$

with the extended infinitesimals given by

$$\eta^{(1)\mu}_{i} = D_i\eta^{\mu} - (D_i\xi^j)u^{\mu}_j, \tag{2.13}$$

and

$$\eta^{(k)\mu}_{i_1\ldots i_k} = D_{i_k}\eta^{(k-1)\mu}_{i_1\ldots i_{k-1}} - (D_{i_k}\xi^j)u^{\mu}_{i_1\ldots i_{k-1}j}, \tag{2.14}$$

where $\mu = 1,...,m$; $i, i_j = 1,...,n$ for $j = 1,...,k$ with $k = 2,3,...$, and summation across j.

Proposition 2.1.1. *The k-th extended or k-th prolonged infinitesimal generator [25, 28] (k-th prolongation of* (2.7)*) is given by*

$$Y^{(k)} = Y + \sum_{i_1=1}^{n}\sum_{\mu=1}^{m}\eta^{(1)\mu}_{i_1}(\boldsymbol{x},\mathbf{u},\partial\mathbf{u})\frac{\partial}{\partial u^{\mu}_{i_1}} + \sum_{i_1,i_2=1}^{n}\sum_{\mu=1}^{m}\eta^{(2)\mu}_{i_1i_2}(\boldsymbol{x},\mathbf{u},\partial\mathbf{u},\partial^2\mathbf{u})\frac{\partial}{\partial u^{\mu}_{i_1i_2}} + \cdots\ \cdots, \tag{2.15}$$

where Y is given by (2.7)*, and infinitesimals are given by* (2.6)*,* (2.13) *and* (2.14)*.*

Definition 2.1.7. For any Lie group of transformations (2.5a)–(2.5b), a smooth function $\Theta(\boldsymbol{x},\mathbf{u})$ is invariant under the group of transformations if and only if $\Theta((x^i)^*,(u^{\mu})^*) = \Theta(\boldsymbol{x},\mathbf{u})$.

Definition 2.1.8. (Point Symmetries) Consider a system $\mathbf{R}\{\boldsymbol{x};\mathbf{u}\}$ of N PDEs of order k with n independent variables $\boldsymbol{x} = (x^1,...,x^n)$ and m dependent variables $\mathbf{u}(\boldsymbol{x}) = (u^1(\boldsymbol{x}),...,u^m(\boldsymbol{x}))$, given by

$$R^{\sigma}(\boldsymbol{x},\mathbf{u},\partial\mathbf{u},...,\partial^k\mathbf{u}) = 0, \quad \sigma = 1,...,N. \tag{2.16}$$

Then, a one-parameter Lie group of point transformations (2.5a)–(2.5b) leaves the PDE system $\mathbf{R}\{\boldsymbol{x},\mathbf{u}\}$ (2.16) invariant if and only if its k-th extension (2.15) leaves invariant the solution manifold of $\mathbf{R}\{\boldsymbol{x},\mathbf{u}\}$ in $(\boldsymbol{x},\mathbf{u},\partial\mathbf{u},...,\partial^k\mathbf{u})$-space, i.e., it maps any family of solution surfaces of the PDE system (2.16) into another family of solution surfaces of PDE system (2.16). In this case, the one-parameter Lie group of point transformations (2.5a)–(2.5b) is called a point symmetry [25, 28] of the PDE system $\mathbf{R}\{\boldsymbol{x};\mathbf{u}\}$ (2.16).

The invariance criteria of the PDE system is not in general a necessary condition for a Lie group to be a symmetry of the PDE system $\mathbf{R}\{\boldsymbol{x};\mathbf{u}\}$ [55]. In order to obtain necessary and sufficient conditions, the PDE system $\mathbf{R}\{\boldsymbol{x};\mathbf{u}\}$ must satisfy the following conditions:
(i) The PDE system is regular.
(ii) The PDE system $\mathbf{R}\{\boldsymbol{x};\mathbf{u}\}$ is of maximal rank.
(iii) $\mathbf{R}\{\boldsymbol{x};\mathbf{u}\}$ is locally solvable.

Definition 2.1.9. Consider a system of PDEs

$$R^{\sigma}(\boldsymbol{x}, \mathbf{u}, \partial\mathbf{u}, ..., \partial^{k}\mathbf{u}) = 0, \ \sigma = 1, ..., N. \tag{2.17}$$

The PDE system (2.17) is of *maximal rank* if the rank of its Jacobian matrix with respect to the variables $(\boldsymbol{x}, ..., \partial^{k}\mathbf{u})$ is N.

Definition 2.1.10. The PDE system (2.17) is *locally solvable* at the point $(\boldsymbol{x}_0, ..., \partial^{k}\mathbf{u}_0)$ if there exists a smooth solution $\mathbf{u} = \mathbf{f}(\boldsymbol{x})$, defined in a neighborhood of $\boldsymbol{x}_0$, which satisfies $\mathbf{u}_0^k = \mathbf{f}^k(\boldsymbol{x}_0)$.

Definition 2.1.11. A k-th order PDE system is *regular* if it is of maximal rank, analytic and contains all its differential consequences up to order k, i.e., no further differential consequences of order k or less can be obtained from the PDE system through differentiation.

Definition 2.1.12. A PDE system $\mathbf{R}\{x; u\}$ is *nondegenerate* if at every point $(\boldsymbol{x}_0, ..., \partial^{k}\mathbf{u}_0)$, it is both of maximal rank and locally solvable. The PDE system is *totally nondegenerate* if it and all its differential consequences are nondegenerate.

Theorem 2.1.13. *Consider the PDE system* $\mathbf{R}\{\boldsymbol{x}; \mathbf{u}\}$ (2.16) *which is regular and nondegenerate. A one-parameter Lie group of point transformations* (2.5) *is admitted by the PDE system* $\mathbf{R}\{\boldsymbol{x}; \mathbf{u}\}$ *if and only if*

$$Y^{(k)} R^{\sigma}(\boldsymbol{x}, \mathbf{u}, \partial\mathbf{u}, ..., \partial^{k}\mathbf{u}) = 0, \qquad \sigma = 1, ..., s, \tag{2.18}$$

whenever

$$R^{\sigma}(\boldsymbol{x}, \mathbf{u}, \partial\mathbf{u}, ..., \partial^{k}\mathbf{u}) = 0 \tag{2.19}$$

for every infinitesimal generator Y (2.7).

A proof of this theorem can be found in [25, 55, 56].

The condition (2.18) is known as the invariance condition. The Theorem 2.1.13 provides a systematic way to find all Lie point symmetries of a k-th order PDE system. In this procedure, one assumes the infinitesimal generator Y (2.7) of the hypothetical one-parameter symmetry group, where the infinitesimals $\xi^i, \ \eta^{\mu}$ are the functions of $\boldsymbol{x}, \ \mathbf{u}$ only. But the prolonged infinitesimal generator $Y^{(k)}$ are the functions of $\boldsymbol{x}, \ \mathbf{u}$ and the derivatives of $\mathbf{u}$ as well as $\xi^i, \ \eta^{\mu}$ and their partial derivatives with respect to $\boldsymbol{x}, \ \mathbf{u}$. When one expands (2.18) and equates the coefficients of the derivatives of $\mathbf{u}$ to zero, there will be a large system of partial differential equations for $\xi^i, \ \eta^{\mu}$. These equations are called the *determining equations* for the symmetry group of the given PDE system.

2.1.1 Lie's algorithm for point symmetries

Consider a k-th order PDE system $\mathbf{R}\{\boldsymbol{x};\mathbf{u}\}$ (2.16) which is regular, of maximal rank, and locally solvable. Then Lie's algorithm for finding point symmetries is as follows:

1. Let the infinitesimal generator Y of the point symmetries be of the form

$$Y=\sum_{i=1}^{n}\xi^i(\boldsymbol{x},\mathbf{u})\frac{\partial}{\partial x^i}+\sum_{j=1}^{m}\eta^j(\boldsymbol{x},\mathbf{u})\frac{\partial}{\partial u^j}, \tag{2.20}$$

where the infinitesimals $\xi^i(\boldsymbol{x},\mathbf{u})$ and $\eta^j(\boldsymbol{x},\mathbf{u})$ are unknown functions of $\boldsymbol{x}$ and $\mathbf{u}$ to be determined.

2. Find the k-th order prolongation/extended infinitesimal generator $Y^{(k)}$ of Y in terms of $\xi^i,\ \eta^\mu$ using the definition in Proposition 2.1.1.

3. Apply the k-th order prolongation $Y^{(k)}$ to $\mathbf{R}\{\boldsymbol{x};\mathbf{u}\}$, and eliminate the dependencies among the derivatives of u arising from $\mathbf{R}\{\boldsymbol{x};\mathbf{u}\}$ itself.

4. Set the coefficients of the remaining derivatives of $\mathbf{u}$ to zero. This step yields a system of linear PDEs for the unknown functions $\xi^i(\boldsymbol{x},\mathbf{u})$ and $\eta^j(\boldsymbol{x},\mathbf{u})$, the determining equations of the infinitesimals of the point symmetries of $\mathbf{R}\{\boldsymbol{x};\mathbf{u}\}$.

5. Solve the determining equations explicitly to obtain the general solutions of $\xi^i(\boldsymbol{x},\mathbf{u})$ and $\eta^j(\boldsymbol{x},\mathbf{u})$.

Example 2.1.1. Consider the one-dimensional nonlinear reaction-diffusion equation

$$u_t-u_{xx}=u^3. \tag{2.21}$$

We want to apply Lie's algorithm to find its point symmetries. Let

$$Y=\xi(x,t,u)\frac{\partial}{\partial x}+\tau(x,t,u)\frac{\partial}{\partial t}+\eta(x,t,u)\frac{\partial}{\partial u} \tag{2.22}$$

be the infinitesimal generator of a point symmetry of the nonlinear reaction-diffusion equation. Then Y is an infinitesimal point symmetry of the nonlinear reaction diffusion equation if and only if its second order prolongation $Y^{(2)}$ satisfies

$$Y^{(2)}(u_t-u_{xx}-u^3)\Big|_{u_t=u_{xx}+u^3}=0, \tag{2.23}$$

where, by (2.15),

$$Y^{(2)}=Y+\eta_t^{(1)}\frac{\partial}{\partial u_t}+\eta_x^{(1)}\frac{\partial}{\partial u_x}+\eta_{tt}^{(2)}\frac{\partial}{\partial u_{tt}}+\eta_{tx}^{(2)}\frac{\partial}{\partial u_{tx}}+\eta_{xx}^{(2)}\frac{\partial}{\partial u_{xx}} \tag{2.24}$$

in terms of

$$\eta_t^{(1)} = D_t\eta - u_t(D_t\tau) - u_x(D_t\xi), \tag{2.25a}$$

$$\eta_x^{(1)} = D_x\eta - u_t(D_x\tau) - u_x(D_x\xi), \tag{2.25b}$$

$$\eta_{xx}^{(2)} = D_x\eta_x^{(1)} - u_{tx}(D_x\tau) - u_{xx}(D_x\xi), \tag{2.25c}$$

and so on. We now substitute the total derivative operators and infinitesimals (2.25) into the invariance condition (2.23). However the terms involving $\eta_x^{(1)},\ \eta_{tt}^{(2)},\ \eta_{tx}^{(2)}$ vanish. After simplifying and equating the coefficients of the similar terms to zero, one obtains the following determining equations

$$\xi_{uu} = 0,\ \xi_u + \tau_{xu} = 0,\ \tau_x = 0,\ \tau_u = 0,\ \tau_{uu} = 0, \tag{2.26a}$$

$$u^3\tau_{uu} - \eta_{uu} + \xi_{xu} = 0, \tag{2.26b}$$

$$2\xi_x - u^3\tau_u + \tau_{xx} - \tau_t = 0, \tag{2.26c}$$

$$\xi_t + u^3\xi_u + \xi_{xx} - 2u^3\tau_{xu} + 2\eta_{xu} = 0, \tag{2.26d}$$

$$\eta_t - \eta_{xx} - 3u^2\eta_u + u^3\eta_u - u^3\tau_t - u^6\tau_u + u^3\tau_{xx} = 0. \tag{2.26e}$$

This system has the following solution:

$$\xi = -C_1x + C_2, \quad \tau = -2C_1t + C_3, \quad \eta = C_1u, \tag{2.27}$$

where $C_1,\ C_2,\ C_3$ are arbitrary constants. Corresponding to each constant, there is one symmetry. Thus the nonlinear reaction-diffusion equation (2.21) only has three point symmetries given by the infinitesimal generators

$$Y_1 = \frac{\partial}{\partial x}, \qquad Y_2 = \frac{\partial}{\partial t}, \qquad Y_3 = x\frac{\partial}{\partial x} + 2t\frac{\partial}{\partial t} - u\frac{\partial}{\partial u}. \tag{2.28}$$

We wish to compute corresponding Lie groups of transformation for the symmetry generators in (2.28). For Y_3, we get

$$\frac{dx^*}{d\varepsilon} = x^* \quad \Longrightarrow\ x^* = e^{\varepsilon}x, \tag{2.29}$$

$$\frac{dt^*}{d\varepsilon} = 2t^* \quad \Longrightarrow\ t^* = e^{2\varepsilon}t, \tag{2.30}$$

$$\frac{du^*}{d\varepsilon} = -u^* \quad \Longrightarrow\ u^* = e^{-\varepsilon}u, \tag{2.31}$$

where we used the fact that $x^*(0) = x,\ t^*(0) = t,\ u^*(0) = u$. Similar procedure can be applied for Y_1 and Y_2. Hence, the corresponding one-parameter Lie groups of transformations generated by Y_i are given by

$$\text{spatial translation} \quad : (x^*, t^*, u^*) \to (x + \varepsilon, t, u), \tag{2.32a}$$

$$\text{time translation} \quad : (x^*, t^*, u^*) \to (x, t + \varepsilon, u), \tag{2.32b}$$

$$\text{scaling} \quad : (x^*, t^*, u^*) \to (e^{\varepsilon}x, e^{2\varepsilon}t, e^{-\varepsilon}u). \tag{2.32c}$$

2.2 Conservation Laws of PDEs

Consider a system $\mathbf{R}\{\boldsymbol{x};\mathbf{u}\}$ of partial differential equations of order k with n independent variables $\boldsymbol{x} = (x^1, x^2, ..., x^n)$ and m dependent variables $\mathbf{u}(\boldsymbol{x}) = (u^1(\boldsymbol{x}),\ u^2(\boldsymbol{x}),\ ...,\ u^m(\boldsymbol{x}))$, given by

$$\mathbf{R}[\mathbf{u}] = R^\sigma(\boldsymbol{x}, \mathbf{u}, \partial\mathbf{u}, ..., \partial^k\mathbf{u}) = 0, \quad \sigma = 1, ..., N. \tag{2.33}$$

Definition 2.2.1. A local *conservation law* [28] of the system (2.33) is a divergence expression

$$\sum_{i=1}^{n} D_{x^i}\Phi^i[\mathbf{u}] = 0 \tag{2.34}$$

holding for all solutions of PDE system (2.33), where $\Phi^i[u] = \Phi^i(\boldsymbol{x}, \mathbf{u}, \partial\mathbf{u}, ..., \partial^r\mathbf{u})$ are called fluxes of the conservation law and the highest-order derivative r in the fluxes $\Phi^i[\mathbf{u}]$ is called the *order* of the conservation law.

If one of the independent variables of $\mathbf{R}\{\boldsymbol{x};\mathbf{u}\}$ (2.33) is time t, the conservation law (2.34) takes the form

$$D_t\Psi[\mathbf{u}] + \sum_{i=1}^{n} D_{x^i}\Phi^i[\mathbf{u}] = 0, \tag{2.35}$$

here $\Psi[\mathbf{u}] = \Psi(\boldsymbol{x}, t, \mathbf{u}, \partial\mathbf{u}, ..., \partial^r\mathbf{u})$ is called density of the conservation law.

Definition 2.2.2. A local conservation law (2.34) of the PDE system is *trivial* if its fluxes are of the form $\Phi^i[\mathbf{u}] = P^i[\mathbf{u}] + Q^i[\mathbf{u}]$, where $P^i[\mathbf{u}]$ and $Q^i[\mathbf{u}]$ are functions of $\boldsymbol{x}$, $\mathbf{u}$ and derivatives of $\mathbf{u}$ such that $P^i[\mathbf{u}]$ vanishes on the solutions of the PDE system, and $D_{x^i}Q^i[\mathbf{u}] \equiv 0$ is identically divergence-free.

Usually a trivial conservation law [55] does not give any information of the given PDE system and holds for the following two cases:
(1) Each of fluxes of the given PDE system vanishes on the solutions of the given PDE system
(2) The conservation law vanishes as a differential identity.

As an example, consider the PDE system

$$v_x = u, \quad v_t = uu_x, \quad x, u, v \in \mathbb{R}. \tag{2.36}$$

Then the conservation law

$$D_t(u(u - v_x)) + D_x(2(v_t - uu_x)) = 0 \tag{2.37}$$

has a first kind of triviality for the PDE system (2.36) and

$$D_t(u_{xx}) + D_x(-u_{xt}) = 0 \tag{2.38}$$

has a second kind of triviality. This observation leads to the following definition of equivalence of conservation laws.

Definition 2.2.3. Two conservation laws $D_{x^i}\Phi_1^i[\mathbf{u}] = 0$ and $D_{x^i}\Phi_2^i[\mathbf{u}] = 0$ are *equivalent* if $D_{x^i}(\Phi_1^i[\mathbf{u}] - \Phi_2^i[\mathbf{u}]) = 0$ is a trivial conservation law. An *equivalence* class of conservation laws consists of all conservation laws equivalent to some given nontrivial conservation law.

Example 2.2.1. Recall the one-dimensional KdV equation

$$u_t + uu_x + u_{xxx} = 0, \tag{2.39}$$

which admits the conservation laws

$$D_t\left(\frac{1}{2}u^2\right) + D_x\left(\frac{1}{3}u^3 + uu_{xx} - \frac{1}{2}u_x^2\right) = 0. \tag{2.40}$$

Then, an equivalent conservation law is in the form

$$D_t\left(\frac{1}{2}u^2 + u_x\right) + D_x\left(\frac{1}{3}u^3 + uu_{xx} - \frac{1}{2}u_x^2 - u_t\right) = 0. \tag{2.41}$$

since it is obvious that subtraction of (2.41) from (2.40) is identically zero, which is the second kind of triviality.

2.2.1 Variational PDE system and Noether's theorem

Noether's Theorem for conservation laws only applies to variational PDE systems. So, it is important to decide if the system is variational. We now briefly discuss the variational formulation of the PDE system.

Definition 2.2.4. Consider a functional $J[\mathbf{U}]$ with n independent variables $\boldsymbol{x} = (x^1, \cdots, x^n)$ and m arbitrary functions $\mathbf{U} = (U^1(\boldsymbol{x}), \cdots, U^m(\boldsymbol{x}))$ and their partial derivatives to order k, defined on a domain Ω, such that

$$J[\mathbf{U}] = \int_\Omega L[\mathbf{U}]\, d\boldsymbol{x} = \int_\Omega L(\boldsymbol{x}, \mathbf{U}, \partial\mathbf{U}, \cdots, \partial^k\mathbf{U})\, d\boldsymbol{x}. \tag{2.42}$$

The functional $J[\mathbf{U}]$ is called an *action integral*.

A *variational problem* consists of finding extrema of the action integral in some class of functions $\mathbf{u} = f(\boldsymbol{x})$ defined over Ω. The integrand $L[\mathbf{U}]$, called the *Lagrangian* of variational problem $J[\mathbf{U}]$, is a smooth function of $\boldsymbol{x}$, $\mathbf{u}$ and derivatives of $\mathbf{u}$.

Definition 2.2.5. The Euler operator with respect to each variable $\mathbf{U}^j$ is given by

$$E_{U^j} = \frac{\partial}{\partial U^j} - D_i\frac{\partial}{\partial U_i^j} + \cdots + (-1)^s D_{i_1}\ldots D_{i_s}\frac{\partial}{\partial U^j_{i_1\ldots i_s}} + \cdots, \quad j = 1, ..., m, \tag{2.43}$$

where D is the total derivative operator given by (2.10), and $U^j_{i_1\ldots i_s}$ is defined in (2.3).

Theorem 2.2.6. *If a smooth function* $\mathbf{U}(\boldsymbol{x}) = \mathbf{u}(\boldsymbol{x})$ *is an extremum of an action integral*

$$J[\mathbf{U}] = \int_{\Omega} L[\mathbf{U}]\, d\boldsymbol{x} \tag{2.44}$$

with $L[\mathbf{U}] = L(\boldsymbol{x}, \mathbf{U}, \partial\mathbf{U}, \cdots, \partial^k\mathbf{U})$*, then* $\mathbf{u}(\boldsymbol{x})$ *satisfies the Euler-Lagrange equations*

$$E_{u^\sigma}(L[\mathbf{u}]) = \frac{\partial L[\mathbf{u}]}{\partial u^\sigma} + \cdots + (-1)^s D_{i_1}...D_{i_s}\frac{\partial L[\mathbf{u}]}{\partial u^\sigma_{i_1...i_s}} = 0, \quad \sigma = 1, ..., m. \tag{2.45}$$

Remark 2.2.1. Not every solution to the Euler-Lagrangian equations is an extremal.

Theorem 2.2.7. *A PDE system admits variational principle if and only if it arises from the Euler-Lagrangian equations.*

Definition 2.2.8. Let $P[u] = P(x, u^l)$ be a differential equation, where $x, u \in \mathbb{R}$ and l is order of the derivative. Then the *linear differential operator* $\mathscr{L}$ is given by the Fréchet derivative of P:

$$\mathscr{L}[u]v = \frac{d}{d\varepsilon}P[u + \epsilon v]\Big|_{\varepsilon=0}, \tag{2.46}$$

where v is an arbitrary function.

The adjoint differential operator $\mathscr{L}^*$ satisfies the relation

$$\int_{\mathbb{R}} w\mathscr{L}[u]v\, dx = \int_{\mathbb{R}} v\mathscr{L}^*[u]w\, dx \tag{2.47}$$

for arbitrary function w. Integration by parts gives an equivalent relation [55] of (2.47) as

$$w\mathscr{L}v = v\mathscr{L}^*w + \text{div } Q, \tag{2.48}$$

where Q is a bilinear expression involving $u,\ v,\ w$ and their derivatives.

Remark 2.2.2. By (2.48), we have

$$E(w\mathscr{L}v) = E(v\mathscr{L}^*w). \tag{2.49}$$

where E is the Euler operator.

Definition 2.2.9. The operator $\mathscr{L}$ is said to be self-adjoint if

$$\mathscr{L}[u] = \mathscr{L}^*[u], \tag{2.50}$$

and it is skew-adjoint if

$$\mathscr{L}[u] = -\mathscr{L}^*[u]. \tag{2.51}$$

Example 2.2.2. Consider the one-dimensional wave equation

$$u_{tt} = u_{xx}. \tag{2.52}$$

The linearizing operator is computed by the Fréchet derivative (2.46) as

$$\begin{aligned}\mathscr{L}[u]v &= \frac{d}{d\varepsilon}(u_{tt} + \varepsilon v_{tt} - u_{xx} - \varepsilon v_{xx})\Big|_{\varepsilon=0} \\ &= v_{tt} - v_{xx} = (\partial_{tt} - \partial_{xx})v. \end{aligned} \tag{2.53}$$

Thus, one has

$$\mathscr{L}[u] = \partial_{tt} - \partial_{xx}. \tag{2.54}$$

We now compute the adjoint operator.

$$\begin{aligned} w\mathscr{L}v &= wv_{tt} - wv_{xx} \\ &= (wv_t - w_t v)_t + (w_x v - wv_x)_x + w_{tt}v - w_{xx}v \\ &= \text{div } Q + v(\partial_{tt} - \partial_{xx})w \end{aligned} \tag{2.55}$$

where $Q = (wv_t - w_t v,\ w_x v - wv_x)$. By the definition (2.48), the adjoint operator is given by

$$\mathscr{L}^*[u] = \partial_{tt} - \partial_{xx}. \tag{2.56}$$

This shows that the linear operator of wave equation (2.52) is self-adjoint.

Definition 2.2.8 can be generalized for a system of N partial differential equations with m dependent and n independent variables. The linearizing operator $\mathscr{L}[\mathbf{U}]$ associated with the PDE system (2.33) is given by the formula

$$\mathscr{L}^{\sigma}_{\mu}[\mathbf{U}]\mathbf{V} = \Big[\frac{\partial R^{\sigma}[\mathbf{U}]}{\partial U^{\mu}} + \frac{\partial R^{\sigma}[\mathbf{U}]}{\partial U^{\mu}_{i}} D_i + \cdots + \frac{\partial R^{\sigma}[\mathbf{U}]}{\partial U^{\mu}_{i_1 \ldots i_k}} D_{i_1} \ldots D_{i_k}\Big] V^{\mu} \tag{2.57}$$

in terms of arbitrary function $\mathbf{V}(\boldsymbol{x}) = (V^1(\boldsymbol{x}), \cdots, V^m(\boldsymbol{x}))$, where $\sigma = 1, ..., N,\ \mu = 1, ..., m$. The operator (2.57) is basically a $\sigma \times \mu$ matrix. The adjoint operator $\mathscr{L}^*[\mathbf{U}]$ associated with the PDE system (2.33) is obtained formally through integration by parts [28] and is given by

$$\mathscr{L}^{*\sigma}_{\mu}[\mathbf{U}]\mathbf{W} = \frac{\partial R^{\sigma}[\mathbf{U}]}{\partial U^{\mu}} W_{\sigma} - D_i\left(\frac{\partial R^{\sigma}[\mathbf{U}]}{\partial U^{\mu}_{i}} W_{\sigma}\right) + \cdots + (-1)^k D_{i_1} \ldots D_{i_k}\left(\frac{\partial R^{\sigma}[\mathbf{U}]}{\partial U^{\mu}_{i_1 \ldots i_k}} W_{\sigma}\right) \tag{2.58}$$

in terms of an arbitrary function $\mathbf{W}(\boldsymbol{x}) = (W_1(\boldsymbol{x}), ..., W_N(\boldsymbol{x}))$.

Theorem 2.2.10. *Let $\mathbf{R}[\mathbf{u}]$ be a system of partial differential equations. Then equations of $\mathbf{R}$ arise as Euler-Lagrange equations for some variational problem $J = \int L\ d\boldsymbol{x}$, i.e., $\mathbf{R} = E(L)$, if and only if the linearizing operator of $\mathbf{R}$ is self-adjoint. In this case, a Lagrangian for $\mathbf{R}$ can be explicitly constructed using the homotopy formula*

$$L[\mathbf{u}] = \int_0^1 \mathbf{u} \cdot \mathbf{R}[\lambda \mathbf{u}]\ d\lambda. \tag{2.59}$$

Proof. See [55].

Example 2.2.3. Recall the one-dimensional wave equation:

$$R[u] \equiv u_{tt} - u_{xx} = 0. \tag{2.60}$$

We already know that the linearizing operator of the wave equation is self-adjoint. According to the Theorem 2.2.10, the Lagrangian is given by

$$\begin{aligned} L[u] &= \int_0^1 u(\lambda u_{tt} - \lambda u_{xx})\ d\lambda \\ &= \frac{1}{2}uu_{tt} - \frac{1}{2}uu_{xx}. \end{aligned} \tag{2.61}$$

It seems the Lagrangian (2.61) is not the same as the Lagrangian

$$L_c = \frac{1}{2}u_t^2 - \frac{1}{2}u_x^2, \tag{2.62}$$

which comes from classical mechanics. Actually (2.61) is equivalent to (2.62) since

$$L[u] = \text{div } Q - \frac{1}{2}u_t^2 + \frac{1}{2}u_x^2, \tag{2.63}$$

where $Q = (\frac{1}{2}uu_t,\ \frac{1}{2}uu_x)$. One can now show that the wave equation (2.60) arises from a Lagrangian. Consider the Euler operator

$$E = \frac{\partial}{\partial u} - D_t\frac{\partial}{\partial u_t} - D_x\frac{\partial}{\partial u_x}, \tag{2.64}$$

where $D_t,\ D_x$ are total derivative operators. Applying the Euler operator (2.64) to the Lagrangian $L[u]$ (2.63), we have

$$\left(\frac{\partial}{\partial u} - D_t\frac{\partial}{\partial u_t} - D_x\frac{\partial}{\partial u_x}\right) L[u] = D_t(u_t) - D_x(u_x) = u_{tt} - u_{xx}. \tag{2.65}$$

Definition 2.2.11. A one-parameter Lie group of point transformations

$$(x^i)^* = x^i + \varepsilon\xi^i(\boldsymbol{x}, \mathbf{U}) + O(\varepsilon^2), \quad i = 1, ..., n, \tag{2.66a}$$

$$(U^\mu)^* = U^\mu + \varepsilon\eta^\mu(\boldsymbol{x}, \mathbf{U}) + O(\varepsilon^2), \quad \mu = 1, ..., m \tag{2.66b}$$

with corresponding infinitesimal generator (2.7) is a *variational symmetry* of the given PDE system if and only if it preserves the action integral $J[\mathbf{U}]$, i.e., if and only if

$$\int_{\Omega^*} L[U^*]\ d\boldsymbol{x}^* = \int_\Omega L[U]\ d\boldsymbol{x}, \tag{2.67}$$

where Ω^* is the image of Ω under the point transformation (2.66).

Example 2.2.4. The one-dimensional wave equation is invariant under space translation. The corresponding infinitesimal generator is $Y = \partial_x$, and a point symmetry is given by

$$x^* = x + \varepsilon, \quad t^* = t, \quad u^*(x^*, t^*) = u(x, t). \tag{2.68}$$

The Lagrangian for which action integral of the one-dimensional wave equation to be extremal is given by

$$L[U] = \frac{1}{2}U_t^2 - \frac{1}{2}U_x^2. \tag{2.69}$$

Ω^* is preserved under transformation (2.68), i.e., $\Omega^* = \Omega$. Also $dx^* = dx,\ dt^* = dt$. We see that

$$\begin{aligned}
J[U] &= \int_\Omega L[U]\, dt\, dx \\
&= \int_\Omega \Big[\frac{1}{2}U_t^2 - \frac{1}{2}U_x^2\Big]\, dt\, dx \\
&= \int_{\Omega^*} \Big[\frac{1}{2}\left(U_{t^*}^* \frac{dt^*}{dt}\right)^2 - \frac{1}{2}\left(U_{x^*}^* \frac{dx^*}{dx}\right)^2\Big]\, dt^* dx^* \\
&= \int_{\Omega^*} \Big[\frac{1}{2}U_{t^*}^{*2} - \frac{1}{2}U_{x^*}^{*2}\Big]\, dt^* dx^* \\
&= \int_{\Omega^*} L[U^*]\, dt^* dx^* \\
&= J[U^*].
\end{aligned} \tag{2.70}$$

Hence, the action integral $J[U]$ is invariant under the transformation (2.68) and so (2.62) is a variational symmetry. Similarly, the symmetries given by $Y^1 = \partial_u$ and $Y^2 = -\partial_t$ are also variational symmetries.

For the infinitesimal generator $Y = u\partial_u$, the scaling symmetry is

$$x^* = x, \quad t^* = t, \quad u^*(x^*, t^*) = \alpha u(x, t), \tag{2.71}$$

where α is a scaling factor. Obviously, $\Omega^* = \Omega$ and $dx^* = dx,\ dt^* = dt$. Now, we see that

$$\begin{aligned}
J[U] &= \int_\Omega L[U]\, dt\, dx \\
&= \int_\Omega \Big[\frac{1}{2}U_t^2 - \frac{1}{2}U_x^2\Big]\, dt\, dx \\
&= \int_{\Omega^*} \Big[\frac{1}{2}\left(\alpha U_{t^*}^* \frac{dt^*}{dt}\right)^2 - \frac{1}{2}\left(\alpha U_{x^*}^* \frac{dx^*}{dx}\right)^2\Big]\, dt^* dx^* \\
&= \int_{\Omega^*} \alpha^2\Big[\frac{1}{2}U_{t^*}^{*2} - \frac{1}{2}U_{x^*}^{*2}\Big]\, dt^* dx^* \\
&= \alpha^2 \int_{\Omega^*} L[U^*]\, dt^* dx^* \\
&\neq J[U^*].
\end{aligned} \tag{2.72}$$

Hence, the action integral $J[U]$ is not invariant under the transformation (2.71), and so (2.71) is not a variational symmetry.

Definition 2.2.12. Recall the PDE system $\mathbf{R}\{\boldsymbol{x}; \mathbf{u}\}$ given by (2.33). Then, *multipliers* or *characteristics* of conservation laws $\sum_{i=1}^n D_{x^i}\Phi^i[\mathbf{u}] = 0$ of the PDE system are a set of functions $\{\Lambda_\sigma(\boldsymbol{x}, \mathbf{U}, \partial\mathbf{U}, \cdots, \partial^k\mathbf{U})\}_{\sigma=1}^N$

such that

$$\sum_{\sigma=1}^{N} \Lambda_\sigma[\mathbf{U}] R^\sigma[\mathbf{U}] \equiv \sum_{i=1}^{n} D_{x^i} \Phi^i[\mathbf{U}] \tag{2.73}$$

holds for arbitrary function $\mathbf{U}(\boldsymbol{x})$. Moreover, k is the order of multipliers, and $\sum_{\sigma=1}^{N} \Lambda_\sigma[\mathbf{u}] R^\sigma[\mathbf{u}]$ is called the *characteristic form* of the conservation law.

The multipliers $\Lambda_\sigma[\mathbf{U}]$ have to be non-singular functions for getting conservation laws of the given PDE system. A singular multiplier can produce a divergence expression which might not be a conservation laws [28]. Singularity of $\Lambda_\sigma[\mathbf{U}]$ means it is a singular function when evaluated on solutions $\mathbf{U}(\boldsymbol{x}) = \mathbf{u}(\boldsymbol{x})$ of the given PDE system [28].

Example 2.2.5. Consider the KdV equation

$$R[u] \equiv u_t + u u_x + u_{xxx} = 0, \tag{2.74}$$

where $u = u(x,t)$ and subscript denotes the partial derivatives. One of its conservation laws is given by

$$D_t\left(\frac{u^2}{2}\right) + D_x\left(\frac{u^3}{3} + u u_{xx} - \frac{u_x^2}{2}\right) = 0. \tag{2.75}$$

This can be written in the characteristic form of the conservation law

$$U R[U] \equiv D_t\left(\frac{U^2}{2}\right) + D_x\left(\frac{U^3}{3} + U U_{xx} - \frac{U_x^2}{2}\right), \tag{2.76}$$

where $\Lambda = U(x,t)$ is a multiplier of the conservation law (2.75).

Noether's Theorem for conservation laws (for details see [28, 55]) states that the variational symmetry of a PDE system has a connection with the conservation law of that system. Recall the variational problem in the classical mechanics. Then the following theorem describes Noether's formulation for constructing conservation laws.

Theorem 2.2.13. (Noether's Formulation) *Suppose a given PDE system* $\mathbf{R}\{\boldsymbol{x};\mathbf{u}\}$ (2.33)*, as written, arises from a variational principle, i.e., the given PDE system is a set of Euler-Lagrange equations* (2.45) *whose solutions* $\mathbf{u}(\boldsymbol{x})$ *are extrema* $\mathbf{U}(\boldsymbol{x}) = \mathbf{u}(\boldsymbol{x})$ *of an action integral* $J[\mathbf{U}]$ (2.42) *with Lagrangian* $L[\mathbf{U}]$*. Suppose the one-parameter Lie group of point transformations*

$$(x^i)^* = x^i + \varepsilon \xi^i(\boldsymbol{x},\mathbf{u}) + O(\varepsilon^2), \quad i = 1,...,n, \tag{2.77}$$

$$(U^\mu)^* = U^\mu + \varepsilon \eta^\mu(\boldsymbol{x},\mathbf{U}) + O(\varepsilon^2), \quad \mu = 1,...,m, \tag{2.78}$$

is a point symmetry of $J[\mathbf{U}]$*. Then*
(i) $\tilde{\eta}^\mu[\mathbf{U}] E_{\mathbf{U}^\sigma}(L[\mathbf{U}])$ *produces a divergence expression, i.e.* $\{\tilde{\eta}^\mu[\mathbf{U}]\}_{\mu=1}^m$ *is a set of local multipliers of the Euler-Lagrange system* (2.45)*, where*

$$\tilde{\eta}^\mu[\mathbf{U}] = \eta^\mu(\boldsymbol{x},\mu) - \sum_{i=1}^{n} \mathbf{U}_i^\mu \xi^i(\boldsymbol{x},\mathbf{U}). \tag{2.79}$$

(ii) The local conservation law of the PDE system $\mathbf{R}\{\boldsymbol{x};\mathbf{u}\}$ *holds for any solution* $\mathbf{U}(\boldsymbol{x}) = \mathbf{u}(\boldsymbol{x})$ *of the Euler-Lagrange system* (2.45).

Example 2.2.6. The one-dimensional wave equation admits u-translation symmetry ($Y^1 = \partial_u$) and time-translation symmetry ($Y^2 = -\partial_t$). They are also variational symmetries. Now corresponding to Y^1 ($\xi^x = \xi^t = 0, \eta = 1$),

$$\tilde{\eta} = 1 - u_x\xi^x - u_t\xi^t = 1. \tag{2.80}$$

By the Noether's Theorem the wave equation admits a conservation law multiplier $\Lambda = 1$ yielding a local conservation law

$$D_t(u_t) + D_x(-u_x) = 0. \tag{2.81}$$

Again corresponding to Y^2 ($\xi^x = 0, \xi^t = -1, \eta = 0$),

$$\tilde{\eta} = 0 - u_x\xi^x - u_t\xi^t = u_t. \tag{2.82}$$

By the Noether's Theorem, we have a conservation law multiplier $\Lambda = u_t$ leads to a local conservation law

$$D_t\left(\frac{1}{2}u_t^2 + \frac{1}{2}u_x^2\right) + D_x\big(-u_tu_x\big) = 0. \tag{2.83}$$

The conservation law (2.81) corresponds to linear momentum and (2.83) to energy conservation of the wave equation.

For Noether's Theorem to be directly applicable to a given PDE system, the following must hold.
(i) The linearized system of the given PDE system is self-adjoint
(ii) PDE system has an explicit action functional.
(iii) One has a one-parameter local transformation that leaves the action functional invariant.

Consequently, if the PDE system is not variational, Noether's formulation is not applicable. However, the 'direct construction method' [68, 69] works to any PDE system, whether it is variational or not.

2.2.2 The direct construction method

Consider a PDE system $\mathbf{R}\{\boldsymbol{x};\mathbf{u}\}$ (2.33). Nontrivial local conservation laws arise from linear combinations of the equations of the PDE system (2.33) with multipliers (or characteristics) that yield nontrivial divergence expressions (see, e.g., [28, 68, 69]). To find such expressions, the dependent variables (and their derivatives) that arise in the PDE system (2.33), or appear in the multipliers, are replaced by arbitrary functions $\mathbf{U}$ (and their derivatives). By their construction, such divergence expressions vanish on all solutions of the PDE system (2.33) [28].

In particular, a set of multipliers $\{\Lambda_\sigma[\mathbf{U}]\}_{\sigma=1}^N = \{\Lambda_\sigma(\boldsymbol{x}, \mathbf{U}, \partial\mathbf{U}, ..., \partial^l\mathbf{U})\}_{\sigma=1}^N$ yields a divergence expression for the PDE system $\mathbf{R}\{\boldsymbol{x}; \mathbf{u}\}$ if the identity

$$\sum_{\sigma=1}^{N} \Lambda_\sigma[\mathbf{U}] R^\sigma[\mathbf{U}] \equiv D_{x^i}\Phi^i[\mathbf{U}] \tag{2.84}$$

holds for arbitrary functions $\mathbf{U}(\boldsymbol{x})$. Then on the solutions $\mathbf{U}(\boldsymbol{x}) = \mathbf{u}(\boldsymbol{x})$ of the PDE system (2.33), if $\Lambda_\sigma[\mathbf{U}]$ is non-singular, one has a local conservation law

$$\sum_{\sigma=1}^{N} \Lambda_\sigma[\mathbf{u}] R^\sigma[\mathbf{u}] \equiv D_{x^i}\Phi^i[\mathbf{u}] = 0. \tag{2.85}$$

The direct conservation law construction method requires finding a set of local multipliers.

By direct calculation, one can show that the Euler operators (2.43) annihilate any divergence expression $D_{x^i}\Phi^i[\mathbf{U}]$. In particular, the following identities hold for arbitrary $\mathbf{U}(\boldsymbol{x})$:

$$E_{U^j}(D_{x^i}\Phi^i(\boldsymbol{x}, \mathbf{U}, \partial\mathbf{U}, ..., \partial^r\mathbf{U})) \equiv 0, \quad j = 1, ..., m. \tag{2.86}$$

The converse also holds. Specifically, the only scalar expressions annihilated by Euler operators are divergence expressions. This leads to the following important theorem.

Theorem 2.2.14. *A set of non-singular local multipliers* $\{\Lambda_\sigma(\boldsymbol{x}, \mathbf{U}, \partial\mathbf{U}, ..., \partial^l\mathbf{U})\}_{\sigma=1}^N$ *yields a local conservation law for the PDE system* $\mathbf{R}\{\boldsymbol{x}; \mathbf{u}\}$ (2.33) *if and only if the set of identities*

$$E_{U^j}\Big[\sum_{\sigma=1}^{4} \Lambda_\sigma(\boldsymbol{x}, \mathbf{U}, \partial\mathbf{U}, ..., \partial^l\mathbf{U}) R^\sigma(\boldsymbol{x}, \mathbf{U}, \partial\mathbf{U}, ..., \partial^k\mathbf{U})\Big] \equiv 0, \quad j = 1, ..., m \tag{2.87}$$

holds for an arbitrary function $\mathbf{U}(\boldsymbol{x})$.

The set of equations (2.87) yields a set of linear determining equations to find sets of local conservation law multipliers of the PDE system $\mathbf{R}\{\boldsymbol{x}; \mathbf{u}\}$ by considering multipliers of all orders $l = 1, 2, ...$ Since equations (2.87) hold for arbitrary $\mathbf{U}(\boldsymbol{x})$, it follows that one can treat each U^μ and each of its derivatives $U^\mu_{x^1}$, $U^\mu_{x^1x^2}$, etc. as independent variables along with x^i. Consequently, the linear PDE system (2.87) splits into an overdetermined linear PDE system of determining equations with unknowns Λ_σ. The solutions of these determining equations form the sets of local multipliers $\{\Lambda_\sigma(\boldsymbol{x}, \mathbf{U}, \partial\mathbf{U}, ..., \partial^l\mathbf{U})\}_{\sigma=1}^N$ of the PDE system $\mathbf{R}\{\boldsymbol{x}; \mathbf{u}\}$ (2.33). Each multiplier set then can be used to produce a local conservation law of of the PDE system $\mathbf{R}\{\boldsymbol{x}; \mathbf{u}\}$ [28].

Definition 2.2.15. (Extended Kovalevskaya form) A PDE system $\mathbf{R}\{\boldsymbol{x}; \mathbf{u}\}$ (2.33) is in extended Kovalevskaya form with respect to an independent variable x^j , if the system is in a solved form for the highest derivative of each dependent variable with respect to x^j , i.e.,

$$\frac{\partial^{s_\sigma}}{\partial(x^j)^{s_\sigma}} u^\sigma = G^\sigma(\boldsymbol{x}, \mathbf{u}, \partial\mathbf{u}, ..., \partial^k\mathbf{u}), \quad 1 \le s_\sigma \le k, \quad \sigma = 1, ..., m, \tag{2.88}$$

where all derivatives with respect to x^j appearing in the right-hand sides of (2.88) are of lower order than those appearing on the left-hand side.

Example 2.2.7. As an obvious example of extended Kovalevskaya form, consider the two-dimensional Euler system for the incompressible fluid given by

$$u_x + w_z = 0, \tag{2.89a}$$

$$u_t + uu_x + wu_z + p_x = 0, \tag{2.89b}$$

$$w_t + uw_x + ww_z + p_z = 0, \tag{2.89c}$$

where (u, w) is the fluid velocity, p is the fluid pressure. The PDE system (2.89) can be written in *extended Kovalevskaya* form with respect to leading x-derivatives:

$$u_x = -w_z, \tag{2.90a}$$

$$p_x = -(u_t - uw_z + wu_z), \tag{2.90b}$$

$$w_x = -\frac{1}{u}(w_t + ww_z + p_z). \tag{2.90c}$$

Note that an extended Kovalevskaya form (2.88) is a special case of a solved form PDE system with respect to the same leading derivatives for all dependent variables. Consequently, a PDE system can admit an extended Kovalevskaya form only if its number of dependent variables equals the number of PDEs in the system [28]. For example, a PDE system that does not admit the extended Kovalevskaya form are Maxwell's equations

$$\mathbf{E}_t - \nabla \times \mathbf{B} = 0, \tag{2.91a}$$

$$\mathbf{B}_t + \nabla \times \mathbf{E} = 0, \tag{2.91b}$$

$$\nabla \cdot \mathbf{E} = 0, \tag{2.91c}$$

$$\nabla \cdot \mathbf{B} = 0, \tag{2.91d}$$

where $\mathbf{E} = (E^1(\mathbf{x}, t),\ E^2(\mathbf{x}, t),\ E^3(\mathbf{x}, t))$, $\mathbf{B} = (B^1(\mathbf{x}, t),\ B^2(\mathbf{x}, t),\ B^3(\mathbf{x}, t))$ are the time-dependent electric and magnetic fields respectively. There are eight PDEs and only six dependent variables in the system (2.91).

A PDE system may not be written in Kovalevskaya form in the current coordinates, but it can be after a point or contact transformation of the PDE system (see, e.g., [28]).

For a PDE system $\mathbf{R}\{\boldsymbol{x}; \mathbf{u}\}$ (2.33) that has an Kovalevskaya PDE form, there is a particularly effective formulation of the direct method to find all local conservation laws as seen in the following Theorem:

Theorem 2.2.16. *Suppose a PDE system admits an extended Kovalevskaya form* (2.88)*. Then all of its nontrivial (up to equivalence) local conservation laws arise from multipliers. Moreover, there is a one-to-one correspondence between equivalence classes of conservation laws and sets of conservation law multipliers with no dependence on derivatives of u^σ with respect to $(x^j)^{s_\sigma}$.*

The proof of this theorem can be found in [49].

2.3 Symmetries of 2D Euler System

As an concrete example we reproduce the Lie point symmetries and conservation laws of two -dimensional Euler system and its vorticity system. Recall the two-dimensional Euler equations for incompressible flow:

$$R^1[u,w] \equiv u_x + w_z = 0, \tag{2.92}$$

$$R^2[u,w,p] \equiv u_t + uu_x + wu_z + p_x = 0, \tag{2.93}$$

$$R^3[u,w,p] \equiv w_t + uw_x + ww_z + p_z = 0, \tag{2.94}$$

with the fluid density $\rho = 1$ without loss of generality.

Consider the infinitesimal generator

$$Y = \xi^{(t)}\frac{\partial}{\partial t} + \xi^{(x)}\frac{\partial}{\partial x} + \xi^{(z)}\frac{\partial}{\partial z} + \eta^{(u)}\frac{\partial}{\partial u} + \eta^{(w)}\frac{\partial}{\partial w} + \eta^{(p)}\frac{\partial}{\partial p}, \tag{2.95}$$

where all the infinitesimals are acting on (x,z,t,u,w,p)–space and are functions of $x,\ z,\ t,\ u,\ w$, and p. Then the determining equations are given by

$$Y^{(1)}R^\sigma(x,z,t,u,w,p) = 0 \quad \text{when } R^\sigma = 0,\ \sigma = 1,2,3. \tag{2.96}$$

where $Y^{(1)}$ is the first prolongation of (2.95) acting on $(x,z,t,u,w,p,\partial u,\partial w,\partial p)$–space and is given by

$$\begin{aligned} Y^{(1)} = Y &+ \eta_t^{1(u)}\frac{\partial}{\partial u_t} + \eta_x^{1(u)}\frac{\partial}{\partial u_x} + \eta_y^{1(u)}\frac{\partial}{\partial u_y} + \eta_t^{1(w)}\frac{\partial}{\partial w_t} + \eta_x^{1(w)}\frac{\partial}{\partial w_x} + \eta_y^{1(w)}\frac{\partial}{\partial w_y} + \\ &\eta_t^{1(p)}\frac{\partial}{\partial p_t} + \eta_x^{1(p)}\frac{\partial}{\partial p_x} + \eta_y^{1(p)}\frac{\partial}{\partial p_y}, \end{aligned} \tag{2.97}$$

in terms of all the extended infinitesimals given by (2.13). Applying (2.97) to the determining equation (2.96) and splitting we get an overdetermined PDE system:

$$\xi_{tt}^{(t)} = 0, \quad \eta_{wt}^{(u)} = 0, \quad \eta_{pt}^{(p)} = 0, \quad \eta_{ww}^{(u)} = 0, \quad \eta_{pp}^{(p)} = 0, \quad \xi_x^{(x)} = \frac{1}{2}\eta_p^{(p)} + \xi_t^{(t)}, \tag{2.98a}$$

$$\xi_x^{(y)} = -\eta_w^{(u)}, \quad \eta_x^{(p)} = -\eta_t^{(u)}, \quad \eta_x^{(u)} = 0, \quad \eta_x^{(w)} = 0, \quad \xi_y^{(t)} = 0, \quad \xi_y^{(x)} = \eta_w^{(u)}, \tag{2.98b}$$

$$\xi_y^{(y)} = \frac{1}{2}\eta_p^{(p)} + \xi_t^{(t)}, \quad \eta_y^{(p)} = -\eta_t^{(w)}, \quad \eta_y^{(w)} = 0, \quad \xi_t^{(x)} = \eta^{(u)} - w\eta_w^{(u)} - \frac{1}{2}u\eta_p^{(p)}, \tag{2.98c}$$

$$\xi_t^{(y)} = \eta^{(w)} + u\eta_w^{(u)} - \frac{1}{2}w\eta_p^{(p)}, \quad \xi_u^{(t)} = 0, \quad \xi_u^{(y)} = 0, \quad \eta_u^{(p)} = 0, \quad \eta_u^{(u)} = \frac{1}{2}\eta_p^{(p)}, \tag{2.98d}$$

$$\eta_u^{(w)} = -\eta_w^{(u)}, \quad \xi_w^{(t)} = 0, \quad \xi_w^{(x)} = 0, \quad \xi_w^{(y)} = 0, \quad \eta_w^{(p)} = 0, \quad \eta_w^{(w)} = \frac{1}{2}\eta_p^{(p)}, \tag{2.98e}$$

$$\xi_p^{(x)} = 0, \quad \xi_p^{(y)} = 0, \quad \eta_p^{(u)} = 0, \quad \eta_p^{(w)} = 0, \quad \xi_x^{(t)} = 0, \quad \eta_y^{(u)} = 0, \quad \xi_u^{(x)} = 0, \tag{2.98f}$$

$$\xi_p^{(t)} = 0. \tag{2.98g}$$

Solving this system of PDEs from the determining equations is tedious. To avoid this tedious calculation by hand, we find and solve these determining equations by using a Maple based software **GeM** [4]. The general solution of the determining equations is found as

$$\xi^{(x)} = C_3x - C_1z + F_2(t) + C_5, \quad \xi^{(z)} = C_1x + C_3z + F_1(t) + C_4, \tag{2.99a}$$

$$\xi^{(t)} = (C_3 - C_2)t + C_6, \qquad \eta^{(u)} = C_2u - C_1w + F_2^{'}(t), \tag{2.99b}$$

$$\eta^{(w)} = C_1u + C_2w + F_1^{'}(t), \quad \eta^{(p)} = 2C_2p - F_2^{''}(t)x - F_1^{''}(t)z + F_3(t), \tag{2.99c}$$

where $C_1,\ C_2,\ C_3,\ C_4,\ C_5,\ C_6$ are constants and $F_1,\ F_2,\ F_3$ are arbitrary functions. Each set of linearly independent solutions in (2.99) can be used in equation (2.96) to yield an infinitesimal generator. Corresponding to these constants and arbitrary functions, we have following symmetry generators:

$$Y_1 = \frac{\partial}{\partial x}, \qquad Y_2 = \frac{\partial}{\partial z}, \qquad Y_3 = \frac{\partial}{\partial t}, \qquad Y_4 = x\frac{\partial}{\partial x} + z\frac{\partial}{\partial z} + t\frac{\partial}{\partial t}, \tag{2.100}$$

$$Y_5 = -z\frac{\partial}{\partial x} + x\frac{\partial}{\partial z} - w\frac{\partial}{\partial u} + u\frac{\partial}{\partial w}, \qquad Y_6 = -t\frac{\partial}{\partial t} + u\frac{\partial}{\partial u} + w\frac{\partial}{\partial w} + 2p\frac{\partial}{\partial p}, \tag{2.101}$$

$$Y_7 = \beta_3(t)\frac{\partial}{\partial p}, \qquad Y_8 = \beta_2(t)\frac{\partial}{\partial x} + \beta_2^{'}(t)\frac{\partial}{\partial u} - x\beta_1^{''}(t)\frac{\partial}{\partial p}, \tag{2.102}$$

$$Y_9 = \beta_1(t)\frac{\partial}{\partial z} + \beta_1^{'}(t)\frac{\partial}{\partial w} - z\beta_1^{''}(t)\frac{\partial}{\partial p}. \tag{2.103}$$

Thus the incompressible 2D Euler equations are invariant under spatial translations (Y_1, Y_2), time-translation (Y_3), and scaling/dilations (Y_4, Y_6). The symmetry Y_5 describes the rotation and Y_7 is the pressure change. The other two symmetries Y_8 and Y_9 give the one-parameter groups of the moving coordinates [55].

2.4 Conservation Laws of 2D Euler System

We apply the direct construction method to the Euler equations (2.92)–(2.94) for finding local conservation laws of the form

$$\frac{\partial \Psi}{\partial t} + \frac{\partial \Phi^1}{\partial x} + \frac{\partial \Phi^2}{\partial z} = 0. \tag{2.104}$$

Consider a set of zeroth order multipliers

$$\Lambda_1 = \Lambda_1(x, z, t, u, w, p), \quad \Lambda_2 = \Lambda_2(x, z, t, u, w, p), \quad \Lambda_3 = \Lambda_3(x, z, t, u, w, p). \tag{2.105}$$

corresponding to the Euler Equations (2.92)–(2.94) respectively. According to the Theorem 2.2.14, the conservation law determining equations are given by

$$E_u\Big(\Lambda_1(x,z,t,u,w,p)(u_x+w_z)+\Lambda_2(x,z,t,u,w,p)(u_t+uu_x+wu_z+p_x)+ \\ \Lambda_3(x,z,t,u,w,p)(w_t+uw_x+ww_z+p_z)\Big)=0, \tag{2.106a}$$

$$E_w\Big(\Lambda_1(x,z,t,u,w,p)(u_x+w_z)+\Lambda_2(x,z,t,u,w,p)(u_t+uu_x+wu_z+p_x)+ \\ \Lambda_3(x,z,t,u,w,p)(w_t+uw_x+ww_z+p_z)\Big)=0, \tag{2.106b}$$

$$E_p\Big(\Lambda_1(x,z,t,u,w,p)(u_x+w_z)+\Lambda_2(x,z,t,u,w,p)(u_t+uu_x+wu_z+p_x)+ \\ \Lambda_3(x,z,t,u,w,p)(w_t+uw_x+ww_z+p_z)\Big)=0, \tag{2.106c}$$

where $E_u,\ E_w,\ E_p$ are the Euler operators (2.43) corresponding to the dependent variables $u,\ w,\ p$. Splitting these determining equations (2.106a)–(2.106c) and equating the coefficients of similar terms to zero, one gets a linear system of partial differential equations with unknowns $\Lambda_1,\ \Lambda_2,\ \Lambda_3$:

$$\Lambda_{1xx}=0,\quad \Lambda_{1xz}=0,\quad \Lambda_{1zz}=0,\quad \Lambda_{1pp}=0,\quad \Lambda_{1px}=0,\quad \Lambda_{1pz}=0, \tag{2.107a}$$

$$\Lambda_{1pt}=0,\quad \Lambda_{2x}=0,\quad \Lambda_{2zz}=0,\quad \Lambda_{2p}=0,\quad \Lambda_{2w}=0,\quad \Lambda_{2t}+w\Lambda_{2z}=-\Lambda_{1x}, \tag{2.107b}$$

$$\Lambda_{2u}=\Lambda_{1p},\quad \Lambda_2=\Lambda_{1u},\quad \Lambda_{3z}=0,\quad \Lambda_{3p}=0,\quad \Lambda_{3u}=0,\quad \Lambda_{3t}+\Lambda_{1z}=u\Lambda_{2z}, \tag{2.107c}$$

$$\Lambda_{3x}=-\Lambda_{2z},\quad \Lambda_3=\Lambda_{1w},\quad \Lambda_{3w}=\Lambda_{1p}, \tag{2.107d}$$

where subscripts denote partial derivatives with respect to those variables. The general solution of this linear system is

$$\Lambda_1=(xw-zu)C_1+\frac{1}{2}(u^2+w^2+2p)C_2+wF_1(t)-zF_{1t}+uF_2(t)-xF_{2t}+F_3(t), \tag{2.108}$$

$$\Lambda_2=-zC_1+uC_2+F_2(t),\quad \Lambda_3=xC_1+wC_2+F_1(t), \tag{2.109}$$

where $C_1,\ C_2$ are arbitrary constants. Corresponding to each constant $C_1,\ C_2$ or to each arbitrary function $F_1(t),\ F_2(t),\ F_3(t)$, there is a set of nontrivial local multipliers of the Euler equations (2.92)–(2.94).

Proposition 2.4.1. *The Euler equations* (2.92)–(2.94) *admit five sets of nontrivial local multipliers of order zero given by*

$$\{\Lambda_1,\Lambda_2,\Lambda_3\}=\{xw-zu,\ -z,\ x\},\quad \{\Lambda_1,\Lambda_2,\Lambda_3\}=\{\frac{1}{2}(u^2+w^2+2p),\ u,\ w\}, \tag{2.110a}$$

$$\{\Lambda_1,\Lambda_2,\Lambda_3\}=\{u\beta(t)-x\beta'(t),\ \beta(t),\ 0\},\quad \{\Lambda_1,\Lambda_2,\Lambda_3\}=\{w\alpha(t)-z\alpha'(t),\ 0,\ \alpha(t)\}, \tag{2.110b}$$

$$\{\Lambda_1,\Lambda_2,\Lambda_3\}=\{\tau(t),\ 0,\ 0\}. \tag{2.110c}$$

Multiplying each set of multipliers obtained in proposition 2.4.1 with the respective equations (2.92)–(2.94), one finds a local conservation law. These yield the following results.

Proposition 2.4.2. *For the multipliers of the form* $\{\Lambda_\sigma(x,z,t,u,w,p)\}_{\sigma=1}^3$ *found in Proposition 2.4.1, the incompressible Euler system* (2.92)–(2.94) *has the following linearly independent local conservation laws*

$$D_t(xw-zu)+D_x(xuw-zu^2-zp)+D_z(-zuw+xw^2+xp)=0, \tag{2.111a}$$

$$D_t\big(\frac{1}{2}(u^2+w^2)\big)+D_x\big(\frac{1}{2}u^3+\frac{1}{2}uw^2+up\big)+D_z\big(\frac{1}{2}w^3+\frac{1}{2}u^2w+wp\big)=0, \tag{2.111b}$$

$$D_t(\beta u)+D_x(\beta u^2-x\beta' u+\beta p)+D_z(\beta uw-x\beta' w)=0, \tag{2.111c}$$

$$D_t(\alpha w)+D_x(\alpha uw-z\alpha' u)+D_z(\alpha w^2-z\alpha' w+\alpha p)=0, \tag{2.111d}$$

$$D_x(\tau u)+D_z(\tau w)=0, \tag{2.111e}$$

where $\alpha=\alpha(t),\ \beta=\beta(t),\ \tau=\tau(t)$, *and prime* $(')$ *stands for the derivative with respect to* t.

The conserved quantities in (2.111a)–(2.111b) produce two conservation laws of the Euler equations (3.3)–(3.4) given by

$$\mathcal{L}=\int_\Omega \mathbf{x}\times\mathbf{u}\ d\mathbf{x}\quad\text{(Angular momentum)}, \tag{2.112}$$

$$\mathcal{E}=\int_\Omega \frac{1}{2}\ |\mathbf{u}|^2\ d\mathbf{x}\quad\text{(Kinetic Energy)}, \tag{2.113}$$

and each conserved quantity in (2.111c) and (2.111d) is a component of generalized momentum

$$\mathcal{P}_u=\int_\Omega \beta u\ d\mathbf{x}\quad\text{(First component)}, \tag{2.114}$$

$$\mathcal{P}_w=\int_\Omega \alpha w\ d\mathbf{x}\quad\text{(Second component)}, \tag{2.115}$$

where $\mathbf{u}=(u,w),\ \mathbf{x}=(x,z)$. These conserved quantities for Euler equations match the known results in [52] as well as conserved quantities we discussed in Section 1.2.1. The formula (2.111e) is the incompressibility condition for 2D Euler system.

2.5 Conservation Laws of the Vorticity System

Let us redefine the velocity field, in 2D, to $\mathbf{u}=(u,w,0)$ and the vorticity field be $\boldsymbol{\omega}=(0,0,\omega)$, where $u=u(x,z,t)$, $w=w(x,z,t)$ and $\omega=\omega(x,z,t)$. We recall the vorticity formulation of the 2D Euler system for incompressible fluid in the component form:

$$u_x+w_z=0, \tag{2.116a}$$

$$\omega=w_x-u_z, \tag{2.116b}$$

$$\omega_t+u\omega_x+w\omega_z=0. \tag{2.116c}$$

The conservation laws for the vorticity system of Navier-Stokes equations as well as Euler equations can be seen in [53]. We reproduce the conservation laws multipliers of the vorticity system by applying direct method resulting the following propositions.

Proposition 2.5.1. *All possible sets of zeroth order conservation law multipliers of the vorticity system* (2.116) *are given by*

$$\{\Lambda_1, \Lambda_2, \Lambda_3\} = \Big\{\frac{1}{2}(x^2+z^2)\omega - xw + zu,\ xu + zw,\ \frac{1}{2}(x^2+z^2)\Big\}, \tag{2.117a}$$

$$\{\Lambda_1, \Lambda_2, \Lambda_3\} = \{g_1(t)x\omega - wg_1(t) + yg_2',\ ug_2(t) + xg',\ xg_2(t)\}, \tag{2.117b}$$

$$\{\Lambda_1, \Lambda_2, \Lambda_3\} = \{g_2(t)z\omega + ug_1(t) - xg_1',\ wg_1(t) + zg_1',\ zg_1(t)\}, \tag{2.117c}$$

$$\{\Lambda_1, \Lambda_2, \Lambda_3\} = \{g_3(t)\omega,\ g_3',\ g_3(t)\}, \tag{2.117d}$$

$$\{\Lambda_1, \Lambda_2, \Lambda_3\} = \Big\{g(\omega),\ 0,\ \frac{dg}{d\omega}\Big\}, \tag{2.117e}$$

$$\{\Lambda_1, \Lambda_2, \Lambda_3\} = \{g_4(t),\ 0,\ 0\}. \tag{2.117f}$$

Using each multiplier set obtained in the proposition 2.5.1 and the vorticity system (2.116a)–(2.116c), one finds one conservation law of the vorticity system. Direct computation yields the following results.

Proposition 2.5.2. *Consider the multipliers set of the form* $\{\Lambda_\sigma(x,z,t,u,w,\omega,p)\}_{\sigma=1}^3$ *in Proposition 2.5.1. By the direct construction method, the vorticity system* (2.116c) *has the following linearly independent local conservation laws*

$$D_t\Big(\frac{1}{2}(x^2+z^2)\omega\Big) + D_x\Big(\frac{1}{2}(x^2+z^2)u\omega + \frac{1}{2}(u^2-w^2)z - xuw\Big) + D_z\Big(\frac{1}{2}(x^2+z^2)w\omega + \frac{1}{2}(u^2-w^2)x + zuw\Big) = 0, \tag{2.118a}$$

$$D_t(g_1x\omega) + D_x\Big(g_1xu\omega - g_1uw + g_1'zu - g_1'xw\Big) + D_z\Big(g_1xw\omega - \frac{1}{2}g_1(u^2-w^2) + g_1'(xu+zw)\Big) = 0, \tag{2.118b}$$

$$D_t(g_2z\omega) + D_x\Big(g_2zu\omega + \frac{1}{2}g_2(u^2-w^2) - g_2'(xu+zw)\Big) + D_z\Big(g_2zw\omega + g_2uw + g_2'zu - g_2'xw\Big) = 0, \tag{2.118c}$$

$$D_t(g_3\omega) + D_x(g_3u\omega - g_3'w) + D_z(g_3w\omega + g_3'u) = 0, \tag{2.118d}$$

$$D_t(g(\omega)) + D_x(ug(\omega)) + D_z(wg(\omega)) = 0, \tag{2.118e}$$

$$D_x(g_4u) + D_z(g_4w) = 0. \tag{2.118f}$$

In the two spatial dimension, the moment of inertia is given by the conservation law (2.118a)

$$\int_{\mathbb{R}^2} \frac{1}{2}|\mathbf{x}|^2\omega\, d\mathbf{x}, \tag{2.119}$$

where $\mathbf{x} = (x, z)$. If $g_1(t),\ g_2(t)$ are constant functions, the equations (2.118b), and (2.118c) represent the first two moments [24, 53]

$$\int_{\mathbb{R}^2} x\omega \, d\mathbf{x}, \quad \text{and} \quad \int_{\mathbb{R}^2} z\omega \, d\mathbf{x}. \tag{2.120}$$

The formula (2.118d), when $g_3(t)$ is constant, gives the $z-$component of the vorticity vector [24, 53]

$$\int_{\mathbb{R}^2} \omega \, d\mathbf{x}. \tag{2.121}$$

The conserved quantity $g(\omega)$ given by (2.118e), in general, is known as Casimirs [31]. The equation (2.118f) again is the incompressibility condition. For the non-constant functions $g_1(t),\ g_2(t),\ g_3(t)$, the conservation laws are not known in the literature [53].

Chapter 3

Fluid Dynamics and Related Models

Internal gravity waves are the waves that travel within the interior of a fluid. Such waves usually arise in a two or multiple layer fluids and owe their existence to the stratified density structure of the fluids [36], with a very small density change producing different wave phenomena. Internal wave is an important phenomenon for the fluid motion. For example, these waves are an essential feature of geophysical fluid dynamics, as stratification is an inherent component of near equilibrium states of ocean and atmosphere. The internal waves most often observed are the *solitary waves* or *solitons* which are the nonlinear, nonsinusoidal travelling waves that preserve their identities (shapes, speeds, orientations) after a pairwise collision. They can propagate over several hundred kilometres and may transport mass and momentum. These waves have a rich application in physics and engineering. For example, they have prominent features in optical fibres.

A vast amount of studies on the two-fluid flow has been performed (e.g., [12, 23, 36, 42, 44, 45, 63, 66, 67, 73, 75, 76, 86]) starting from 1950s. Although Russel [48] observed the solitary wave first in the shallow water in 1834, it was Keulegan [23] who initiated such wave in the two-layer fluids; and Robert R. Long who observed such kind of wave in a two-fluid system in the course of experiment in [66, 67] where Long found the wave is of elevation if the ratio of undisturbed depth of upper fluid to the total depth is less than $\frac{1}{2}$ and of depression if that is greater than $\frac{1}{2}$. Both Keulegan and Long considered the fixed upper boundaries. The similar problem has been carried out with free upper boundaries by Peters and Stoker in [10] where the fluid density decreases exponentially with fluid height. They investigate solitary wave solution and also recognised that their theory would yield a periodic solution. Shen [44, 45] then extended the methods of Peters and Stoker to deal with compressible heavy fluids. A nonlinear model for internal waves was first conducted by Miyata [50], and later by Choi and Camassa [85, 86] rigorously.

3.1 The Choi-Camassa Two-Fluid Model

Choi and Camassa [85] derived the general evolution equations for two-dimensional weakly nonlinear waves at the free surface in the two-fluid system of arbitrary depth. Later on in [86], they derive a new fully nonlinear two-fluid model by approximating the original 2D Euler equations. The model describes the evolution of the internal waves at the interface of two non-mixing incompressible inviscid fluids in a closed channel as

shown in Figure 3.1. Mathematically this is an interesting model having solitary wave solutions with a bidirectional wave propagation for both shallow and deep water configurations. For a small ratio of wave amplitude and wave length, it leads to the Korteweg-de Vries (KdV) equation. The Choi-Camassa model for internal waves has been shown to agree better with experimental data [12] and numerical solutions of Euler equations compared to shallow water models (e.g., KdV model). When a depth ratio is close to the critical ratio

$$h_1/h_2 = (\rho_1/\rho_2)^{1/2}, \tag{3.1}$$

the approximation is given by the modified Korteweg-de Vries equation with a cubic nonlinear term, and if the depth of the lower fluid is much larger than that of upper fluid, this model leads to the Intermediate Long Wave equation ([47] and ref. therin). For deep water configuration, the nonlinear model posses solitary wave solution which undergo a collision with overtaking the slower wave or with moving head-on. In the collision they have a nonlinear interaction producing a phase shift of the solitary waves. All the features of this solitary wave solution in all cases are consistent with that of the numerical solution of Euler equations.

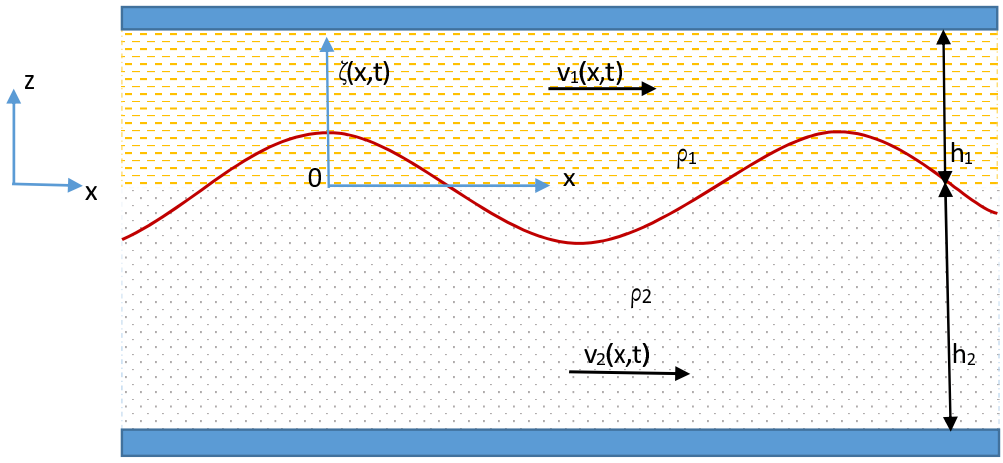

Figure 3.1: Choi-Camassa model for a two-layers fluid system

Mathematically the Choi-Camassa model is given by four nonlinear partial differential equations. The derivation of the Choi-Camassa model equations is briefly outlined here. Consider the original Euler system for inviscid and incompressible fluid with constant fluid density ρ:

$$u_{ix} + w_{iz} = 0, \tag{3.2}$$

$$u_{it} + u_i u_{ix} + w_i u_{iz} = -\frac{p_{ix}}{\rho_i}, \tag{3.3}$$

$$w_{it} + u_i w_{ix} + w_i w_{iz} = -\frac{p_{iz}}{\rho_i} - g, \tag{3.4}$$

where g is the gravitational acceleration, (x, z) are the spatial variables and t is time, and where the scalar valued function $p_i(x, z, t)$ is the fluid pressure, (u_i, w_i) are the fluid velocity components in Cartesian coordinates. Here $u_i = u_i(x, z, t)$ and $w_i = w_i(x, z, t)$. The index $i = 1$ $(i = 2)$ stands for the upper (lower) fluid (see Figure 3.1) and $\rho_1 < \rho_2$ is assumed for a stable stratification.

At the upper and lower rigid surfaces, the kinematic boundary conditions are given by

$$w_1(x, h_1, t) = 0, \quad w_2(x, -h_2, t) = 0, \tag{3.5}$$

where $h_1(h_2)$ is the undisturbed thickness of upper (lower) fluid layer. The boundary conditions at the interface of the two fluids are the continuity of normal velocity and pressure:

$$\zeta_t + u_1\zeta_x = w_1, \quad \zeta_t + u_2\zeta_x = w_2, \quad p_1 = p_2 \tag{3.6}$$

at $z = \zeta(x, t)$. To derive the two-fluid model equations, an assumption is made by the authors [86] that the fluid depth is much smaller that the characteristic wavelength:

$$\frac{h_i}{L} = \epsilon \ll 1, \tag{3.7}$$

where L is the typical wavelength. Then, the continuity equation yields

$$\frac{w_i}{u_i} = O(h_i/L) = O(\epsilon) \ll 1. \tag{3.8}$$

For finite amplitude waves, the authors [86] assumed that

$$\frac{w_i}{U_0} = O(\zeta/h_i) = O(1),$$

where U_0 is the characteristic speed given by $U_0 = (gh_1)^{1/2}$. The pressure at the interface of the two fluids is asymptotically given by the formula

$$P(x, t) = (z - \zeta) + p_1^{(0)}, \tag{3.9}$$

with the leading pressure term $p_1^{(0)}$. The horizontal velocities v_1 and v_2 of upper and lower fluids, averaged over vertical coordinate (z), are defined as

$$v_1(x, t) = \frac{1}{h_1 - \zeta} \int_{\zeta}^{h_1} u_1(x, z, t)\, dz, \tag{3.10}$$

$$v_2(x, t) = \frac{1}{h_2 + \zeta} \int_{-h_2}^{\zeta} u_2(x, z, t)\, dz, \tag{3.11}$$

where the quantity ζ is a displacement at the interface of the fluids, $u_1(u_2)$ is the horizontal component of the upper (lower) fluid for the Euler system.

Then, integrating the original Euler system (3.3)–(3.4) across the upper and lower fluids and imposing the boundary conditions (3.5)–(3.6), and using the mean velocities (3.10)–(3.11), a nonlinear model for the two incompressible fluids of different densities $\rho_1,\ \rho_2$ has been derived in [86]. The model is formulated as

$$F^1[\zeta, v_1, v_2] \equiv \zeta_t - (h_1 - \zeta)v_{1x} + v_1\zeta_x = 0, \tag{3.12}$$

$$F^2[\zeta, v_1, v_2] \equiv \zeta_t + (h_2 + \zeta)v_{2x} + v_2\zeta_x = 0, \tag{3.13}$$

$$F^3[\zeta, v_1, v_2, P] \equiv v_{1t} + v_1v_{1x} + g\zeta_x + (h_1 - \zeta)G_1\zeta_x - \frac{1}{3}(h_1 - \zeta)^2G_{1x} = -\frac{P_x}{\rho_1}, \tag{3.14}$$

$$F^4[\zeta, v_1, v_2, P] \equiv v_{2t} + v_2v_{2x} + g\zeta_x - (h_2 + \zeta)G_2\zeta_x - \frac{1}{3}(h_2 + \zeta)^2G_{2x} = -\frac{P_x}{\rho_2} \tag{3.15}$$

with

$$G_1 = v_{1tx} + v_1v_{1xx} - (v_{1x})^2 = \frac{D_1^2\zeta}{h_1 - \zeta}, \tag{3.16}$$

$$G_2 = v_{2tx} + v_2v_{2xx} - (v_{2x})^2 = -\frac{D_2^2\zeta}{h_2 + \zeta}, \tag{3.17}$$

where dependent variables $\zeta,\ v_1,\ v_2,\ P$ depend on spacial variable x and time variable t, and where $\rho_1 \neq \rho_2$, P is the fluid pressure at interface. Note that the differential operators D_i are given by

$$D_i = \partial_t + u_i^0\partial_x. \tag{3.18}$$

The first two equations (3.12)–(3.13) come from continuity equation (3.2) while the last two equations (3.14)–(3.15) have been derived by approximating Euler equations (3.3)–(3.4).

A travelling wave solution at the interface has an initial condition

$$\zeta(x, 0) = \zeta_0(x) \tag{3.19}$$

and boundary conditions

$$\lim_{x\to\pm\infty} \zeta(x, t) = 0 \tag{3.20}$$

for the solitary waves. Eliminating ζ_t from (3.12)–(3.13), one gets

$$\big((h_1 - \zeta)v_1\big)_x + \big((h_2 + \zeta)v_2\big)_x = 0. \tag{3.21}$$

Now imposing the zero boundary conditions at infinity, i.e.,

$$\lim_{x\to\pm\infty} v_i(x, t) = 0, \quad i = 1, 2 \tag{3.22}$$

one can express v_2 in terms of v_1 as

$$v_2 = -\frac{h_1 - \zeta}{h_2 + \zeta}v_1. \tag{3.23}$$

If the upper fluid layer is neglected and P is regarded as the external pressure applied to the free surface, (3.13) and (3.15) are the complete set of evolution equations for a homogeneous layer, originally derived by

Green & Naghdi [2]. Therefore (3.12)–(3.15) can be regarded as the coupled Green-Naghdi (GN) equations for one-dimensional internal waves in a two-fluid system.

For convenience, we use the notation

$$\eta_1 = h_1 - \zeta, \quad \eta_2 = h_2 + \zeta. \tag{3.24}$$

3.2 Known Results of Choi-Camassa Model

Work in various directions has been done in the literature based on the Choi-Camassa model. Some extensive works are reviewed below.

(1) **A Regularized model**

A local stability analysis for the solitary waves has been conducted in [79]. The analysis shows that the solitary waves suffer from the Kelvin-Helmhotz instability due to a tangential velocity discontinuity across the interface. This jump discontinuity [79] is given, from (3.12)–(3.13), by

$$\Delta v \equiv v_1 - v_2 = -\frac{c(h_1 + h_2)\zeta}{(h_1 - \zeta)(h_2 + \zeta)}, \tag{3.25}$$

where c is the travelling-wave speed. The maximum jump is seen at $x = 0$ and $\Delta v \to 0$ as $|x| \to \infty$. The maximum jump is given by

$$\Delta v_{max} \equiv (v_1 - v_2)\Big|_{x=0} = -\frac{c(h_1 + h_2)A}{(h_1 - A)(h_2 + A)} \tag{3.26}$$

with maximum wave amplitude A at $x = 0$.

The Choi-Camassa model may be regularized to eliminate the shear instability due to jump of the velocities at the interface. The regularized model [87] has been derived in terms of the horizontal velocities evaluated at the top and bottom boundaries instead of the depth-averaged velocities. Under the long-wave approximation, the horizontal velocities $u_i(x, z, t)$ of Euler's equations can be expressed (see [21]) as

$$u_i(x, z, t) = u_i^{(0)}(x, t) - \frac{1}{2}(z \pm h_i)^2 u_{ixx}^{(0)} + O(\epsilon^4). \tag{3.27}$$

Therefore, from the definition (3.10)–(3.11) depth-mean horizontal velocities v_i are found as

$$v_i(x, t) = u_i^{(0)}(x, t) - \frac{1}{6}\eta_i^2 u_{ixx}^{(0)} + O(\epsilon^4). \tag{3.28}$$

On the other hand, the horizontal velocities u_i can be evaluated at fixed vertical levels i.e. at fixed $z = \tilde{z}_1,\ z = -\tilde{z}_2$. Let $\tilde{u}_i$ denotes the approximated velocities at the fixed level. Then $\tilde{u}_i$ are given by the formula

$$\tilde{u}_i(x, t) = u_i^{(0)}(x, t) - \frac{1}{2}H_i^2 u_{ixx}^{(0)} + O(\epsilon^4), \tag{3.29}$$

where

$$H_i = h_i - \tilde{z}_i, \quad \tilde{u}_1(x,t) = u_1(x,z,t)|_{z=\tilde{z}_1}, \quad \tilde{u}_2(x,t) = u_2(x,z,t)|_{z=-\tilde{z}_2} \tag{3.30}$$

with $0 \le \tilde{z}_i \le h_i$. Then, the depth-mean velocities v_i are related to $\tilde{u}_i$ by

$$v_i = \tilde{u}_i - \frac{1}{6}\eta_i^2 \tilde{u}_{ixx} + \frac{1}{2}H_i^2 \tilde{u}_{ixx} + O(\epsilon^4). \tag{3.31}$$

Now by substituting (3.31) into the equations (3.12)–(3.15) and neglecting the terms $O(\epsilon^4)$ or higher, a new system of nonlinear evolution equations is derived for $\zeta,\ \tilde{u}_i,\ P$:

$$(\eta_i)_t + \left(\eta_i\big(\tilde{u}_i - \frac{1}{6}\eta_i^2\tilde{u}_{ixx} + \frac{1}{2}H_i^2\tilde{u}_{ixx}\big)\right)_x = 0, \tag{3.32}$$

$$\tilde{u}_{it} + \tilde{u}_i\tilde{u}_{ix} + g\zeta_x - \left(\frac{1}{2}\eta_i^2(\tilde{u}_{ixt} + \tilde{u}_i\tilde{u}_{ixx} - \tilde{u}_{ix}^2)\right)_x + \frac{1}{2}H_i^2(\tilde{u}_{ixt} + \tilde{u}_i\tilde{u}_{ixx})_x = -\frac{P_x}{\rho_i}, \tag{3.33}$$

where it is used $\eta_{it} = -(\eta_i\tilde{u}_i)_x$ to construct the equations (3.33). The authors [87] showed through a local stability analysis that internal solitary waves are locally stable to perturbations of arbitrary wavelengths if the wave amplitudes are smaller than a critical value A_{cr}, where A_{cr} is given by the root of the equation

$$3\rho_1\rho_2(h_1+h_2)^2A^2 = (h_1-A)(h_2+A)[\rho_1(h_2+A) + \rho_2(h_1-A)]. \tag{3.34}$$

The domain of physical parameters (density and depth ratios) for which the internal solitary waves are stable for all possible wave amplitudes are determined by

$$(3-\sqrt{\rho})h^2 - 8\sqrt{\rho}h + 3\rho - \sqrt{\rho} \le 0, \tag{3.35}$$

where ρ and h are the density and depth ratios respectively, defined by $\rho = \rho_2/\rho_1 > 1$ and $h = h_2/h_1$. From (3.35), one can see that the maximum amplitude wave is stable if

$$h^- \le h \le h^+ \quad \text{for } 1 < \rho < 9, \qquad h^- \le h < \infty \quad \text{for } \rho \ge 9, \tag{3.36}$$

where $h^\pm$ are the roots of the quadratic equation for h in (3.35). The authors of [79] have solved the regularized nonlinear two-fluid model to construct solitary wave solutions numerically. These solutions have been compared [87] with the solitary wave solutions of the original Choi-Camassa equations (3.12)–(3.15) and they found both solutions are asymptotically equivalent.

(2) **Non-uniform bottom topography**

In the Choi-Camassa two-fluid model, the equations are obtained considering a uniform rigid boundary. But it is also interesting to look at the uneven bottom boundary which can be seen, for example, in the ocean topography.

With the uneven bottom topography as shown in the Figure 3.2, the Choi-Camasssa model requires to be slightly modified (see in [88, 78]) and are given by

$$\eta_{1t} + (\eta_1 v_1)_x = 0, \tag{3.37}$$

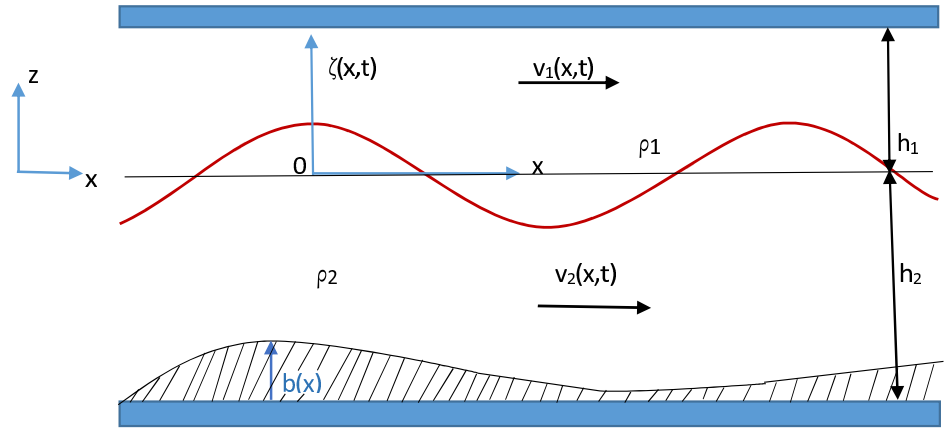

Figure 3.2: Choi-Camassa model with uneven bottom topography

$$\eta_{2t} + (\eta_2 v_2)_x = 0, \tag{3.38}$$

$$v_{1t} + v_1 v_{1x} + g\zeta_x = \frac{P_x}{\rho_1} + \frac{1}{\eta_1}\left(\frac{1}{3}\eta_1^3 G_1\right)_x, \tag{3.39}$$

$$v_{2t} + v_2 v_{2x} + g\zeta_x = \frac{P_x}{\rho_2} + \frac{1}{\eta_2}\left(\frac{1}{3}\eta_2^3 G_2\right)_x + \frac{1}{\eta_2}\left(\frac{1}{2}\eta_2^2 H_2\right)_x + \left(\frac{1}{2}\eta_2^2 G_2 + H_2\right) b'(x), \tag{3.40}$$

where $v_1,\ G_1,\ \eta_1$ remains same as given by (3.10), (3.16) and (3.24) respectively, and where

$$\eta_2 = h_2 + \zeta - b(x), \tag{3.41}$$

$$v_2(x,t) = \frac{1}{\eta_2}\int_{-h_2+b(x)}^{\zeta} u_2(x,z,t)\, dz, \tag{3.42}$$

$$G_2(x,t) = v_{2tx} + v_2 v_{2xx} - (v_{2x})^2, \tag{3.43}$$

$$H_2 = -(\partial_t + v_2\partial_x)(v_2 b'), \tag{3.44}$$

where ∂ denotes partial derivatives. The equations (3.37)–(3.38) are exact while the equations (3.39)–(3.40) have error of order four ($O(\epsilon^4)$). The bottom topography $b(x)$ is assumed to be slowly varying and we recover the original Choi-Camassa model [86] when $b(x) = 0$.

Let us denote the total depth and characteristic velocity respectively by

$$H = h_1 + h_2, \quad \text{and} \quad V = \sqrt{gH}. \tag{3.45}$$

Assuming

$$\frac{\zeta}{H} \ll 1, \quad \frac{v_i}{V} = O\left(\frac{\zeta}{H}\right),\ i = 1, 2, \tag{3.46}$$

the system (3.37)–(3.40) reduce to the weakly nonlinear model in terms of ζ and v_1:

$$\zeta_t - \big((h_1 - \zeta)v_1\big)_x = 0, \tag{3.47}$$

$$v_{1t} + q_1 v_1 v_{1x} + (q_2 + q_3\zeta)\zeta_x = q_4 v_{1txx}, \tag{3.48}$$

where q_i are slowly varying functions defined by

$$q_1 = \frac{\rho_1\tilde{h}_2^2 - \rho_2 h_1\tilde{h}_2 - 2\rho_2 h_1^2}{\tilde{h}_2(\rho_1\tilde{h}_2 + \rho_2 h_1)}, \quad q_2 = \frac{g\tilde{h}_2(\rho_1 - \rho_2)}{\rho_1\tilde{h}_2 + \rho_2 h_1}, \tag{3.49}$$

$$q_3 = \frac{g\rho_2(\rho_1 - \rho_2)(h_1 + \tilde{h}_2)}{(\rho_1\tilde{h}_2 + \rho_2 h_1)^2}, \quad q_4 = \frac{h_1\tilde{h}_2(\rho_1 h_1 + \rho_2\tilde{h}_2)}{3(\rho_1\tilde{h}_2 + \rho_2 h_1)}, \tag{3.50}$$

with $\tilde{h}_2 = h_2 - b(x)$.

The solitary wave solutions are constructed numerically for different stability criteria [78]. The interaction solutions, produced by the collision of the two solitary waves with different speeds, are also constructed in [78]. Two different collision exist: 1) *overtake collision* – faster wave overtakes the slower wave; 2) *head-on collision* – two waves collide face to face. For either collision, the solitary waves remain unchanged after collision except producing a position shift and a phase shift. The interaction solutions of the complex solitons of the Choi-Camassa model has been studied in [37].

With the non-uniform bottom topography $\tilde{h}_2(x) = h_2 - b(x)$, the weakly nonlinear model (3.47)–(3.48) can be reduce to the KdV equation for ζ as developed by Djordjevic and Redekopp [84] :

$$\zeta_t + c_0(x)\zeta_x + c_1(x)\zeta\zeta_x + c_2(x)\zeta_{xxx} + \frac{1}{2}c_0'(x)\zeta = 0, \tag{3.51}$$

where the variable coefficients are defined as

$$c_0^2 = \frac{gh_1\tilde{h}_2(\rho_2 - \rho_1)}{\rho_1\tilde{h}_2 + \rho_2 h_1}, \quad c_1 = \frac{q_2}{2c_0}\left(2 + q_1 - \frac{q_3 h_1}{q_2}\right), \quad c_2 = \frac{1}{2}q_4 c_0 \tag{3.52}$$

with q_i given by (3.49)–(3.50).

This model with non-uniform bottom topography again suffers from the Kelvin-Helmholtz instability due to velocity jump at the interface. For a stable model, one needs to consider some physical effects, for example, viscosity, surface tension or continuous stratification. For validity of this model, it is required to compare the solution curves of the model equations (3.37)–(3.40) with those of the Euler equations.

(3) **Shear currents**

Large amplitude internal waves interacting with a linear shear current in a system of two layer fluids of different densities have been studied in [89]. The authors have derived a modified Choi-Camassa model considering shear currents.

For an inviscid and incompressible fluid of density ρ_i, the velocity components in Cartesian coordinates $(u_i^*,\ w_i^*)$ and the pressure p_i^* satisfy the continuity equation (3.2) and the Euler equations (3.3)–(3.4). Here, $i = 1$ ($i = 2$) stands for the upper (lower) fluid as seen in the Figure 3.3.

The boundary conditions at the interface and kinematic boundary conditions are given by (3.6) and (3.5) respectively in terms of the variables with star. The total velocity can be decomposed into a background

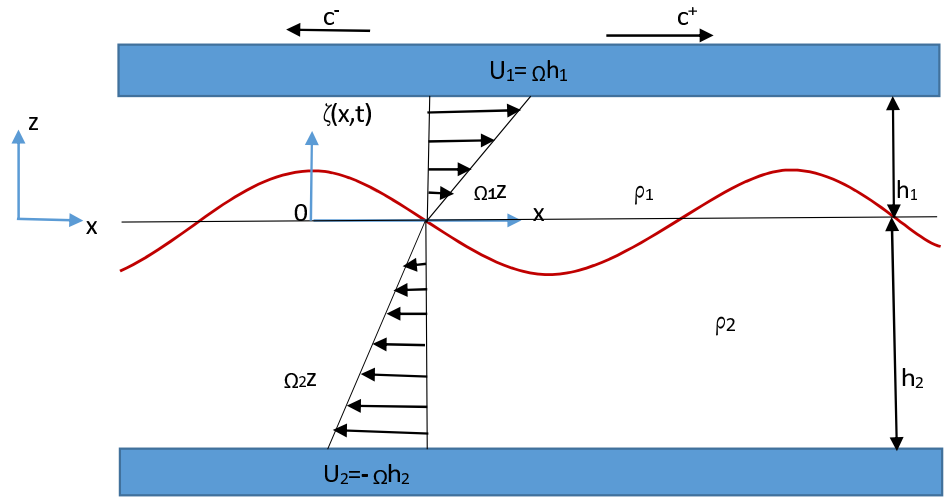

Figure 3.3: Choi-Camassa model with shear currents

uniform shear of constant vorticity Ω_i and a perturbation so that

$$u_i^* = \Omega_i z + u_i(x,z,t), \quad w_i^* = w_i(x,z,t), \tag{3.53}$$

where u_i^* and w_i^* are the total horizontal and vertical velocities, respectively, while u_i and w_i represent the perturbation velocities. Then, the complete set of equations for the four unknowns ($\zeta,\ v_1,\ v_2,\ P$) is, in the dimensional form with shear currents, given by

$$\eta_{it} + U_i\eta_{ix} - \frac{U_i}{h_i}\eta_i\eta_{ix} + (\eta v_i)_x = 0, \tag{3.54}$$

$$v_{it} + U_i v_{ix} + v_i v_{ix} + g\zeta_x = -\frac{1}{\rho_i}P_x + \frac{1}{\eta_i}\left(\frac{\eta_i^3}{3}\left(v_{itx} + U_i v_{ixx} - \frac{U_i}{h_i}\eta_i v_{ixx} + v_i v_{ixx} - v_{ix}^2\right)\right)_x, \tag{3.55}$$

where U_i are the velocities at the rigid boundaries, given by

$$U_1 = \Omega_1 h_1, \quad U_2 = -\Omega_2 h_2. \tag{3.56}$$

For $\Omega_i = 0$, the system given by (3.54)–(3.55) is reduced to the original Choi-Camassa model equations [86].

(4) **Domain of validity**

The parameter domains of validity of the Choi-Camassa model (3.14)–(3.15) have been analyzed by Camassa *et al* [61]. The authors compared and validated the analytical and numerical results of Choi-Camassa model equations with the experimental results of internal gravity waves and with the numerical solutions of the Euler equations at the interface of two fluids. For all the cases they focused on the solitary wave solutions.

Considered the shallow water configuration first. The authors [61] began with the comparison of wave profiles from the numerical computation of Euler vs. the analytic expression from the Choi-Camassa model.

The solitary wave solutions of the Choi-Camassa model are quite close to Euler's for the small values of amplitudes. Let a be the wave amplitude. The largest discrepancies occur for waves in the mid-amplitude range between $|a|/h_1 \simeq 0.3$ and $|a|/h_1 \simeq 0.7$, where the effective wavelength is shortest and so a long-wave theory such as the strongly nonlinear model can be expected to fare the worst.

Next, the authors looked at the variation of effective wavelength λ_I/h_1 and wave velocity c/c_0 with amplitude a/h_1, where λ_I is the integral wavelength introduced by Koop & Butler [12]

$$\lambda_I = \frac{1}{a}\int_{\xi_m}^{\infty} \zeta(\xi)\, d\xi, \tag{3.57}$$

where $\xi = x - ct$ is a travelling-wave coordinate, ξ_m is the location of maximum displacement. The authors showed that the agreement between Euler and the Choi-Camassa model is remarkable, with the largest discrepancy occurring in the mid-amplitude range. They found both wavelength and velocity plots terminate at the maximum amplitude [86], a_m, given by

$$a_m = \frac{h_1 - h_2\sqrt{\rho_1/\rho_2}}{1 + \sqrt{\rho_1/\rho_2}}. \tag{3.58}$$

Finally, they compared by looking at the variation of fluid velocity with depth. The averaged fluid velocity was reconstructed at the height z. It was found that the Euler solutions and the Choi-Camassa model are equivalent.

The authors [61] also focused on testing the performance of the Choi-Camassa model with respect to experimental data pertaining to the shallow-water configuration. They presented experimental data for wave profiles together with those from the nonlinear internal wave theory. The wave profiles were computed from the solution of the travelling-wave equation at several different amplitudes using the measured parameters of the experiment. These amplitudes and parameters correspond to the Euler and Choi-Camassa model wave profiles, and by a comparison it can be seen that, from the viewpoint of the experimental data, the Euler and Choi-Camassa model solutions are indistinguishable. Further, the experimental data for variation of effective wavelength and wave speed with amplitude were compared with the corresponding Choi-Camassa model solution curves. The agreement between the experimental data [32] and the model has been shown to be reasonable though discrepancies seem to occur mostly at the lower and largest amplitudes.

The nonlinear Choi-Camassa model for the shallow configuration is fairly robust, in the sense that it does not require an overly small long-wave parameter for a favourable comparison with the Euler theory, and it performs well even for fairly skewed depth ratios, at least the solitary wave test is concerned. This remains true across all types of comparison that the authors have used, from the basic waveform test to the horizontal fluid parcel velocity profiles vs. depth. Moreover, for the shallow configuration, their results show that both the asymptotic model and the fundamental Euler theory are within good experimental accuracy.

(5) **A special asymptotic reduction of the Choi-Camassa system**

The authors of [86, 91] derived a single equation for the interfacial waves by introducing the dimensionless quantities and assuming a relation between ζ and v_1. This equation has been derived for shallow water configuration by considering a weakly nonlinear assumption [86]. Assume that the fluid in each layer is homogeneous, inviscid, incompressible, and irrotational.

Let $\phi_1(x,z,t)$ and $\phi_2(x,z,t)$ be the velocity potentials for the upper and the lower fluids respectively. Then, following the Whitham method [21] for KdV equation, the authors of [86, 91] derived a single decoupled equation for the interfacial elevation ζ :

$$\zeta_t + c_0\zeta_x + c_1\zeta\zeta_x + c_2\zeta_{xxx} + c_3(\zeta^3)_x + (c_4\zeta_x^2 + c_5\zeta\zeta_{xx})_x + c_6\zeta_{xxxxx} = 0, \tag{3.59}$$

where

$$c_0^2 = \frac{gh_1h_2(\rho_2-\rho_1)}{\rho_1h_2+\rho_2h_1}, \quad c_1 = \frac{3c_0(\rho_2h_1^2-\rho_1h_2^2)}{2(\rho_1h_1h_2^2+\rho_2h_1^2h_2)}, \quad c_2 = \frac{c_0h_1h_2(\rho_1h_1+\rho_2h_2)}{6(\rho_1h_2+\rho_2h_1)}, \tag{3.60}$$

$$c_3 = \frac{7c_1^2}{18c_0} - \frac{c_0(\rho_1h_2^3+\rho_2h_1^3)}{h_1^2h_2^2(\rho_1h_2+\rho_2h_1)}, \quad c_4 = \frac{17c_1c_2}{12c_0} + \frac{c_0h_1h_2(\rho_1-\rho_2)}{12(\rho_1h_2+\rho_2h_1)}, \tag{3.61}$$

$$c_5 = \frac{7c_1c_2}{3c_0} + \frac{c_0h_1h_2(\rho_1-\rho_2)}{6(\rho_1h_2+\rho_2h_1)}, \quad c_6 = \frac{3c_2^2}{2c_0} - \frac{c_0h_1h_2(\rho_1h_1^3+\rho_2h_2^3)}{90(\rho_1h_2+\rho_2h_1)}. \tag{3.62}$$

This is a fifth order KdV equation with higher order nonlinear terms that posses the solitary wave solutions. If we neglect the dispersive terms (set $c_4 = c_5 = c_6 = 0$) then the equation (3.59) reduces to the combined KdV and mKdV equation. For the special case of (3.59), when $c_4 = c_5 = c_6 = 0$, it posses solitary wave solutions and conserved quantities analogous to KdV mass, momentum and energy (see, e.g., [9]).

The equation (3.59) is already in conserved form and the conserved integral, with zero boundary condition at infinity,

$$\int_{-\infty}^{\infty} \zeta\, dx \tag{3.63}$$

is analogous to the KdV mass conservation. However, these models do not seem to admit conservation laws that contain the energy-like variables ζ^2.

(6) **Variational formulation**

The variational method for water waves has been studied by Whitham in [22]. Ostrovsky and Grue [40] claimed the Choi-Camassa equations are variational, but they have not proved their claim, and have rather just made some assumptions by following Whitham's method [22]. According to [22, 40], the velocity potentials for the upper and the lower fluids are

$$\phi_1(x,z,t) = f_1(x,t) - \frac{1}{2}z^2 f_{1xx}, \tag{3.64}$$

$$\phi_2(x,z,t) = f_2(x,t) - \frac{1}{2}z^2 f_{2xx}, \tag{3.65}$$

where $f_1(f_2)$ is the velocity potential at the bottom of the upper (lower) fluid. The dynamic fluid depth is $h_1 - \zeta$ for the upper fluid and $h_2 + \zeta$ for the lower fluid. Thus the surface potentials [22, 40]

$$F_1(x, z, t) = f_1(x, t) - \frac{1}{2}\eta_1^2 f_{1xx}, \tag{3.66}$$

$$F_2(x, z, t) = f_2(x, t) - \frac{1}{2}\eta_2^2 f_{2xx} \tag{3.67}$$

with $\eta_1 = h_1 - \zeta,\ \eta_2 = h_2 + \zeta$. Then the Lagrangian for the Choi-Camassa model is given by

$$L = L_1 + L_2 \tag{3.68}$$

in terms of Lagrangian

$$L_1 = \rho_1\eta_1\left(F_{1t} + \frac{1}{2}F_{1x}^2\right) + \frac{1}{2}\rho_1 g\eta_1^2 - \frac{1}{6}\rho_1\eta_1^3 F_{1xx}^2 \tag{3.69}$$

for the upper fluid and

$$L_2 = \rho_2\eta_2\left(F_{2t} + \frac{1}{2}F_{2x}^2\right) + \frac{1}{2}\rho_2 g\eta_2^2 - \frac{1}{6}\rho_2\eta_2^3 F_{2xx}^2 \tag{3.70}$$

for the lower fluid. The averaged velocities as seen in [40] in terms of $F_1,\ F_2$ are given by

$$v_i = \frac{1}{\eta_i}\int_0^{\eta_i} \phi_{ix} dy = f_{ix} - \frac{1}{6}\eta_i^2 f_{ixxx} = F_{ix} + \frac{1}{3}\eta_i^2 F_{ixxx} + \eta_i\eta_{ix}F_{ixx}, \quad i = 1, 2. \tag{3.71}$$

Applying the Euler operator to the Lagrangian L with respect to four different variables $\eta_1,\ \eta_2,\ F_1,\ F_2$, one can derive four variational equations. The authors of [40] then mentioned that the Choi-Camassa equations arise from these four equations after using the formula (3.71).

In fact, the mass conservation equations (3.12)–(3.13) arise explicitly from their Lagrangian given by (3.68)–(3.70), but the momentum balance equations (3.14)–(3.15) arise as a combined single equation as found after eliminating P_x from both equations. A clear variational formulation of Choi-Camassa equations is thus not contained in [40].

3.3 Some Related Models

The Choi-Camassa model is a one-dimensional two-layer fluid model that describe the motion of two superposed fluids of different density in a channel. Several models related to Choi-Camassa model are seen in the literature. Few of them are described briefly as under:

(1) **Korteweg-de Vries (KdV) model**

It is well known that the third order KdV equation is the generic model of weakly nonlinear waves. The equation models water waves with small amplitude and long wavelength on shallow water. The KdV equation involves a balance between weak nonlinearity and linear dispersion. The generalized Korteweg-de Vries

(gKdV) equation [48, 54] is given by

$$u_t + \eta u^m u_x + \gamma u_{xxx} = 0, \quad t \geq 0, \ -\infty < x < \infty, \tag{3.72}$$

where x is the space variable and t is the time variable, η is real parameter, $\gamma > 0$, m is a positive integer. For $m = 1$, this is the standard KdV [48, 54] equation which models shallow water waves, while for $m = 2$ the equation (3.72) is called modified Korteweg-de Vries (mKdV) equation. For $m = 1, 2$, N-soliton solutions can be obtained for integer $N \geq 1$ (see, e.g., [48, 54]). The exact closed form solution [48, 54] of the generalized KdV equation (3.72) is given by

$$u(x,t) = \Big[\frac{(m+1)(m+2)c}{2\eta}\ \mathrm{sech}^2\left(\frac{m\sqrt{c}}{2\sqrt{\gamma}}(x - ct - x_0)\right)\Big]^{1/m} \tag{3.73}$$

centered at x_0 and moves with a constant speed $c > 0$. The solution (3.73) is a localized, stable, nonlinear travelling wave that is single-peaked and unidirectional. The KdV solitary wave (3.73) is proportional to its speed resulting the faster soliton is taller while the slower soliton is smaller. It carries mass, momentum, energy, which are constants of motion for the standard KdV equation. Then the 1-soliton (solitary wave) solution of the standard KdV equation is shown in the Figure 3.4. For simplicity we use $\eta = 6, \ \gamma = 1$.

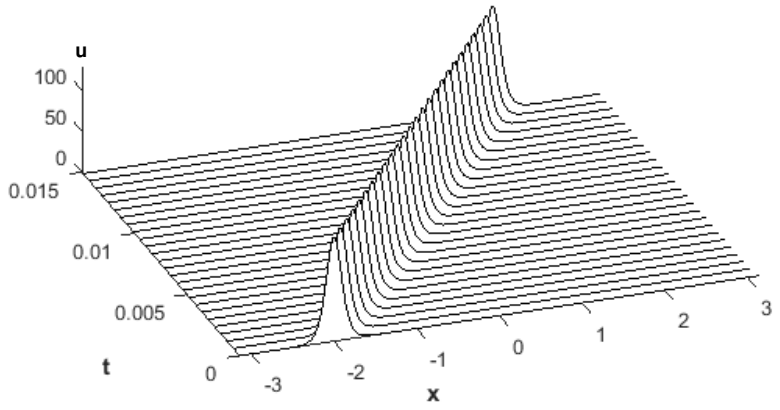

Figure 3.4: KdV 1-soliton solution

A collision of KdV multi solitary waves produce a multi-soliton solution. Note that the KdV multi-soliton solutions do not satisfy the linear superposition of single solitons [48, 54]. These solutions can be produced by a nonlinear superposition of single solitons. A collision occurs when a faster solitary wave overtakes a slower solitary wave. These KdV solitary waves retain their initial identities (shapes, speeds, integrability

etc.) after a pair-wise collision, but gets a shift in position [48, 54]. The 2-soliton (collision) solution of the standard KdV equation is by using MATLAB software as shown in the Figure 3.5.

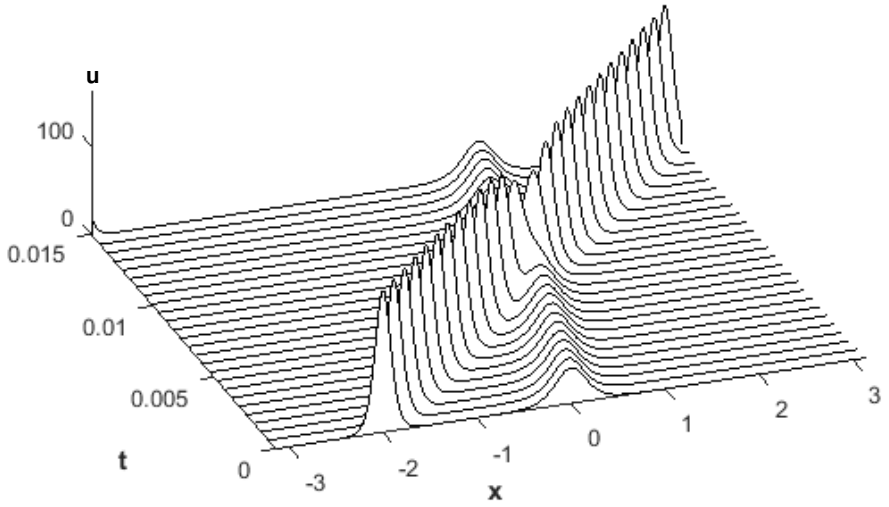

Figure 3.5: KdV 2-soliton solution

From the KdV 2-soliton solution in the Figure 3.5, it is clear that the faster (taller) soliton gets shifted forward while the slower (shorter) soliton gets shifted backward. After collision both solitary waves retain their initial speeds, shapes and orientations.

(2) **Su-Gardner (SG) model**

Significant efforts have been directed towards the derivation of relatively simple models enabling the quantitative description of the propagation of fully nonlinear waves, and also amenable to analytical study. In the context of one-dimensional shallow-water waves such a model was derived using a long-wave asymptotic expansion of the full Euler equations for irrotational flow by Su and Gardner (SG) [13].

The SG system describing fully nonlinear, unsteady, shallow water waves has the form

$$\eta_t + (\eta u)x = 0, \tag{3.74}$$

$$u_t + uu_t + \eta_x = \frac{1}{\eta}\left(\frac{1}{3}\eta^3(u_{tx} + uu_{xx} - u_x^2)\right)_x. \tag{3.75}$$

Here η is the total depth and u is the layer-mean horizontal velocity; all variables are nondimensionalized by their typical values. The first equation is the exact equation for conservation of mass and the second equation can be regarded as an approximation to the equation for conservation of horizontal momentum.

The system (3.74)–(3.75) has the typical structure of the well-known Boussinesq-type systems for shallow water waves, but differs from them in retaining full nonlinearity in the leading-order dispersive term. Note that the system (3.74)–(3.75) represents a one-layer reduction of the system of Choi-Camassa model [86] for fully nonlinear internal shallow-water waves.

(3) **Green-Naghdi (GN) model**

One of popular simple mathematical models is the Green-Naghdi model obtained in the multi-dimensional case by Green *et al* [2] within the context of a homogeneous one-layer fluid. In the literature, this model is usually called Green-Naghdi model (GN model or GN system). The Green-Naghdi equations are given by

$$\eta_t + \nabla \cdot (\eta \mathbf{u}) = 0, \tag{3.76}$$

$$\mathbf{u}_t + \mathbf{u} \cdot \nabla \mathbf{u} + g \nabla \eta = -\frac{1}{3\eta} \nabla (\eta^2 \mathbf{G}), \tag{3.77}$$

with

$$\mathbf{G} = \frac{D}{Dt}(\eta_t + \mathbf{u} \cdot \nabla \eta), \quad \frac{D}{Dt} = \partial_t + \mathbf{u} \cdot \nabla, \tag{3.78}$$

where $\eta(x, y, t)$ is the position of the free surface, $\mathbf{u} = (u, v)$ is the averaged over depth horizontal velocity of the fluid, g is the acceleration of the gravity. Here $u = u(x, y, t)$ and $v = v(x, y, t)$ are the components of the averaged velocity. The system describes long dispersive three-dimensional gravity waves on a surface of an incompressible ideal fluid. The GN equations for one spatial dimension have the form [60]

$$\eta_t + (\eta U)_x = 0, \tag{3.79}$$

$$U_t + U U_x + g \eta_x = \frac{1}{3\eta} (\eta^2 G)_x, \tag{3.80}$$

with

$$G = (\eta U_x)_t + U (\eta U_x)_x, \tag{3.81}$$

where $\eta(x, t)$ and $u(x, t)$ represent the surface displacement and the horizontal velocity, respectively.

(4) **Camassa-Holm equation**

Completely integrable nonlinear partial differential equations arise at various levels of approximation in shallow water theory. The Camassa-Holm equation [59] is one such well-known completely integrable dispersive model. The equation is given by

$$u_t + k u_x - u_{xxt} + 3 u u_x = 2 u_x u_{xx} + u u_{xxx}, \tag{3.82}$$

where $u(x,t)$ is the fluid velocity in the x direction (or equivalently the height of the water's free surface above a flat bottom), k is a constant related to the critical shallow water wave speed, and subscripts denote partial derivatives. The Camassa-Holm equation posses solitary wave solutions with a limiting case for $k = 0$. In the limiting case ($k = 0$), the Camassa-Holm equation has peakon solutions (i.e., at peaks the first derivatives are discontinuous). The equation (3.82) is bi-Hamiltonian, i.e., it can be expressed in Hamiltonian form in two different ways. The ratio of its two (compatible) Hamiltonian operators is a recursion operator that produces an infinite sequence of conservation laws [59].

(5) **KP equation**

The Kadomtsev-Petviashvili equation [11, 48] (or simply the *KP equation*) is a nonlinear partial differential equation with two spatial and one temporal coordinates which describes the evolution of nonlinear, long waves of small amplitude with slow dependence on the transverse coordinate. There are two distinct versions of the KP equation, which can be written in normalized form as follows:

$$(u_t + 6uu_x + u_{xxx})_x + 3\sigma^2 u_{yy} = 0, \tag{3.83}$$

where $u = u(x,y,t)$ is a scalar function, x and y are respectively the longitudinal and transverse spatial coordinates, subscripts $x,\ y,\ t$ denote partial derivatives, and $\sigma^2 = \pm 1$. The case $\sigma = 1$ is known as the KPII equation, and models, for instance, water waves with small surface tension. The case $\sigma = i$ is known as the KPI equation, and may be used to model waves in thin films with high surface tension. The KP equation is a universal integrable system in two spatial dimensions in the same way that the KdV equation can be regarded as a universal integrable system in one spatial dimension. In fact, KP equation also known as 2D KdV equation.

(6) **Shallow water model**

The shallow water equations are derived from equations of conservation of mass and conservation of momentum (the Navier-Stokes equations), which hold even when the assumptions of shallow water break down, such as across a hydraulic jump. In the case of no frictional or viscous forces, the shallow-water equations are:

$$h_t + (hu)_x = 0, \tag{3.84}$$

$$(hu)_t + (hu^2)_x + \left(\frac{1}{2}gh^2\right)_x = -ghb_x, \tag{3.85}$$

where $h(x,t)$ is water depth, $u(x,t)$ is the velocity of water, $b(x)$ describes the topography for non-uniform bottom surface, and g is gravitational acceleration.

In two spatial dimensions, the shallow water equations are given by

$$h_t + (hu)_x + (hv)_y = 0, \tag{3.86}$$

$$(hu)_t + \left(hu^2 + \frac{1}{2}gh^2\right)_x + (huv)_y = -ghb_x, \tag{3.87}$$

$$(hv)_t + (huv)_x + \left(hv^2 + \frac{1}{2}gh^2\right)_y = -ghb_y, \tag{3.88}$$

where, u is velocity in x direction, v is velocity in y direction. For the uniform bottom surface, $b = 0$.

(7) **Multi-layer fluid model**

Consider the governing equations (3.2)–(3.4) for an inviscid and incompressible fluid of densities ρ_i with the velocity components (u_i, w_i) and fluid pressure p_i, where $i = 1, 2, ..., N$ and $\rho_i < \rho_{i+1}$ for stable stratification. The boundary conditions at the upper and lower interfaces of the i-th layer require the continuity of normal velocity and pressure:

$$\eta_{it} + u_i\eta_{ix} = w_i, \quad \text{at} \quad z = \eta_i(x,t), \tag{3.89}$$

$$\eta_{(i+1)t} + u_i\eta_{(i+1)x} = w_i, \quad \text{at} \quad z = \eta_{(i+1)}(x,t), \tag{3.90}$$

$$p_i = p_{i-1}, \quad \text{at} \quad z = \eta_i(x,t). \tag{3.91}$$

Here $\eta_i(x,t),\ i = 1, ..., N$, is the location of the upper interface of the i-th layer [88] given by

$$\eta_i = \zeta_i - \sum_{j=1}^{i-1} h_j, \tag{3.92}$$

where h_i is the undisturbed thickness of the i-th layer and $\zeta_i(x,t)$ in the interfacial displacement. One gets

$$\eta_{N+1} = \zeta_{N+1} - \sum_{j=1}^{N} h_j = \zeta_{N+1} - h, \tag{3.93}$$

where $\zeta_N(x,t)$ describes the bottom topography and h is the total depth of the fluid. By applying the similar mechanism as seen in the Section 3.1 (see [86]), the authors of [88] have derived a nonlinear model that describes the evolution of finite-amplitude long internal waves in a multi-layer system:

$$H_{it} + (H_i v_i)_x = 0, \quad H_i = \eta_i - \eta_{i+1}, \tag{3.94}$$

$$v_{it} + v_i v_{ix} + g\eta_{ix} = -P_{ix}/\rho_i + \frac{1}{H_i}\left(\frac{1}{3}H_i^3 a_i + \frac{1}{2}H_i^2 b_i\right)_x + \left(\frac{1}{2}H_i^3 a_i + b_i\right)(\eta_{i+1})_x, \tag{3.95}$$

where

$$a_i(x,t) = v_{itx} + v_i v_{ixx} - (v_{ix})^2, \tag{3.96}$$

$$b_i(x,t) = -D_i^2\eta_{i+1}, \quad D_i = \partial_t + u_i^{(0)}\partial_x. \tag{3.97}$$

For $1 \le i \le N$, (3.94)–(3.95) determines the evolution of $2N$ unknowns $v_i,\ \zeta_i$ and P_i, where

$$P_{i+1} = P_i + \rho_i\left(gH_i - \frac{1}{2}a_i H_i^2 - b_i H_i\right). \tag{3.98}$$

For $N = 1$, the coupled system (3.94)–(3.95) reduces to the homogeneous Green-Nagdhi system, and for $i = 1, 2$, the system reduces to the 1D Choi-Camassa model.

Chapter 4

Conservation Laws of the Choi-Camassa Model

In this chapter we derive systematically the conservation laws of the Choi-Camassa equations (3.12)–(3.15). We derive an explicit formula for each conserved density and spatial flux analogous to the Euler system. We also derive additional conservation laws of the Choi-Camassa equations if exist.

4.1 Conservation Laws

The Choi-Camassa system has four equations (3.12)–(3.15) with four dependent variables. To apply the direct method for constructing conservation law, we seek multipliers $\Lambda_\sigma,\ \sigma = 1, ..., 4$ up to a finite order to form a conservation law

$$D_t T + D_x X = 0 \tag{4.1}$$

on the solution of the Choi-Camassa system, where the density T and the flux X are the functions of $x,\ t,\ \zeta,\ v_1,\ v_2,\ P$ and derivatives of $\zeta,\ v_1,\ v_2,\ P$ up to some finite order. Following the direct construction method, one use the formula (2.84) to seek conservation laws in the form

$$\sum_{\sigma=1}^{4} \Lambda_\sigma F^\sigma[\zeta, v_1, v_2, P] \equiv D_t T + D_x X, \tag{4.2}$$

where Λ_σ are functions of $x,\ t,\ \zeta,\ v_1,\ v_2,\ P$ and derivatives of $\zeta,\ v_1,\ v_2,\ P$. We are interested in finding the conserved quantities of the Choi-Camassa system analogous to the conserved quantities (2.112)–(2.115) of the Euler equations. In addition to this, we also wish to find other physical quantities of the Choi-Camassa equations.

First, we seek zeroth order multipliers of the form

$$\Lambda_\sigma(x, t, \zeta, v_1, v_2, P) \tag{4.3}$$

to derive the conserved densities and spatial fluxes. Following the theorem 2.2.14, with the multipliers (4.3),

the conservation law determining equations are given by

$$E_\zeta\left(\sum_{\sigma=1}^{4}\Lambda_\sigma(x,t,\zeta,v_1,v_2,P)F^\sigma[\zeta,v_1,v_2,P]\right)=0, \tag{4.4}$$

$$E_{v_1}\left(\sum_{\sigma=1}^{4}\Lambda_\sigma(x,t,\zeta,v_1,v_2,P)F^\sigma[\zeta,v_1,v_2,P]\right)=0, \tag{4.5}$$

$$E_{v_2}\left(\sum_{\sigma=1}^{4}\Lambda_\sigma(x,t,\zeta,v_1,v_2,P)F^\sigma[\zeta,v_1,v_2,P]\right)=0, \tag{4.6}$$

$$E_P\left(\sum_{\sigma=1}^{4}\Lambda_\sigma(x,t,\zeta,v_1,v_2,P)F^\sigma[\zeta,v_1,v_2,P]\right)=0, \tag{4.7}$$

where $E_\zeta,\ E_{v_1},\ E_{v_2},\ E_P$ are the Euler operators up to third order derivatives given by (2.43).

Now applying the Euler operators, where the total derivative operators are given by (2.10), and splitting the determining equations of the Choi-Camassa system by Maple **GeM** package [4], we obtain an overdetermined linear PDE system for unknowns Λ_σ. We then use Maple **rifsimp** operation to reduce the determining equations into a simple PDE system, and finally use Maple **pdsolve** to get the solution of this reduced PDE system. We found a general solution involving three arbitrary constants and one arbitrary function. Thus, we obtain three nontrivial local multiplier sets for the three linearly independent solutions corresponding to three arbitrary constants given in the Theorem 4.1.1, and one multiplier set for the linearly independent solution corresponding to the arbitrary function given in the Theorem 4.1.2 below. For simplicity we write

$$h_1-\zeta=\eta_1 \quad \text{and} \quad h_2+\zeta=\eta_2 \tag{4.8}$$

hereafter in the equations (4.9)–(6.9).

Theorem 4.1.1. *The Choi-Camassa system* (3.12)–(3.15) *has three sets of zeroth-order multipliers admitted by the determining equations of the system:*

$$(i)\ \Lambda_1=1,\quad \Lambda_2=0,\quad \Lambda_3=0,\quad \Lambda_4=0 \quad or \quad \Lambda_1=0,\quad \Lambda_2=1,\quad \Lambda_3=0,\quad \Lambda_4=0, \tag{4.9}$$

$$(ii)\ \Lambda_1=-\rho_1 v_1,\quad \Lambda_2=\rho_2 v_2,\quad \Lambda_3=\rho_1\eta_1,\quad \Lambda_4=\rho_2\eta_2, \tag{4.10}$$

$$(iii)\ \Lambda_1=\rho_1(x-tv_1),\quad \Lambda_2=-\rho_2(x-tv_2),\quad \Lambda_3=\rho_1 t\eta_1,\quad \Lambda_4=\rho_2 t\eta_2. \tag{4.11}$$

Note that we find the determining equations and the multiplier sets (4.9)–(4.11) off the solution space of the Choi-Camassa equations. Now using each multiplier set in the theorem 4.1.1 and the Choi-Camassa equations, we produce a divergence expression. As a consequence, we find three local conservation laws on the solutions of the Choi-Camassa equations (3.12)–(3.15).

(i) For the multiplier set (4.9), we have one locally conserved density, but two spatial fluxes for top fluid and bottom fluid:

$$T^{(1)} = \zeta, \tag{4.12}$$

$$X^{(1)} = -\eta_1 v_1 \quad \text{(upper fluid)}, \tag{4.13}$$

$$\text{or} \quad X^{(1)} = \eta_2 v_2 \quad \text{(lower fluid)}. \tag{4.14}$$

(ii) For the multiplier set (4.10), the corresponding density and flux are found as

$$T^{(2)} = \rho_1\eta_1 v_1 + \rho_2\eta_2 v_2, \tag{4.15}$$

$$X^{(2)} = \frac{1}{2}g(\rho_1 - \rho_2)\zeta^2 + \sum_{i=1}^{2}\frac{1}{3}\rho_i\eta_i^3(v_{ix}^2 - v_i v_{ixx} - v_{itx}) + g\rho_i\eta_i\zeta + \rho_i\eta_i v_i^2 + \eta_i P. \tag{4.16}$$

(iii) For the multiplier set (4.11), the density and flux are given by

$$T^{(3)} = x(\rho_1 - \rho_2)\zeta + t\big(\rho_1\eta_1 v_1 + \rho_2\eta_2 v_2\big), \tag{4.17}$$

$$X^{(3)} = \frac{1}{2}gt(\rho_1 - \rho_2)\zeta^2 + \sum_{i=1}^{2} t\big(\frac{1}{3}\rho_i\eta_i^3(v_{ix}^2 - v_i v_{ixx} - v_{itx}) + \eta_i(g\rho_i\zeta + \rho_i v_i^2 + P)\big) - x\rho_i\eta_i v_i. \tag{4.18}$$

Theorem 4.1.2. *In addition to* (4.9)–(4.11)*, the Choi-Camassa system* (3.12)–(3.15) *has the following set of zeroth-order multipliers with arbitrary function admitted by the determining equations of the system:*

$$\Lambda_1 = -\frac{\partial}{\partial\varpi}\Upsilon(\varpi, t), \quad \Lambda_2 = \frac{\partial}{\partial\varpi}\Upsilon(\varpi, t), \quad \Lambda_3 = 0, \quad \Lambda_4 = 0, \tag{4.19}$$

where $\varpi = \eta_1 v_1 + \eta_2 v_2$.

Applying the multipliers in the Theorem 4.1.2 to the equations (3.12)–(3.15), one gets

$$\frac{\partial}{\partial x}\Upsilon(\varpi, t) = 0 \tag{4.20}$$

where $\Upsilon \neq 0$. This implies $\varpi = f(t)$. So the conserved flux corresponding to these multipliers is

$$X^{(4)} = \Upsilon(\varpi, t) \tag{4.21}$$

provided $f(t) \neq 0$. If $f(t) = 0$, then

$$v_2 = -\frac{\eta_1}{\eta_2}v_1 \tag{4.22}$$

and $\varpi = 0$. In this case, one can eliminate P_x from (3.14) by (3.15), and use (4.22) for v_2. Equations (3.12) and (3.14) then become a closed system of equations for ζ and v_1.

Next, we seek multipliers of the form

$$\Lambda_\sigma(x, t, \zeta, v_1, v_2, P, \zeta_x, v_{1x}, v_{2x}, P_x, v_{1xx}, v_{2xx}) \tag{4.23}$$

involving derivatives up to some second order, and classify the densities and fluxes. Again we find the determining equations off the solutions of the Choi-Camassa system (3.12)–(3.15). With the multipliers (4.23) the conservation law determining equations are given by

$$E_\zeta\left(\sum_{\sigma=1}^{4}\Lambda_\sigma(x,t,\zeta,v_1,v_2,P,\zeta_x,v_{1x},v_{2x},P_x,v_{1xx},v_{2xx})F^\sigma[\zeta,v_1,v_2,P]\right)=0, \tag{4.24}$$

$$E_{v_1}\left(\sum_{\sigma=1}^{4}\Lambda_\sigma(x,t,\zeta,v_1,v_2,P,\zeta_x,v_{1x},v_{2x},P_x,v_{1xx},v_{2xx})F^\sigma[\zeta,v_1,v_2,P]\right)=0, \tag{4.25}$$

$$E_{v_2}\left(\sum_{\sigma=1}^{4}\Lambda_\sigma(x,t,\zeta,v_1,v_2,P,\zeta_x,v_{1x},v_{2x},P_x,v_{1xx},v_{2xx})F^\sigma[\zeta,v_1,v_2,P]\right)=0, \tag{4.26}$$

$$E_P\left(\sum_{\sigma=1}^{4}\Lambda_\sigma(x,t,\zeta,v_1,v_2,P,\zeta_x,v_{1x},v_{2x},P_x,v_{1xx},v_{2xx})F^\sigma[\zeta,v_1,v_2,P]\right)=0. \tag{4.27}$$

Similarly splitting the determining equations of the Choi-Camassa system by Maple **GeM** package we find that it forms an overdetermined linear PDE system for unknowns Λ_σ. We then use Maple **rifsimp**, and finally use Maple **pdsolve** to get the general solution of the determining equations. In this stage, in addition to the zeroth order multipliers, we obtain one nontrivial local multiplier set of first order given in the Theorem 4.1.3, and three multiplier sets of order two given in the Theorem 4.1.4.

Theorem 4.1.3. *The Choi-Camassa system* (3.12)–(3.15) *has following set of first order multipliers admitted by the determining equations of the system:*

$$\Lambda_1=-\frac{1}{2}\rho_1(2g\zeta+v_1^2-\eta_1^2v_{1x}^2)-P,\quad \Lambda_2=\frac{1}{2}\rho_2(2g\zeta+v_2^2+\eta_2^2v_{2x}^2)+P,$$
$$\Lambda_3=\rho_1\eta_1v_1,\quad \Lambda_4=\rho_2\eta_2v_2. \tag{4.28}$$

Now using this multiplier set (4.28) to the Choi-Camassa equations and writing in the form (4.2), we find a local conservation law, where conserved density and corresponding flux are given by

$$T^{(5)}=\frac{1}{2}g(\rho_2-\rho_1)\zeta^2+\sum_{i=1}^{2}\frac{1}{2}\rho_i(\eta_iv_i^2+\frac{1}{3}\eta_i^3v_{ix}^2), \tag{4.29}$$

$$X^{(5)}=\sum_{i=1}^{2}g\rho_i\eta_i\zeta v_i+\frac{1}{2}\rho_i\eta_iv_i^3+\frac{1}{6}\rho_i\eta_i^3v_i(3v_{ix}^2-2v_iv_{ixx}-2v_{itx})+\eta_iv_iP. \tag{4.30}$$

Theorem 4.1.4. *The Choi-Camassa system* (3.12)–(3.15) *has the following three sets of multipliers up to some second order derivatives admitted by the determining equations of the system:*

$$(i)\ \Lambda_1=-\frac{1}{3}\rho_1\eta_1v_{1xx},\quad \Lambda_2=0,\quad \Lambda_3=\rho_1,\quad \Lambda_4=0, \tag{4.31}$$

$$(ii)\ \Lambda_1=0,\quad \Lambda_2=\frac{1}{3}\rho_2\eta_2v_{2xx},\quad \Lambda_3=0,\quad \Lambda_4=\rho_2, \tag{4.32}$$

$$(iii)\ \Lambda_1=-\rho_1v_1+\frac{1}{3}\rho_1\eta_1(\eta_1+\zeta)v_{1xx},\ \Lambda_2=\rho_2v_2-\frac{1}{3}\rho_2\eta_2(\eta_2-\zeta)v_{2xx},$$
$$\Lambda_3=-\rho_1\zeta,\ \Lambda_4=\rho_2\zeta. \tag{4.33}$$

Again using these three multiplier sets (4.31)–(4.33) and the Choi-Camassa equations and writing in the form of (4.2), we find three local conservation laws as follows.

(i) For the multiplier set (4.31), the corresponding local density and flux are

$$T^{(6)} = \rho_1 v_1 + \frac{1}{6}\rho_1 \eta_1^2 v_{1xx}, \tag{4.34}$$

$$X^{(6)} = \frac{1}{6}\rho_1 \eta_1^2 (3v_{1x}^2 - 2v_1 v_{1xx} - 3v_{1tx}) + g\rho_1 \zeta + \frac{1}{2}\rho_1 v_1^2 + P. \tag{4.35}$$

(ii) For the multiplier set (4.32), the corresponding local density and flux are

$$T^{(7)} = \rho_2 v_2 + \frac{1}{6}\rho_2 \eta_2^2 v_{2xx}, \tag{4.36}$$

$$X^{(7)} = \frac{1}{6}\rho_2 \eta_2^2 (3v_{2x}^2 - 2v_2 v_{2xx} - 3v_{2tx}) + g\rho_2 \zeta + \frac{1}{2}\rho_2 v_2^2 + P. \tag{4.37}$$

(iii) For the multiplier set (4.33), the corresponding local density and flux are

$$T^{(8)} = \sum_{i=1}^{2} (-1)^i \rho_i \zeta \left(v_i - \frac{1}{6} h_i (h_i + \eta_i) v_{ixx} \right), \tag{4.38}$$

$$\begin{aligned} X^{(8)} = {} & \frac{1}{2} g(\rho_2 - \rho_1)\zeta^2 + \frac{1}{6} \sum_{i=1}^{2} (-1)^i \rho_i \Big((v_{ix}^2 - v_i v_{ixx} - v_{itx})(2\zeta - 3h_i)\zeta^2 + h_i v_i v_{ixx} \zeta^2 \\ & - 2(h_i^2 v_i v_{ixx} - 3v_i^2)\zeta \Big) - \rho_i h_i (h_i^2 v_{ix}^2 - 3v_i^2). \end{aligned} \tag{4.39}$$

Among the above densities and fluxes for the Choi-Camassa system, the density $T^{(3)}$ and corresponding flux have not appeared in the literature before. The densities $T^{(1)},\ T^{(2)},\ T^{(5)},\ T^{(6)}$, and $T^{(7)}$ have been studied in [86], but the corresponding fluxes have not been presented. The fourth conservation law involving only spatial flux with an arbitrary function is also a new result. We also note that all the multiplier sets found in the Theorems 4.1.1–4.1.4 appear for the first time in the literature here.

The density $T^{(8)}$ can be written as a linear combination in terms of the densities $T^{(2)},\ T^{(6)}$, and $T^{(7)}$ as

$$T^{(8)} = T^{(2)} - h_1 T^{(6)} - h_2 T^{(7)} + \tilde{T}, \tag{4.40}$$

where

$$\tilde{T} = \frac{1}{6} h_1^3 \rho_1 v_{1xx} + \frac{1}{6} h_2^3 \rho_2 v_{2xx}. \tag{4.41}$$

Similarly $X^{(8)}$ can be written as a linear combination in terms of the fluxes $X^{(2)},\ X^{(6)}$, and $X^{(7)}$ as

$$X^{(8)} = X^{(2)} - h_1 X^{(6)} - h_2 X^{(7)} + \tilde{X}, \tag{4.42}$$

where

$$\tilde{X} = -\frac{1}{6} h_1^3 \rho_1 v_{1xt} - \frac{1}{6} h_2^3 \rho_2 v_{2xt}. \tag{4.43}$$

It is obvious that $\tilde{T}$ and $\tilde{X}$ hold a trivial conservation law since $D_t\tilde{T} + D_x\tilde{X}$ becomes zero due to differential identities. Hence, the conservation law given by (4.38) and (4.39) is trivial.

4.1.1 Comparison and completeness

We already have seen mass conservation of the Euler equations in Chapter 1, and as such, one might expect same physical quantity for the Choi-Camassa model. The quantity ζ is the height of the fluid under travelling wave. Let us consider a stripe of fluid under the travelling-wave at the interface of the two fluids with Δx a small displacement along the x-axis. Then the mass element for the stripe is $\rho\zeta\Delta x$. Hence, mass under the travelling-wave is given by

$$M = \rho \int \zeta \, dx. \tag{4.44}$$

As such, $T^{(1)} = \zeta$ is the mass density of the Choi-Camassa equations.

The Euler equations have a conserved momentum given by (1.40). The Choi-Camassa model has an analogous quantity given by the horizontal momentum density:

$$T^{(2)} = \rho_1\eta_1 v_1 + \rho_2\eta_2 v_2. \tag{4.45}$$

Another important physical quantity, kenetic energy, of the Euler equations has been shown in (1.62). The energy density of the Choi-Camassa model is given by

$$T^{(5)} = \frac{1}{2}g(\rho_2 - \rho_1)\zeta^2 + \sum_{i=1}^{2}\frac{1}{2}\rho_i(\eta_i v_i^2 + \frac{1}{3}\eta_i^3 v_{ix}^2) \tag{4.46}$$

which is a combination of Kinetic energy density and potential energy density.

The irrotationalty density [86] for the upper fluid is

$$T^{(6)} = \rho_1 v_1 + \frac{1}{6}\rho_1\eta_1^2 v_{1xx} \tag{4.47}$$

and that for the lower fluid is

$$T^{(7)} = \rho_2 v_2 + \frac{1}{6}\rho_2\eta_2^2 v_{2xx}. \tag{4.48}$$

The Euler equations admits conservation of angular momentum, but the Choi-Camassa model does not have any conserved angular momentum density. However, we do not know the meaning of the other two conservation laws given by (4.17)–(4.18) and (4.21) of the Choi-Camassa model.

We derived conservation laws with an ordinary solved form of the Choi-Camassa equations. With the current settings we obtained seven different conservation laws. We do not know if the above conservation laws (4.12)–(4.18), (4.21), (4.29)–(4.30), and (4.34)–(4.39) form a complete set of all possible conservation laws up to some second order derivatives. To get a full set, one needs to re-write the system in the extended Kovalevskaya form and then derive the conservation laws. To find the extended Kovalevskaya form one should first write the equations (3.12)–(3.13) in the solved form for the leading derivatives $\zeta_x,\ v_{2x}$:

$$\zeta_x = \frac{(h_1 - \zeta)v_{1x} - \zeta_t}{v_1}, \tag{4.49}$$

$$v_{2x} = -\frac{v_2\zeta_x + \zeta_t}{h_2 + \zeta}, \tag{4.50}$$

It is clear that the equations (4.49)–(4.50) already have the extended Kovalevskaya form. Then one can solve the other two equations (3.14) and (3.15) for v_{1xxx} and P_x respectively. The variables $\zeta_x,\ v_{2x}$ and their differential consequences in (3.14)–(3.15) can be replaced by (4.49) and (4.50). Thus, the variables $\zeta_x,\ v_{2x}$ and their differential consequences do not exist on the right side of (3.14) while solving for leading derivatives v_{1xxx} and P_x. The extended Kovalevskaya form for the Choi-Camassa equations thus can be derived and used for constructing all conservation laws of the Choi-Camassa model. However, computing the conservation laws of the extended Kovalevskaya form of the Choi-Camassa model is more difficult because the fourth equation becomes too large with a few hundreds terms, the determining equations (2.87) contain a large number of equations which are impossible to solve with the current limits of computer systems.

4.1.2 Global conserved densities

A quantity T is said to be conserved globally if it has the property

$$\frac{d}{dt}\int_{-\infty}^{+\infty} T\ dx = \int_{-\infty}^{+\infty} -\frac{dX}{dx}\ dx = -X\Big|_{-\infty}^{+\infty} = 0 \tag{4.51}$$

after eliminating all pure time derivatives of $\zeta,\ v_1,\ v_2$ using the equations (3.12)–(3.15), where X is the conserved flux corresponding to T. Hence, we can define the integrated form of any density T by

$$\mathcal{C} = \int_{-\infty}^{+\infty} T\ dx = \text{constant}. \tag{4.52}$$

Recall the asymptotic boundary conditions (3.20) and (3.22). Then, for the first conservation law given by (4.12)–(4.13), we have

$$\frac{d}{dt}\int_{-\infty}^{+\infty} \zeta\ dx = \int_{-\infty}^{+\infty} [\eta_1 v_1]_x\ dx = \eta_1 v_1\Big|_{-\infty}^{+\infty} \longrightarrow\ 0 \tag{4.53}$$

as $v_1 \to 0$ when $x \to \pm\infty$. Hence, mass is conserved globally and can be written in the integral form (4.52):

$$\int_{-\infty}^{+\infty} \zeta\ dx. \tag{4.54}$$

Next, for the second conservation law given by (4.15)–(4.16)

$$\begin{aligned}
&\frac{d}{dt}\int_{-\infty}^{+\infty} [\rho_1\eta_1 v_1 + \rho_2\eta_2 v_2]\ dx \\
&= -\int_{-\infty}^{+\infty} \left[\frac{1}{2}g(\rho_1-\rho_2)\zeta^2 + \sum_{i=1}^{2}\frac{1}{3}\rho_i\eta_i^3(v_{ix}^2 - v_i v_{ixx} - v_{itx}) + g\rho_i\eta_i\zeta + \rho_i\eta_i v_i^2 + \eta_i P\right]_x\ dx \\
&= -\left[\frac{1}{2}g(\rho_1-\rho_2)\zeta^2 + \sum_{i=1}^{2}\frac{1}{3}\rho_i\eta_i^3(v_{ix}^2 - v_i v_{ixx} - v_{itx}) + g\rho_i\eta_i\zeta + \rho_i\eta_i v_i^2 + \eta_i P\right]\Bigg|_{-\infty}^{+\infty} \\
&\longrightarrow\ 0
\end{aligned} \tag{4.55}$$

as $v_1,\ v_2,\ P \to 0$ when $x \to \pm\infty$. Hence, total horizontal momentum is conserved globally and can be written in the integral form:

$$\int_{-\infty}^{+\infty} [\rho_1\eta_1 v_1 + \rho_2\eta_2 v_2]\, dx. \tag{4.56}$$

Similarly, one can show that energy density given by (4.29) is conserved globally and has an integral form (4.52). Hence, total energy is

$$\int_{-\infty}^{+\infty} \left[\frac{1}{2}g(\rho_2-\rho_1)\zeta^2 + \sum_{i=1}^{2}\frac{1}{2}\rho_i\Big(\eta_i v_i^2 + \frac{1}{3}\eta_i^3 v_{ix}^2\Big)\right]\, dx. \tag{4.57}$$

The irrotationality density given by (4.34) and (4.36) for the upper and lower fluid respectively are also conserved globally under boundary conditions (3.20) and (3.22). Then, the irrotationality [86] is given by

$$\int_{-\infty}^{+\infty} \left[\rho_i v_i + \frac{1}{6}\rho_i\eta_i^2 v_{ixx}\right]\, dx, \quad i = 1, 2. \tag{4.58}$$

The density (4.17) decays exponentially for large x. The corresponding flux (4.18) vanishes on the solitary wave solution as $x \to \pm\infty$. Therefore, the density (4.17) is conserved globally and can be written in the integral form (4.52).

$$\int_{-\infty}^{+\infty} [x(\rho_1-\rho_2)\zeta + t(\rho_1\eta_1 v_1 + \rho_2\eta_2 v_2)]\, dx. \tag{4.59}$$

All the globally conserved integrals (4.54), (4.56)–(4.59) are constants of motion on the solitary wave solution of Choi-Camassa model.

4.2 Computational Remarks

The Choi-Camassa equations (3.12)–(3.15) have 46 terms with four parameters $h_1,\ h_2,\ \rho_1,\ \rho_2$, and one constant g. The highest order of derivative of the equations is three. As such all computations for constructing conservation laws of the Choi-Camassa model cannot be done by hand written calculations. One might need to use computational software to save time, and to find accurate results.

For computing conservation laws, we used the Maple-based software **GeM** [4]. First, we declare the arbitrary constants, independent variables, dependent variables and Choi-Camassa equations (3.12)–(3.15) in the solved form with respect to the leading terms $\zeta_t,\ \zeta_x,\ v_{1txx},\ v_{2txx}$ respectively. Note that it is not necessary to write the system as a solved form in the leading derivatives, rather it could be solved for any function or derivative in the equation. We input the multipliers of the form $\Lambda_\sigma(x, t, \zeta, v_1, v_2, P),\ \sigma = 1, ..., 4$, a function of independent and dependent variables only. Since there are no derivatives in our considered Λ_σ, it is herein called zeroth order multiplier. The Euler operators given by (2.43) are the integrated tools in the **GeM** package which reads these operators automatically when one calls for conservation law determining equations. The determining equations (4.4)–(4.4) are obtained by applying the Euler operators

$E_\zeta,\ E_{v_1},\ E_{v_2},\ E_P$ for the respective variables $\zeta,\ v_1,\ v_2,\ P$ to the linear combination of the equations (3.12)–(3.15) and multipliers Λ_σ. Since Euler operators involve terms up to 3rd order derivatives and total derivative operators (2.10), the application of the Euler operators accumulates thousands of terms and splits into an overdetermined linear homogeneous PDE system with 324 equations for four unknowns $\Lambda_\sigma,\ \sigma = 1, ..., 4$. The split is done by collecting the coefficients of the similar terms and equating to zero. For solving this overdetermined PDE system one may need substitution, separation of variables, integration, etc. Before doing these operations, a differential reduction has been done by the Maple **rifsimp** algorithm which is essentially an extension of the Gaussian elimination algorithm to a system of PDEs. The determining equations do not involve any transcendental functions, and so **rifsimp** works fine. After applying **rifsimp** operation, there remain 17 linear partial differential equations to solve. Some of these equations involve more than one unknown and they are not separable. The dimension of the solution space was infinity. The general solution is found by using Maple **pdsolve** solver. Since the dimension of the solution space is infinite, the solution here is particular. The solution involved one arbitrary function $\Upsilon(\varpi, t)$, where $\varpi = \eta_1 v_1 + \eta_2 v_2$, and three arbitrary constants. For each arbitrary function and for each arbitrary constant, there is a linearly independent solution set. Thus we obtained four sets of conservation laws multipliers which can be seen in the Theorems 4.1.1 and 4.1.2. For computing fluxes, the direct conservation law construction method has been used. By applying multipliers to the Choi-Camassa equations and then by hand calculations, we derive all the densities and corresponding fluxes. Thus, we have four conservation laws for the zeroth order multipliers as shown in Section 4.1.

Next, one may consider multipliers involving independent variables, dependent variables, and all first order derivatives of $\zeta,\ v_1,\ v_2$, and P. It was beyond our ability to perform computation with multiplier functions up to all first order derivatives. This is because the reductions became impossible due to complex structures of the determining equations. Further, one can consider multiplier functions up to second order derivatives or higher. However, we were unable to find conservation laws with all possible second order derivatives due to tons of terms in the determining equations with a complex structure. For both cases, we have used a powerful computer with 128 GB memory to solve the determining equations. But it was even not possible to finish the **rifsimp** operation.

Instead, we input the multipliers of the form $\Lambda_\sigma(x, t, \zeta, v_1, v_2, P, v_{1x}, v_{2x}, v_{1xx}, v_{2xx}),\ \sigma = 1, ..., 4$, a function of independent and dependent variables and up to some second order derivatives. This time the determining equations gather a large number of terms (few thousands) yielding a split system containing 528 linear homogeneous PDEs. As a consequence, the **rifsimp** operation takes a long time to finish its differential reduction. With the current form of the multipliers, the reduced determining system has been solved again by using MAPLE **pdsolve** solver. The general solution to the determining system contains an arbitrary function, and six arbitrary constants. Writing this general solution into seven linearly independent solu-

tions, we got seven sets of multipliers of which three are exactly as we found for the zeroth order multipliers. Hence, in this case, we have four new conservation law multiplier sets, one of which is first order given in the Theorem 4.1.3 and three of which are second order given in the Theorem 4.1.4. Again by hand calculations, we get seven conservation laws, three of which are included in the zeroth order conservation laws, one first order, and three second order conservation laws. Thus we compute a subset of all local conservation laws of the Choi-Camassa model. Note that one can use Kovalevskaya form of the Choi-Camassa equations (3.12)–(3.15) to derive a complete set of conservation laws.

To verify the correctness of our computed local conservation laws, we also use **GeM** package under MAPLE. We apply total derivative operators to the density and corresponding flux of each conservation law, and use the equations (3.12)–(3.15) to substitute the expressions for $\zeta_t,\ v_{1t},\ v_{2t}$ and for their differential consequences. We then simplify and see that all the terms cross out. Hence, conservation law is verified. We repeat the process for verifying other conservation laws.

Chapter 5

Solutions to the Choi-Camassa Model

The Choi-Camassa equations admit an internal solitary wave solution for zero boundary conditions (3.22) at infinity. Because of the complicated nature of fluids, the closed form of exact solutions of the Choi-Camassa equations are yet to be studied. Until now the only way to solve the system is numerically after reducing the equations to an ODE using the travelling wave ansatz with zero boundary condition at anfinity. Camassa *et al* [62] studied and analyzed the structure of the periodic solutions with non-zero boundary condition, for which they have obtained approximate solutions. With one zero asymptotic state and one non-zero asymptotic state the system admits kink solutions. A complicated structure has been established for kink solutions (see, e.g., [38]), but the authors [38] did not produce any explicit kink solution. In this chapter, we briefly review the periodic solutions, produce space plots of the solitary wave solutions and the kink solutions of the Choi-Camassa model. We then plot the conserved densities of the Choi-Camassa model on the solitary wave solution and on the kink solution.

5.1 Periodic Solutions

The Choi-Camassa equations (3.12)–(3.15) for inviscid, incompressible fluids admit periodic travelling-wave solutions. These solutions for the Choi-Camassa model of long internal wave propagation are derived in [62], with the aim of providing structure to the parametric space of existence of such waves for the parent Euler system. To construct the periodic solutions, the authors in [62] considered a travelling wave ansatz:

$$\xi = x - ct, \quad v_i(x,t) = v_i(\xi), \quad P(x,t) = P(\xi), \tag{5.1}$$

where ξ is travelling wave coordinate, and c is the wave speed. By the transformation (5.1), the equations (3.12)–(3.13) become a system of ODEs in ξ. After one integration in ξ, one gets

$$-c\eta_i + \eta_i v_i = C_i, \quad i = 1, 2 \tag{5.2}$$

with $\eta_1(\xi) = h_1 - \zeta(\xi),\ \eta_2(\xi) = h_2 + \zeta(\xi)$, where $C_1,\ C_2$ are integrating constants. Eliminating pressure between the two momentum equations (3.14)–(3.15), and substituting (5.2) yields a third order ODE:

$$\left(\frac{\rho_1 C_1^2}{\eta_1^3} + \frac{\rho_2 C_2^2}{\eta_2^3} - \gamma\right)\zeta' = \frac{\rho_1}{\eta_1}\left(\frac{1}{3}\eta_1^3 G_1\right)' - \frac{\rho_2}{\eta_2}\left(\frac{1}{3}\eta_2^3 G_2\right)' \tag{5.3}$$

with $\gamma = g(\rho_2 - \rho_1)$, where $'$ denotes derivative with respect to ξ. In order to separate variables, the authors [62] integrate this ODE (5.3) once directly and once with the integrating factor η_1, and collect two more integration constants $C_3,\ C_4$. By eliminating the common second derivative ζ'' between the resulting equations, one obtains the following nonlinear ODE for the interfacial displacement $\zeta(\xi)$:

$$\zeta'^2 = 3\,\frac{\rho_1 C_1^2\eta_2 + \rho_2 C_2^2\eta_1 - \gamma\zeta^2\eta_1\eta_2 + 2C_3\eta_1^2\eta_2 - 2C_4\eta_1\eta_2}{\rho_1 C_1^2\eta_2 + \rho_2 C_2^2\eta_1} \equiv \frac{3\tilde{P}(\zeta)}{\rho_1 C_1^2\eta_2 + \rho_2 C_2^2\eta_1}, \tag{5.4}$$

where $\tilde{P}(\zeta)$ is a polynomial of degree four given by

$$\tilde{P}(\zeta) = \rho_1 C_1^2\eta_2 + \rho_2 C_2^2\eta_1 - \gamma\zeta^2\eta_1\eta_2 + 2C_3\eta_1^2\eta_2 - 2C_4\eta_1\eta_2. \tag{5.5}$$

The numerator of (5.4) is positive for large ζ with

$$\lim_{\zeta\to\pm\infty} \tilde{P}(\zeta) = +\infty,$$

while the denominator of (5.4) is always positive inside the physical domain $[-h_2, h_1]$ since $\rho_1 C_1^2\eta_2 + \rho_2 C_2^2\eta_1 > 0$ [62]. Let r_d denotes the root of the denominator of (5.4). Consequently r_d is outside the physical domain. For periodic solutions to exist, there needs to be two roots of the numerator $\tilde{P}(\zeta)$, with $\tilde{P} > 0$ between these two roots. Hence, there must be four real roots of the polynomial $\tilde{P}(\zeta)$ to have periodic solutions (see [62] for details). These roots can be ordered by magnitude, $r_1 < r_2$, etc., and periodic solutions will vary between the trough at r_2 and the crest at r_3, see Figure 5.1.

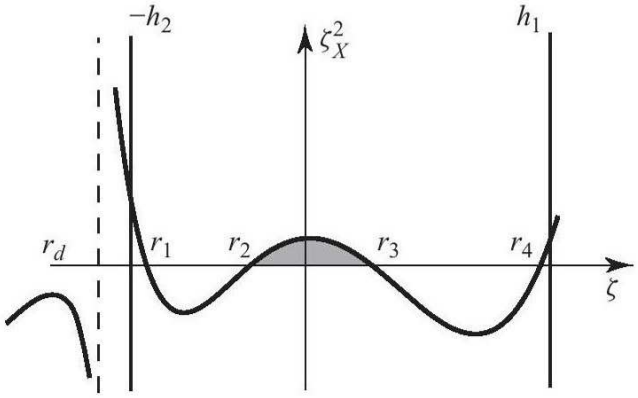

Figure 5.1: Potential of the quadrature (5.4) [62]

The two constants of integration in the quadrature C_1 and C_2 are related to the phase speed and mean heights

$$C_1 = -c\tilde{h}_1, \quad C_2 = -c\tilde{h}_2, \tag{5.6}$$

where $\tilde{h}_1$ ($\tilde{h}_2$) denotes the period-average of η_1 (η_2). The constants C_3 and C_4 can be determined by seeking waves of amplitude A and imposing the mean interface displacement $\tilde{\zeta}$ to zero:

$$\mathscr{A}(c, C_3, C_4) = A, \quad \tilde{\zeta}(c, C_3, C_4) = 0. \tag{5.7}$$

The authors [62] first related the two remaining constants of integration C_3 and C_4 to the position of the crest and the position of the trough, which are given by the middle roots of the quartic polynomial from the numerator of (5.3). If α is the position of the crest (so αA is the position of the trough), then C_3 and C_4 are functions of α since α and αA must be roots of the polynomial $P(\zeta)$. By imposing this condition and solving the resulting linear system, one has

$$C_3(\alpha) = \frac{c^2\rho_1 h_1^2}{2(h_1-\alpha)(h_1-\alpha+A)} - \frac{c^2\rho_2 h_2^2}{2(h_2+\alpha)(h_2+\alpha-A)} - \gamma(\alpha - A/2), \tag{5.8}$$

$$C_4(\alpha) = C_3(\alpha)(A+h_1-\alpha) + \frac{c^2\rho_1 h_1^2}{2(A+h_1-\alpha)} - \frac{c^2\rho_2 h_2^2}{2(A-h_2-\alpha)} - \frac{\gamma}{2}(A-\alpha)^2. \tag{5.9}$$

The quadrature (5.4) remains to be solved for the periodic solutions. Several results [62] have been presented by the authors. First, they have identified analytically the domain of existence of the periodic solutions in the two-parameter space of amplitude and speed. A class of numerical solutions of the periodic waves were then constructed for the two parameter family (speed and amplitude). Second, they worked to determine the regions within the domain of existence of periodic solutions of the nonlinear Choi-Camassa model where one can expect good agreement with Euler solutions. Third, they validated the Choi-Camassa model for periodic waves by comparison to the Euler solutions. The model predictions are very good approximations of the full Euler system.

The authors of [62] showed the existence condition for periodic solutions. They considered α-range by

$$\alpha_{min}(A,c) \equiv \alpha(A,c)\Big|_{r_1(\alpha;A,c)=r_2(\alpha;A,c)} \tag{5.10}$$

and

$$\alpha_{max}(A,c) \equiv \alpha(A,c)\Big|_{r_3(\alpha;A,c)=r_4(\alpha;A,c)}. \tag{5.11}$$

The polynomial $P(\zeta)$ has double roots given by

$$\beta_e(A,c) = r_1 = r_2 = \alpha_{min}(A,c) - A, \tag{5.12}$$

$$\beta_d(A,c) = r_3 = r_4 = \alpha_{max}(A,c). \tag{5.13}$$

Note also that these are not limiting forms of the class of periodic waves that satisfy the requirements described earlier. Thus, the necessary condition for existence of a periodic solution [62] is given by

$$\beta_e(A,c) < 0 < \beta_d(A,c). \tag{5.14}$$

The solution plots are shown in the Figure 5.2 with the parameters given by

$$h_1/h_2 = 1/3, \quad \rho_1/\rho_2 = 0.99, \quad c/c_0 = 0.55, \quad A/h_1 = 1. \tag{5.15}$$

The solid curves in the Figure 5.2 denote the travelling wave solution profiles, and the right half for solitary waves. The location of the targeted mean level is marked by the dashed horizontal line and the quadratic

function $\tilde{P}(\zeta)$, shown by the dash-dotted curve, varies according to the placement of α in the allowable range from (a) to (c):

$$(a)\ \alpha = \beta_e(A,c) + A, \quad (b)\ \beta_e(A,c) < \alpha < \beta_d(A,c), \quad (c)\ \alpha = \beta_d(A,c). \tag{5.16}$$

The fluid is confined between the top and bottom walls at $z = h_1$ and $z = -h_2$, respectively. The dark grey strip 'highlights' the range of the interface function $\zeta(\xi)$ between the roots at α and $\alpha - A$, while the light grey strip identifies the allowable range determined by root coalescence at $\alpha - A = \beta_e(A,c)$ and $\alpha = \beta_d(A,c)$, corresponding to solitary waves of elevation and depression, respectively.

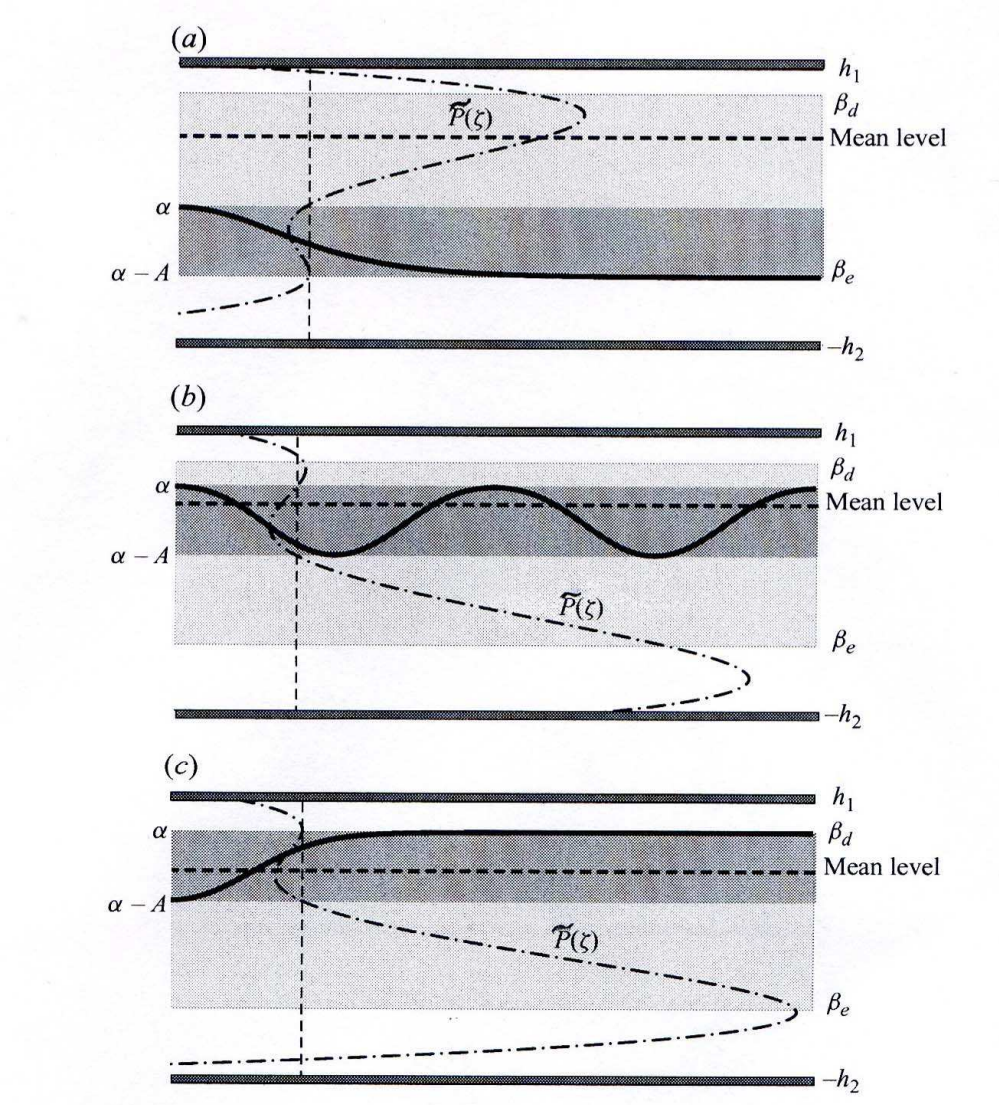

Figure 5.2: Periodic solution (solid line) of the Choi-Camassa model [62]

5.2 Kink Solution Structure

Important equations in terms of kink coordinates for the Choi-Camassa model equations have been obtained and analyzed in [38]. Consider first stationary solutions of the Choi-Camassa model equations which depend on a single variable $\xi = x - ct$, where $c =$ constant. Then, after elementary transformations, the system is reduced to a second-order ordinary differential equation (ODE) for the displacement ζ:

$$M(\zeta)\zeta'' + \frac{1}{2}M_\zeta \zeta'^2 + W_\zeta(\zeta) = 0, \tag{5.17}$$

where

$$M(\zeta) = \frac{\rho_1 B_1^2}{3\eta_1} + \frac{\rho_2 B_2^2}{3\eta_2}, \quad W(\zeta) = \frac{3}{2}M(\zeta) + \frac{\rho_1 - \rho_2}{2}g\zeta^2 + B_3\zeta, \tag{5.18}$$

with integration constants B_1, B_2, and B_3. To construct the solitary wave solution, the authors of [38] considered the asymptotic boundary conditions

$$\zeta = 0 \quad \text{and} \quad v_{1,2} = 0 \quad \text{as } x \to \pm\infty. \tag{5.19}$$

The integration constants are given by

$$B_1 = -ch_1, \quad B_2 = -ch_2, \quad B_3 = \frac{3}{2}M(0). \tag{5.20}$$

The equation (5.17) gives a family of solitary wave solutions with boundary conditions (5.19). These solutions can be characterized by two independent parameters: the coordinate of the soliton center S and its velocity c or, equivalently, its amplitude a. The possible values of the wave parameters lie within the intervals $c_0^2 < c^2 < c_m^2$ and $0 < a^2 < a_m^2$, where the maximum amplitude a_m is given by (3.58), and where c_0 and maximum velocity c_m are given by

$$c_0^2 = gh_1h_2\frac{\rho_2 - \rho_1}{\rho_1 h_2 + \rho_2 h_1}, \quad c_m = g(h_1 + h_2)\frac{1 - \sqrt{\rho_1/\rho_2}}{1 + \sqrt{\rho_1/\rho_2}}. \tag{5.21}$$

As $c \to c_m$ the solitary wave infinitely increases; at velocities close to c_m it has a tabletop shape with an amplitude close to a_m and relatively sharp edges kinks [38]. A single kink is a transition between two constant states. It has a unique velocity, $\zeta = c_m$, and is characterized by a single parameter, S, which is the coordinate of its center. The corresponding solution structure of (5.17) can be represented as

$$\frac{V+1}{|V-1|}\left(\frac{|V - V_m|}{V + V_m}\right)^{V_m} = Ae^{\pm K_0(\xi - S)}, \tag{5.22}$$

where S is the coordinate of the kink, and where

$$\zeta = \frac{a_m}{2} \quad \text{as } \xi = S, \tag{5.23}$$

$$V = \sqrt{1 + \zeta/a_*}, \quad V_m = \sqrt{1 + a_m/a_*}, \tag{5.24}$$

$$a_* = \frac{h_1 h_2(\rho_1 h_1 + \rho_2 h_2)}{\rho_1 h_1^2 - \rho_2 h_2^2}, \quad K_0^2 = \frac{3g(\rho_2 - \rho_1)a_m^2}{(\rho_2 h_2^2 - \rho_1 h_1^2)}, \tag{5.25}$$

$$A = \frac{V_{1/2}+1}{|V_{1/2}-1|}\left(\frac{|V_{1/2}-V_m|}{V_{1/2}+V_m}\right)^{V_m}, \quad V_{1/2} = \sqrt{1+\frac{a_m}{2a_*}}. \tag{5.26}$$

The signs + and − in (5.22) refer to the kinks of different polarities corresponding to frontal kink (ζ_f) and rear kink (ζ_r). For the frontal kink the transition happens from $\zeta = 0,\ u_{1,2} = 0$ as $\xi \to +\infty$ to $\zeta = a_m,\ u_{1,2} = U_{1,2} = \mp c_m a_m(h_{1,2} + a_m)$ as $\xi \to -\infty$, while for the rear kink it is from $\zeta = a_m,\ u_{1,2} = U_{1,2}$ as $\xi \to +\infty$ to $\zeta = 0,\ u_{1,2} = 0$ as $\xi \to -\infty$. The behaviour of kinks near their asymptotes $\zeta = 0$ and $\zeta = a_m$ is exponential. The soliton can be represented by joining two kinks together and has a tabletop shape with permanent form with an amplitude closer to the maximum amplitude a_m. Some non-trivial features of the two soliton interaction have also been studied in [38].

5.3 Solitary Wave Solutions

Consider a travelling-wave coordinate

$$\xi = x - ct - x_0 \tag{5.27}$$

with wave speed c and initially centered at x_0. Then using travelling-wave ansatz

$$\zeta(x,t) = \zeta(\xi),\ v_1(x,t) = v_1(\xi),\ v_2(x,t) = v_2(\xi), \tag{5.28}$$

the equations (3.12)–(3.13) can be converted into two ODEs which have the following solutions [86]

$$v_1(\xi) = \frac{-c\zeta(\xi)}{h_1 - \zeta(\xi)} \quad \text{and} \quad v_2(\xi) = \frac{c\zeta(\xi)}{h_2 + \zeta(\xi)} \tag{5.29}$$

respectively, where asymptotically

$$\zeta(\xi) \to 0 \text{ as } |\xi| \to \infty. \tag{5.30}$$

Using these results in equations (3.14)–(3.15) and then integrating twice one gets a 1st order ordinary differential equation [86]

$$\frac{d\zeta}{d\xi} = \pm\sqrt{\left(\frac{3g(\rho_2-\rho_1)}{c^2(\rho_1 h_1^2 - \rho_2 h_2^2)}\right)\frac{\zeta^2(\zeta - a_-)(\zeta - a_+)}{(\zeta - \kappa)}}, \tag{5.31}$$

where

$$\kappa = -\frac{h_1 h_2(h_1\rho_1 + h_2\rho_2)}{\rho_1 h_1^2 - \rho_2 h_2^2} \tag{5.32}$$

and $a_\pm$ are given by the two roots of the quadratic

$$a^2 + (h_2 - c^2/g - h_1)a + h_1 h_2(c^2/c_0^2 - 1) = 0 \tag{5.33}$$

with

$$c_0^2 = \frac{g h_1 h_2(\rho_2 - \rho_1)}{\rho_2 h_1 + \rho_1 h_2}. \tag{5.34}$$

The solitary wave solution exists [86] if either one of the three conditions

$$(i)\ h_1/h_2 > (\rho_2/\rho_1)^{1/2}, \quad \kappa < 0 < \zeta \le a_- < a_+, \tag{5.35}$$

$$(ii)\ h_1/h_2 < (\rho_2/\rho_1)^{1/2}, \quad \kappa > 0 > \zeta \ge a_+ > a_-, \tag{5.36}$$

$$(iii)\ (\rho_1/\rho_2)^{1/2} < h_1/h_2 < (\rho_2/\rho_1)^{1/2}, \quad 0 < \zeta \le a_- < a_+ < \kappa \tag{5.37}$$

is satisfied. The solitary wave solution of the ODE (5.31) is of *elevation* [86] if the heights and densities of the two fluids satisfy a relation

$$h_1/h_2 > (\rho_2/\rho_1)^{1/2} \tag{5.38}$$

which implies that $a_- > 0$, and of *depression* if

$$h_1/h_2 < (\rho_2/\rho_1)^{1/2}. \tag{5.39}$$

No solitary wave solution exists for $h_1/h_2 = (\rho_2/\rho_1)^{1/2}$. The wave speed c is given by

$$c^2 = c_0^2 \frac{(h_1 - \chi)(h_2 - \chi)}{h_1 h_2 - (c_0^2/g)\chi} \tag{5.40}$$

with wave amplitude χ, and satisfies the relation

$$c^2 > c_0^2. \tag{5.41}$$

The wave amplitude and speed are limited by

$$\chi \le \frac{h_1 - h_2\sqrt{\rho_1/\rho_2}}{1 + \sqrt{\rho_1/\rho_2}}, \quad c^2 \le g(h_1 + h_2)\frac{1 - \sqrt{\rho_1/\rho_2}}{1 + \sqrt{\rho_1/\rho_2}}. \tag{5.42}$$

With the asymptotic result (5.30), the ODE (5.31) has an asymptotic form for $|\xi| \to \infty$:

$$\frac{d\zeta}{d\xi} \simeq \pm\sqrt{\mu}\,\zeta, \quad \mu = \frac{3ga_-a_+(\rho_1 - \rho_2)}{\kappa c^2(\rho_1 h_1^2 - \rho_2 h_2^2)} > 0. \tag{5.43}$$

The solution of the ODE (5.43) is

$$\zeta \simeq \zeta_0 \exp(\pm\sqrt{\mu}\,\xi) \tag{5.44}$$

for an initial solution ζ_0 at $\xi = 0$. Hence, the equation (5.31) admits a solitary wave solution with exponential diminishing tail.

We now produce some space plots of solution parameters. Under the space translation $x \to x + x_0$ we transfer the center of the travelling wave coordinate at 0 initially. We list here the fixed parameters

$$g = 9.8\ \text{m/s}^2, \quad h_2 = 1\ \text{m}, \quad \rho_2 = 1000\ \text{kg/m}^3. \tag{5.45}$$

We take $h_1 = 5$ m, $\rho_1 = 600$ kg/m^3 to satisfy the condition (5.38) and compute $c_0,\ a_\pm,\ \kappa$. The initial solution $\zeta_0 = a_- - 10^{-6}$ is chosen such that to satisfy (5.35) and to produce the numerical solution with different wave speed as seen in the Figure 5.3.

One can produce similar solitary wave solutions satisfying any one of the existence conditions (5.36) and (5.37). For the condition (5.36), the solitary waves have bottom orientations.

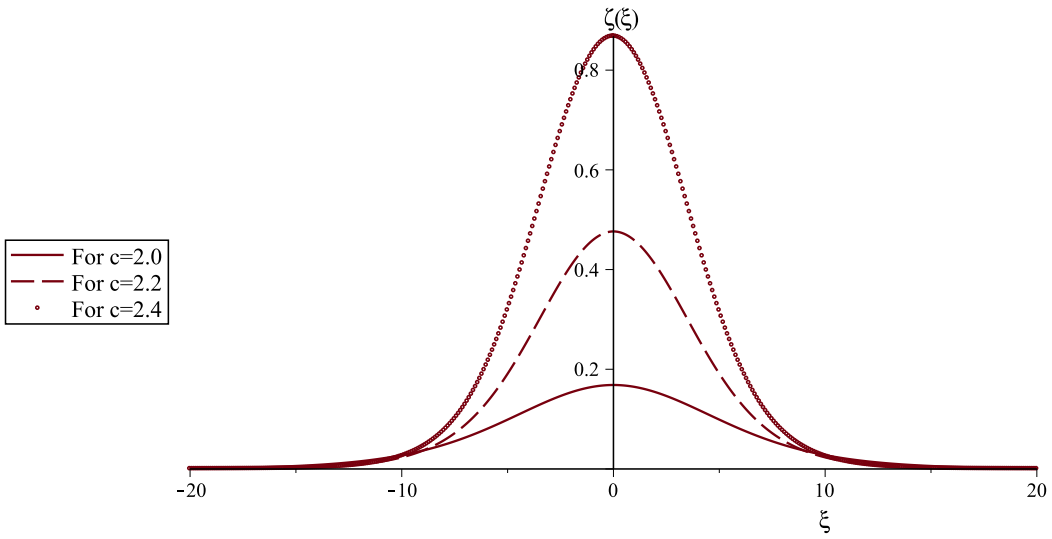

Figure 5.3: Solitary wave solutions for three different wave speeds

5.4 Kink and Anti-Kink Solutions

We are now interested in finding the kink and the anti-kink solutions of the two-fluid system considering the property that the solution ζ approaches 0 as $\xi \to -\infty$ and a constant as $\xi \to +\infty$ for the kink while ζ interpolates between 0 as $\xi \to +\infty$ and a constant as $\xi \to -\infty$ for the anti-kink. Thus $\zeta(\xi)$ satisfies the condition $\zeta \to \zeta_{\pm} = const$. This implies the asymptotic boundary conditions

$$\frac{d\zeta}{d\xi}(\pm\infty) = \frac{d^2\zeta}{d\xi^2}(\pm\infty) = 0. \tag{5.46}$$

The kink and the anti-kink solutions exist subject to the same conditions (5.35)–(5.41). We now determine the values of ζ at the boundary. At $\xi \to \pm\infty$, we use the boundary condition (5.46) into the ODE (5.31) to get

$$\zeta(\pm\infty) = 0 \quad \text{or} \quad \zeta(\pm\infty) = a_- \quad \text{or} \quad \zeta(\pm\infty) = a_+. \tag{5.47}$$

But for $\zeta(\pm\infty) = 0$, the solution reduces to the above exponentially decaying solitary wave (5.44). Hence, for the kinks wave either $\zeta_{\pm} = a_-$ or $\zeta_{\pm} = a_+$ with

$$a_{\pm} = \frac{1}{2}(h_1 - h_2) + \frac{c^2}{2g} \pm \sqrt{\frac{1}{4}(h_1 - h_2 + \frac{c^2}{g})^2 + h_1 h_2 (1 - \frac{c^2}{c_0^2})}. \tag{5.48}$$

First, we consider the condition (5.35) where $\zeta > 0$ always. The ODE (5.31) with positive sign corresponds to the kink wave and negative sign corresponds to the anti-kink. To produce the kink and the anti-kink solution of the wave of elevation, we compute a_- from (5.48). Then, we use the same parametric values and same initial solution as we have taken for the solitary wave solution above. The space plots for solution parameters with three different values of c are seen in the Figure 5.4.

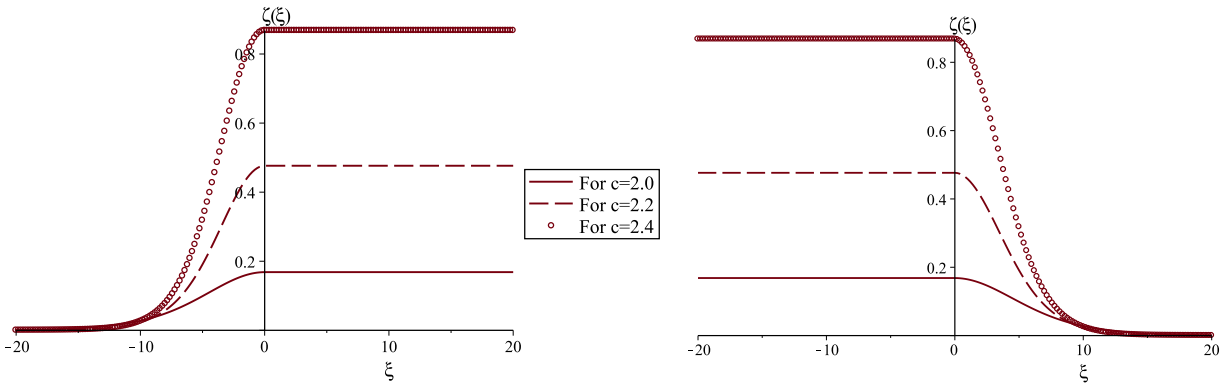

Figure 5.4: Kink and anti-kink solutions for $\kappa < 0 < \zeta \leq a_- < a_+$

Next we consider the condition (5.36) where $\zeta < 0$ always. In this case, the ODE (5.31) with negative sign corresponds to the kink solution and that is with positive sign corresponds to the anti-kink. We compute a_+ from the formula (5.48) and list the fixed parameters:

$$g = 9.8 \text{ m/s}^2, \quad h_1 = 1 \text{ m}, \quad \rho_2 = 1000 \text{ kg/m}^3 \tag{5.49}$$

Take $h_2 = 5$ m, $\rho_1 = 600$ kg/m^3 to satisfy the condition (5.41) and compute c_0, a_-, κ. Let the initial solution $\zeta_0 = a_+ + 10^{-6}$ and produce the numerical solution with different wave speed as seen in the Figure 5.5.

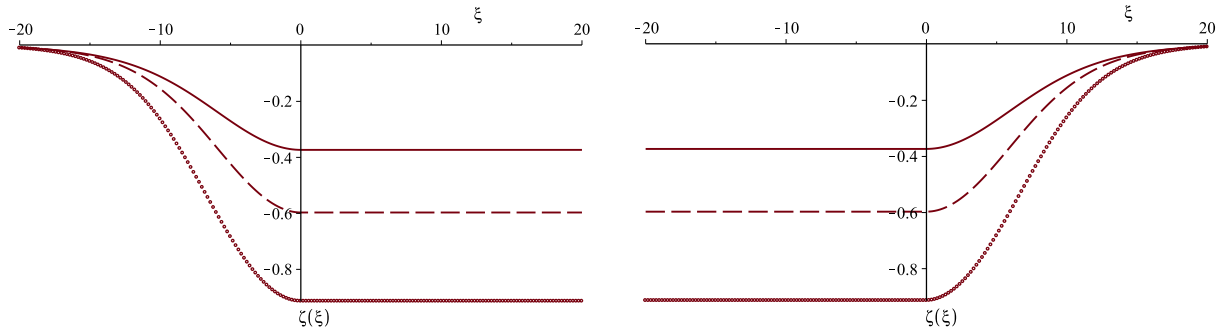

Figure 5.5: Kink and anti-kink solutions for $\kappa > 0 > \zeta \geq a_+ > a_-$

The same ODE (5.31) is found if we consider a left travelling-wave ansatz $\zeta(x,t) = \zeta(\xi)$, $\xi = x + ct$ and all the conditions (5.35)–(5.41) remain invariant for $c \to -c$. Therefore, the same kink and anti-kink solutions are produced as shown in the Figures 5.4 and 5.5 for the negative wave speed apart from changing the direction of the fluid motions. For this reason, kinks waves with wave profile $\zeta(x + ct)$ with negative wave speed also show the same asymptotic behaviour as shown for the wave profile $\zeta(x - ct)$ with positive wave speed.

5.5 Plots of Local Conserved Quantities for Solitary Waves and Kink Waves

On the solitary wave solution $\zeta(x,t)$ of the two-fluid system, the computed densities will be localized conserved quantities if and only if the densities $T^{\alpha},\ \alpha = 1,...,7$ decays rapidly as $x \to \pm\infty$ and also the corresponding fluxes vanish for $x \to \pm\infty$. We will now determine which of the densities produce a localized conserved quantity for the solitary wave solution obtained in the previous section. To do that we first substitute the solutions $v_1,\ v_2$, given by (5.29), into the densities after converting an ODE by transformations (5.27)–(5.28). Then we insert the numerical solution of $\zeta(\xi)$ into the converted ODE and plot to compare with the solution $\zeta(\xi)$. We observe that all densities have exponentially decaying tails for $\xi \to \pm\infty$. These decaying behaviours are seen in the Figures 5.6, 5.7 and 5.8:

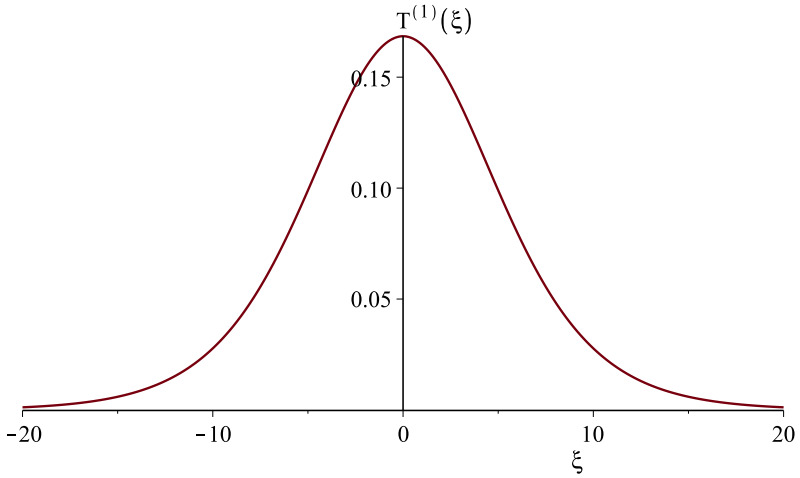

Figure 5.6: The density $T^{(1)}$ for the solitary wave solution

Similarly on the kink waves, the densities will be finite conserved quantity if and only if the densities $T^{\alpha},\ \alpha = 1,...,7$ decays rapidly for one asymptotic state and approaches a constant for another asymptotic state, and also the corresponding fluxes vanish for $x \to \pm\infty$. We plot all the densities by similar procedure as we have done for solitary wave solution above. These plots are shown in the Figures 5.9, 5.10 and 5.11.

It is clear that all these densities are localized conserved quantities for the solitary wave solution. But for the kinks solution, all densities except $T^{(3)}$ are conserved and finite. The density $T^{(3)}$ is conserved but not finite on the kinks solution. Thus the solitary wave and kinks wave for the two-fluid system do not gain or lose any amount in the physical quantities $T^{(\alpha)},\ \alpha \neq 3$ during their propagation.

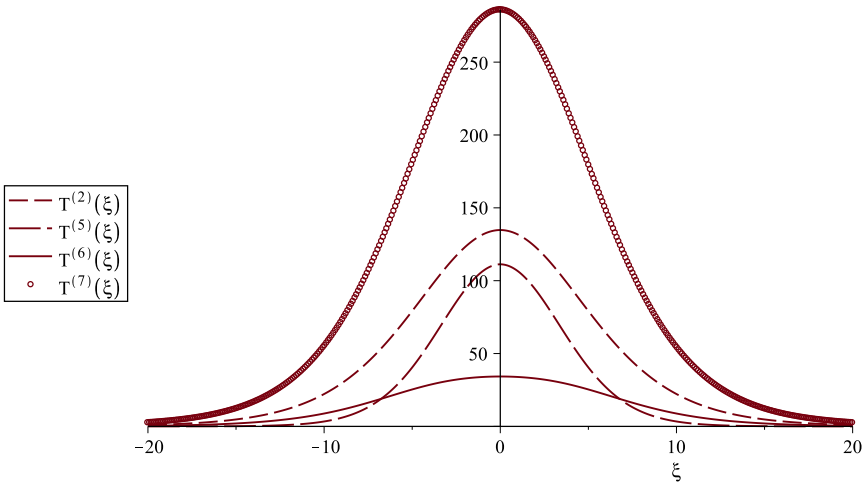

Figure 5.7: The densities $T^{(2)}$, and $T^{(5)} - T^{(7)}$ for the solitary wave solution

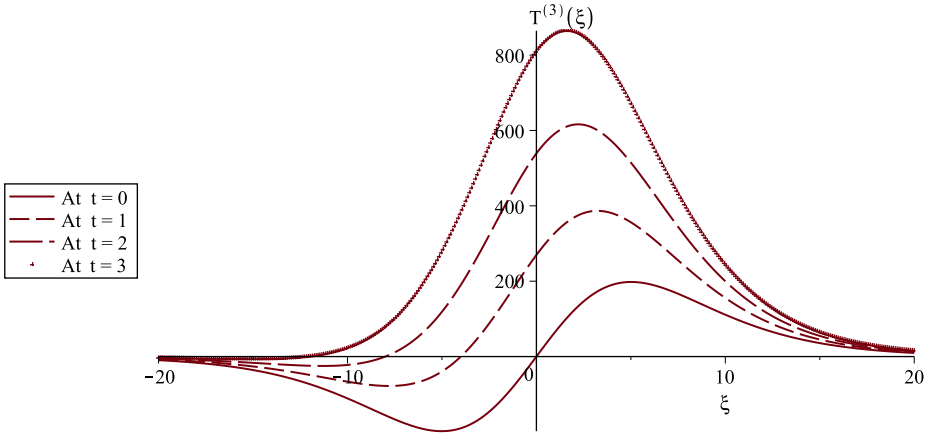

Figure 5.8: The density $T^{(3)}$ at various times for the solitary wave solution

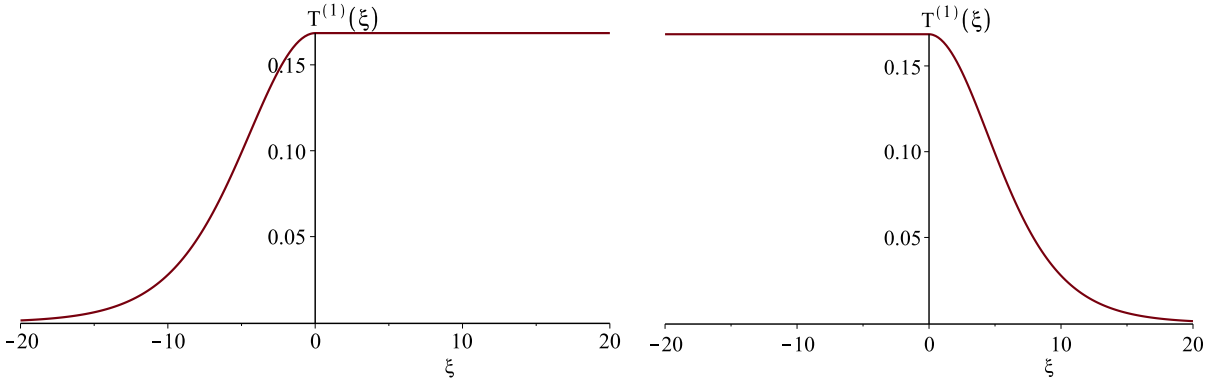

Figure 5.9: The density $T^{(1)}$ for the kink and anti-kink solutions

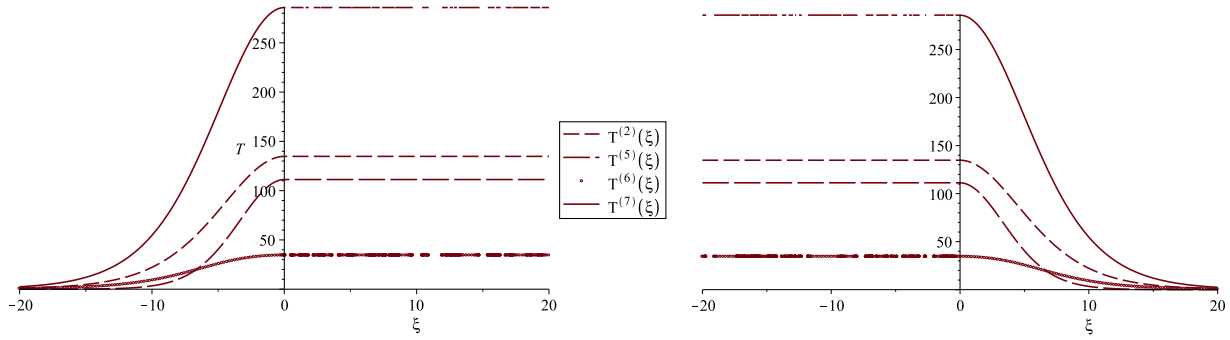

Figure 5.10: The densities $T^{(2)}$, and $T^{(5)} - T^{(7)}$ for the kink and anti-kink solutions

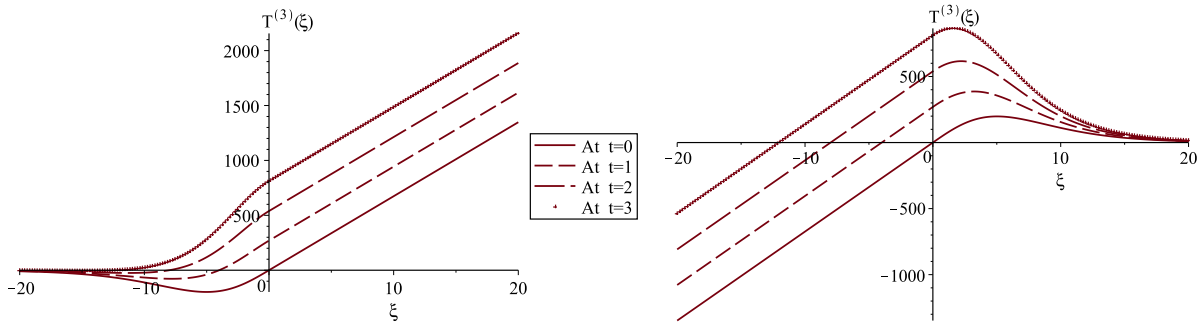

Figure 5.11: The density $T^{(3)}$ at various times for the kink and anti-kink solutions

Chapter 6

Conclusion

We divide this Chapter into two portions: (i) discussion about our accomplished results, and (ii) open problems related to the Choi-Camassa model.

Discussion

We systematically constructed local conservation laws of the Choi-Camassa model equations (3.12)–(3.17) by applying the direct conservation law construction method, where we considered multipliers involving independent variables $x,\ t$, dependent variables $\zeta,\ v_1,\ v_2,\ P$, and derivatives of $v_1,\ v_2$ with respect to x. In Chapter 4, we obtained several new results. First, we derived non-singular multipliers function up to second order derivatives as presented in the Theorems 4.1.1 to 4.1.4. Second, using these multipliers, we derived local conserved densities and corresponding fluxes for mass, total horizontal momentum, energy, and irrotationality. In addition to these physical quantities, we constructed two additional local conserved densities and corresponding fluxes. The meaning of these two conservation laws is yet to be understood.

In Chapter 5, we studied the periodic solution, solitary wave solution, and kink solution of the Choi-Camassa model. With non-zero boundary condition of $\zeta,\ v_1,\ v_2$ periodic travelling wave solutions are presented in Section 5.1, while for zero boundary condition at infinity, the solitary wave solutions were given in Section 5.3. For zero boundary condition at one asymptotic state ($x \to -\infty$) together with non-zero boundary condition at another asymptotic state ($x \to \infty$), kink travelling wave solutions were presented in Section 5.4. We then plotted the conserved quantities of the Choi-Camassa model on the solitary wave solutions and on the kink solutions in Section 5.5. All these quantities have exponentially decaying behavior on the solitary wave solutions, which guarantee their global conservation. On the kink solutions, all these conserved quantities except $T^{(3)}$ have an exponentially decaying tail at one asymptotic state and are constant at another asymptotic state. These quantities are conserved globally except $T^{(3)}$.

The computed conservation laws are important in many aspects. For example, the derived conservation laws can be used for developing conserved numerical schemes to get more stable numerical solutions of the Choi-Camassa system, and can be an essential starting point for finding nonlocally related PDE systems of the Choi-Camassa equations.

Open Problems Related to Choi-Camassa Model

In this work, we derived conservation laws multipliers including some second order derivatives and computed basic local conservation laws of the Choi-Camassa model. Fluid model, the Euler system (1.38) and (1.45), admits special types of conserved physical quantities like conservation of vorticity, center of vorticity, helicity of vorticity, etc. It is unknown whether such conserved quantities hold for the Choi-Camassa model. The one way to verify this is to find all possible conservation laws of the Choi-Camassa system. To find a full set of conservation laws for each order, one needs to re-write the Choi-Camassa equations in the extended Kovalevskaya form and then find the conservation laws of this Kovalevskaya form. This, however, presents a significant computational challenge.

Another related research direction is to find the nonlocally related PDE systems. The nonlocally related PDE system is also known as potential system of the given PDE system. Let $v(t,x)$ be a nonlocal variable. Then, the conservation laws (4.1) yields a couple of potential equations

$$v_x = T(x,t,\zeta,v_1,v_2,P,\cdots), \tag{6.1}$$

$$v_t = X(x,t,\zeta,v_1,v_2,P,\cdots). \tag{6.2}$$

Thus each conservation law in Chapter 4 gives a distinct potential system with different non-local variables. The relationship between the given PDE system and the potential system is nonlocal, i.e., there does not exist a one-to-one local transformation connecting the solutions of the given PDE system and the potential system. Within such a relationship, it follows that a conservation law of a potential PDE system yields a conservation law of the given PDE system, and the converse statement also holds. Nonlocally related PDE systems may be useful to find the solution of the given PDE system from solutions of the nonlocally related PDE systems. Hence potential systems of the Choi-Camassa system are promising in many aspects.

The Lie point symmetries of the Choi-Camassa system are presented here. To compute these, we consider a symmetry generator of the form

$$Y = \xi^{(t)}\frac{\partial}{\partial t} + \xi^{(x)}\frac{\partial}{\partial x} + \eta^{(\zeta)}\frac{\partial}{\partial \zeta} + \eta^{(v_1)}\frac{\partial}{\partial v_1} + \eta^{(v_2)}\frac{\partial}{\partial v_2} + \eta^{(P)}\frac{\partial}{\partial P}. \tag{6.3}$$

where all the symmetry components are function of $x,\ t,\ \zeta,\ v_1,\ v_2,\ P$. Then proceeding the Lie's algorithm described in Chapter 2 and using the Maple based software **GeM**, the point symmetries for the Choi-Camassa system (3.12)–(3.15), with the condition $h_1 + h_2 \neq 0$, are found as

$$Y_1 = \frac{\partial}{\partial x}, \qquad Y_2 = \frac{\partial}{\partial t}, \qquad Y_3 = t\frac{\partial}{\partial x} + \frac{\partial}{\partial v_1} + \frac{\partial}{\partial v_2}, \tag{6.4}$$

$$Y_4 = \Upsilon\Big((h_1-\zeta)v_1 + (h_2+\zeta)v_2, t\Big)\frac{\partial}{\partial P}. \tag{6.5}$$

For the symmetry generators $Y_1, ..., Y_4$, the Choi-Camassa system (3.12)–(3.15) has four classes of Lie groups of point transformations:

$$\text{space translation} \qquad G_1 : (x + \lambda, t, \zeta, v_1, v_2, P), \tag{6.6}$$

$$\text{time translation} \qquad G_2 : (x, t + \lambda, \zeta, v_1, v_2, P), \tag{6.7}$$

$$\text{Galilean boosts} \qquad G_3 : (x - \lambda t, t, \zeta, v_1 + \lambda, v_2 + \lambda, P), \tag{6.8}$$

$$\text{pressure translation} \qquad G_4 : (x, t, \zeta, v_1, v_2, P + \Upsilon(t, w)\lambda), \tag{6.9}$$

where $-\infty < \lambda < +\infty$, $w = (h_1 - \zeta)v_1 + (h_2 + \zeta)v_2$, and Υ is an arbitrary function. One can easily verify that the Choi-Camassa system is invariant under these transformations. The Choi-Camassa system is also invariant under the time inversion:

$$t \to -t,\ \zeta \to \zeta,\ v_1 \to -v_1,\ v_2 \to -v_2,\ P \to P. \tag{6.10}$$

It remains an open problem to provide a variational formulation of the Choi-Camassa system, if it exists (see Chapter 2). If such a formulation exists, the Noether's theorem and variational symmetries could be used to compute conservation laws of the Choi-Camassa model.

Considering the analogy of 1D Choi-Camassa model [86] and the regularized model [87], Barros & Choi derived a two-dimensional nonlinear model [90] in a closed channel for two incompressible fluids with different densities. Also a hydrostatic model for N-layers fluid has been developed in [88] by approximating the two-dimensional Euler system for incompressible fluid in a closed channel. The 2D model and the multi-layers fluid model also admit conservation of mass, momentum and energy. Additional conservation laws similar to the 1D Choi-Camassa model might posses for these two models. The methodology that we have used in this thesis can be carried out to derive the conservation laws for both the hydrostatic model of N-fluids and the 2D model of two fluids. Solitary wave solutions and kink solutions exist under certain conditions on each fluid depth and density similar to the conditions (5.35)–(5.37).

Bibliography

[1] A. Enciso, D. P. Salas, Knots and links in steady solutions of the Euler equation, *Annals of Mathematics*, Vol. 175(1), pp. 345–367 (2012).

[2] A. E. Green, P. M. Naghdi, A derivation of equations for wave propagation in water of variable depth, *Journal of Fluid Mechanics*, Vol. 78 (02), pp. 237–246 (1976).

[3] A. E. Green, G. I. Taylor, Mechanism of the production of small eddies from larger ones, *Proceedings Royal Society A*, Vol. 158 (1937).

[4] A. F. Cheviakov, GeM software package for computation of symmetries and conservation laws of differential equations *Computer Physics Communications*, Vol. 176, pp. 48–61 (2007).

[5] A. F. Cheviakov, G. W. Bluman, On locally and nonlocally related potential systems, *Journal of Mathematical Physics*, Vol. 51(7) (2010).

[6] A. R. Paterson, *A First Course in Fluid Dynamics*, Cambridge University Press (1983).

[7] A. J. Chorin, J. E. Marsden, *A Mathematical Introduction to Fluid Mechanics*, New York: Springer, Vol. 3, (1990).

[8] A. J. Majda, A. L. Bertozzi, *Vorticity and Incompressible Flow*, Cambridge University Press (2002)

[9] A. S. Mia, Collision effects of solitary waves for the Gardner equation, *Interdisciplinary Topics in Applied Mathematics, Modeling and Computational Science, Springer International Publishing*, Chap. 44, pp. 309–314 (2015).

[10] A. S. Peters, J. J. Stoker, Solitary waves in liquids having non-constant density, *Communications on Pure and Applied Mathematics*, Vol. 13(1), pp. 115–164 (1960).

[11] B. B. Kadomtsev, V. I. Petviashvili, On the stability of solitary waves in weakly dispersing media, *Soviet Physics Doklady*, Vol. 15(6), pp. 539–541 (1970).

[12] C. G. Koop, G. Butler, An investigation of internal solitary waves in a two-fluid system, *Journal of Fluid Mechanics*, Vol. 112, pp. 225–251 (1981).

[13] C. H. Su, C. S. Gardner, Korteweg-de Vries equation and generalizations. III. Derivation of the Korteweg-de Vries equation and Burgers equation, *Journal of Mathematical Physics*, Vol. 10 (1969).

[14] C. Marchioro, M. Pulvirenti, *Mathematical Theory of Incompressible Nonviscous Fluids*, Springer Science & Business Media, Vol. 96 (1994).

[15] C. R. Ethier, D. A. Steinman, Exact fully 3D Navier-Stokes solutions for benchmarking, *International Journal for Numerical Methods in Fluids*, Vol. 19, pp. 369–375 (1994).

[16] C. R. Shalizi, Advanced data analysis from an elementary point of view, URL: `http://www.stat.cmu.edu/cshalizi/ADAfaEPoV/13`, 24 (2013).

[17] C. W. Shu, W. S. Don, D. Gottlieb, O. Schilling, L. Jameson, Numerical convergence study of nearly incompressible, inviscid Taylor-Green vortex flow, *Journal of Scientific Computing*, Vol. 24(1), pp. 1–27 (2005).

[18] C. Y. Wang, Exact solutions of the steady-state Navier-Stokes equations, *Annual Review of Fluid Mechanics*, Vol. 23(1), pp. 159–177 (1991).

[19] D. G. Dritschel, Generalized helical Beltrami flows in hydrodynamics and magnetohydrodynamics, *Journal of Fluid Mechanics*, Vol. 222, pp. 525–541 (1991).

[20] D. McLaughlin, O. Pironneau, Some notes on periodic Beltrami fields in Cartesian geometry, *Journal of Mathematical Physics*, Vol. 32(3), pp. 797–804 (1991).

[21] G. B. Whitham, Linear and nonlinear wave, *Journal of Applied Mechanics*, Vol. 46 (1976).

[22] G. B. Whitham, Variational methods and applications to water waves, *Proceedings of the Royal Society of London: Series A. Mathematical and Physical Sciences* Vol. 299 (1456), pp. 6–25 (1967).

[23] G. H. Keulegan, Characteristics of internal solitary waves, *Journal of Research of the National Bureau of Standards*, Vol. 51(3) (1953).

[24] G. K. Batchelor, *An Introduction to Fluid Dynamics*, Cambridge university press (2000).

[25] G. W. Bluman, S. Kumei, *Symmetries and Differential Equations*, Springer-Verlag NY (1989).

[26] G. W. Bluman, S. C. Anco, *Symmetry and Integration Methods for Differential Equations*, Springer Science & Business Media, Vol. 154 (2002).

[27] G. W. Bluman, A. F. Cheviakov, S. C. Anco, Construction of conservation laws: how the direct method generalizes Noether's theorem, *4th Workshop "Group Analysis of Differential Equations & Integrable Systems"*, pp. 13–35 (2009).

[28] G. W. Bluman, A. F. Cheviakov, S. C. Anco, *Applications of Symmetry Methods to Partial Differential Equations*, Springer Science+Business Media, LLC (2010).

[29] H. K. Moffatt, Helicity in laminar and turbulent flow, *Annual Review of Fluid Mechanics*, Vol. 24, pp. 281–312 (1992).

[30] J. B. Etnyre, R. W. Ghrist, Stratified integrals and unknots in inviscid flows, *Contemporary Mathematics*, Vol. 246, pp. 99–111 (1999).

[31] J. C. Bowman, Casimir cascades in two-dimensional turbulence, *Advances in Turbulence XII, Springer Proceedings in Physics*, Vol. 132, pp. 685–688 (2009).

[32] J. Grue, A. Jensen, P. O. Russ, J. K. Sveen, Properties of large-amplitude internal waves, *Journal of Fluid Mechanics*, Vol. 380, pp. 257–278 (1999).

[33] J. Hietarinta, A search for bilinear equations passing Hirota's three-soliton condition. I. KdV type bilinear equations, *Journal of Mathematical Physics*, Vol. 28(8), pp. 1732–1742 (1987).

[34] J. Hietarinta, A search for bilinear equations passing Hirota's three-soliton condition. II. mKdV-type bilinear equations, *Journal of Mathematical Physics*, Vol. 28(9), pp. 2094–2101 (1987).

[35] J. L. Johnson, C. R. Oberman, R. M. Kruskal, E. A. Frieman Some stable hydromagnetic equilibria, *Physics of Fluids*, Vol. 1(4), 281296 (1958).

[36] J. R. Apel, *Principles of Ocean Physics*, Academic Press (1987).

[37] K. A. Gorshkov, L. A. Ostrovskii, I. A. Soustova, N. V. Zaitseva, L. M. Shevts, Study of interaction between intense internal wave solitons in the context of the Choi-Camassa model, *Izvestiya, Atmospheric and Oceanic Physics*, Vol. 47(3), pp. 336–349 (2011).

[38] K. Gorshkov, L. A. Ostrovsky, I. Soustova, Dynamics of strongly nonlinear kinks and solitons in a two-layer fluid, *Studies in Applied Mathematics*, Vol. 126(1), pp.49–73 (2011).

[39] L. C. Berselli, On the large eddy simulation of the Taylor-Green vortex, *Journal of Mathematical Fluid Mechanics*, Vol. 7(2), pp. S164–S191 (2005).

[40] L. Ostrovsky, J. Grue, Evolution equations for strongly nonlinear internal waves, *Physics of Fluids*, Vol. 15, pp. 2934–2948 (2003).

[41] L. Prandtl, On fluid motions with very small friction, *Proceedings of the Third International Mathematical Congress, Heidelberg*, Vol. 3, pp. 484–491 (1904).

[42] L. R. Walker, Interfacial solitary waves in a two-fluid medium, *Physics of Fluids*, Vol. 16, 1796 (1973).

[43] M. Bineau, On the existence of force-free magnetic fields, *Communication on Pure and Applied Mathematics*, Vol. 25(1), pp. 77–84 (1972).

[44] M. C. Shen, Solitary waves in compressible media, *New York Univ Inst Mathematical Science*, Rep. IMM-NYU 325 (1964).

[45] M. C. Shen, Solitary waves in running gases, *New York Univ Inst Mathematical Science*, Rep. IMM-NYU 341 (1965).

[46] M. F. White, *Fluid Mechanics*, McGraw-Hill, Boston (2003).

[47] M. J. Ablowitz, A. S. Fokas, J. Satsuma, H. Segur, On the periodic intermediate long wave equation, *Journal of Physics A: Mathematics and General*, Vol. 15(3) (1982).

[48] M. J. Ablowitz, P.A. Clarkson , Solitons, *Nonlinear Evolution Equations and Inverse Scattering*, Cambridge University Press (1991).

[49] M. L. Alonso, On the Noether map, *Letters in Mathematical Physics*, Vol. 3(5), pp. 419–424 (1979).

[50] M. Miyata, Long internal waves of large amplitude, *Nonlinear Water Waves. Springer Berlin Heidelberg*, pp. 399–406 (1988).

[51] M. W. Dingemans, Water wave propagation over uneven bottoms: Linear wave propagation, *World Scientific*, Vol. 13 (1997).

[52] N. H. Ibragimov, *CRC Handbook of Lie Group Analysis of Differential Equations*, CRC Press Incorporation, Vol. 2 (1995).

[53] O. Kelbin, A. F. Cheviakov, M. Oberlack, New conservation laws of helically symmetric, plane and rotationally symmetric viscous and inviscid flows, *Journal of Fluid Mechanics*, Vol. 721, pp. 340–366 (2013).

[54] P. G. Drazin, R. S. Johnson, *Solitons: An Introduction*, Cambridge Texts in Applied Mathematics (1989).

[55] P. J. Olver, *Applications of Lie Groups to Differential Equations*, Springer-Verlag NY Incorporation, (1986).

[56] P. E. Hydon, *Symmetry Methods for Differential Equations: A Beginners Guide*, Cambridge University Press (2000).

[57] R. Barros, W. Choi, On regularizing the strongly nonlinear model for two-dimensional internal waves, *Physica D*, Vol. 264, pp. 27-34 (2013).

[58] R. Bruno, The solar wind as a turbulence laboratory, *Living Reviews in Solar Physics*, Vol. 10(2) (2013).

[59] R. Camassa, D. D. Holm, An integrable shallow water equation with peaked solitons, *Physical Review Letters*, Vol. 71(11) (1993).

[60] R. Camassa, D. D. Holm, C. D. Levermore, Long-time effects of bottom topography in shallow water, *Physica D: Nonlinear Phenomena*, Vol. 98(2), pp. 258–286 (1996).

[61] R. Camassa, W. Choi, H. Michallet, P. Rusas, J. K. Sveen, On the realm of validity of strongly nonlinear asymptotic approximations for internal waves, *Journal of Fluid Mechanics*, Vol. 549, pp. 1–24 (2006).

[62] R. Camassa, P. O. Rusas, A. Saxena, R. Tiron, Fully nonlinear periodic internal waves in a two-fluid system of finite depth, *Journal of Fluid Mechanics*, Vol. 652, pp. 259–298 (2010).

[63] R. E. Davis, A. Acrivos, Solitary internal waves in deep water, *Journal of Fluid Mechanics*, Vol. 29, part 3, pp. 593-607 (1967).

[64] R. L. Pego, I. Michael, Weinstein, Asymptotic stability of solitary waves, *Communications in Mathematical Physics*, Vol. 164, pp. 3005–349 (1994).

[65] R. K. Helfrich, W. K. Melville, Long nonlinear internal waves, Âannual Review of Fluid Mechanics, Vol. 38, pp. 395–425 (2006).

[66] R. R. Long, Long waves in a two-fluid system, *Journal of Meteorology*, Vol. 13 (1955).

[67] R. R. Long, Solitary waves in the one and the two-fluid systems, *Tellus A*, Vol. 8(4) (1956).

[68] S. C. Anco, G. Bluman, Direct construction method for conservation laws of partial differential equations. Part I: Examples of conservation law classifications, *European Journal of Applied Mathematics*, Vol. 13(5), pp. 545–566 (2002).

[69] S. C. Anco, G. Bluman, Direct construction method for conservation laws of partial differential equations. Part II: General treatment, *European Journal of Applied Mathematics*, Vol. 13(5), pp. 567–588 (2002).

[70] S. Lie, *Theorie der transformationgruppen*, B.G. Teubner, Leipzig, Vol. I (1880).

[71] S. Lie, *Theorie der transformationgruppen*, B.G. Teubner, Leipzig, Vol. II (1890).

[72] S. Lie, *Theorie der transformationgruppen*, B.G. Teubner, Leipzig, Vol. III (1893).

[73] S. V. Raman, Solitary waves in a two-fluid system in a channel of arbitrary cross section, *Tellus A*, Vol. 20, No. 4 (1968).

[74] T. Amari, C. Boulbe, T. Z. Boulmezaoud, Computing Beltrami fields, *SIAM Journal on Scientific Computing*, Vol. 31(5), pp. 3217–3254 (2009).

[75] T. B. Benjamin, Internal waves of finite amplitude and permanent form, *Journal of Fluid Mechanics*, Vol. 25, part 2, pp. 241–270 (1966).

[76] T. B. Benjamin, Internal waves of permanent form in fluids of great depth, *Journal of Fluid Mechanics*, Vol. 29, part 3, pp. 559–592 (1967).

[77] T. B. Benjamin, The stability of solitary waves, *Proceedings of the Royal Society of London*, A. 328, pp. 153–183 (1972).

[78] T. C. Jo, W. Choi, Dynamics of strongly nonlinear internal solitary waves in shallow water, *Studies in Applied Mathematics*, Vol. 109(3), pp. 205–227 (2002).

[79] T. C. Jo, W. Choi, On Stabilizing the strongly nonlinear internal wave model, *Studies in Applied Mathematics*, Vol. 120, pp. 65–85 (2008).

[80] T. Dombre, U. Frisch, J. M. Greene, M. Henon, A. Mehr, A. M. Soward, Chaotic streamlines in the ABC flows, *Journal of Fluid Mechanics*, Vol. 167, pp. 353–391 (1986).

[81] T. H. Boyer, Continuous symmetries and conserved currents, *Annals of Physics*, Vol. 42, pp. 445–466 (1967).

[82] T. Z. Boulmezaoud, Y. Maday, T. Amari, On the linear force-free fields in bounded and unbounded three-dimensional domains, *Mathematical Modelling and Numerical Analysis*, Vol. 33(2), pp. 359–393 (1999).

[83] T. Z. Boulmezaoud, T. Amari, On the existence of non-linear force-free fields in three-dimensional domains, *Zeitschrift fr angewandte Mathematik und Physik ZAMP*, Vol. 51(6), pp. 942–967 (2000).

[84] V. D. Djordjevi, L. G. Redekopp, On the development of packets of surface gravity waves moving over an uneven bottom, *Journal of Applied Mathematics and Physics*, Vol.29(6), pp. 950–962 (1978).

[85] W. Choi, R. Camassa, Weakly nonlinear internal waves in a two-fluid system, *Journal of Fluid Mechanics*, Vol. 313, pp. 83–103 (1996).

[86] W. Choi, R. Camassa, Fully nonlinear internal waves in a two-fluid system, *Journal of Fluid Mechanics*, Vol. 396, pp. 1–36 (1999).

[87] W. Choi, R. Barros, T. C. Jo, A regularized model for strongly nonlinear internal solitary waves, *Journal of Fluid Mechanics*, Vol. 629, pp. 73-85 (2009).

[88] W. Choi, Modelling of strongly nonlinear internal gravity waves, *Proceedings of the 4th International Conference 7-9 September*, Hydrodynamics, Yokohama, pp. 453-458 (2000).

[89] W. Choi, The effect of a background shear current on large amplitude internal solitary waves, *Physics of Fluids*, Vol. 18(3) (2006).

[90] R. Barros, W. Choi, On regularizing the strongly nonlinear model for two-dimensional internal waves, *Physica D: Nonlinear Phenomena*, Vol. 264, pp. 27–34 (2013).

[91] Y. Hong-Li, S. Jin-Bao, Y. Lian-Gui, L. Yong-Jun, A kind of extended Korteweg-de Vries equation and solitary wave solutions for interfacial waves in a two-fluid system, *Chinese Physics*, Vol. 16(12) (2007).

Appendix A

Scaling Symmetry of Korteweg-de Vries (KdV) Model

The standard KdV equation [48, 54] is

$$u_t + 6uu_x + u_{xxx} = 0. \tag{A.1}$$

Scaling symmetry [28] of the KdV equation is given by the symmetry generator

$$Y = -x\partial_x - 3t\partial_t + 2u\partial_u. \tag{A.2}$$

For Y, one gets

$$\frac{dx^*}{d\varepsilon} = -x^* \quad \Longrightarrow\ x^* = e^{-\varepsilon}x, \tag{A.3}$$

$$\frac{dt^*}{d\varepsilon} = -3t^* \quad \Longrightarrow\ t^* = e^{-3\varepsilon}t, \tag{A.4}$$

$$\frac{du^*}{d\varepsilon} = 2u^* \quad \Longrightarrow\ u^* = e^{2\varepsilon}u, \tag{A.5}$$

where we used the fact that $x^*(0) = x,\ t^*(0) = t,\ u^*(0) = u$. Hence, the corresponding one-parameter (ε) scaling group of transformations generated by Y is given by

$$x^* = f(x, t, u, \varepsilon) = e^{-\varepsilon}x, \tag{A.6a}$$

$$t^* = g(x, t, u, \varepsilon) = e^{-3\varepsilon}t, \tag{A.6b}$$

$$u^* = h(x, t, u, \varepsilon) = e^{2\varepsilon}u. \tag{A.6c}$$

The equation (A.1) in invariant under the scaling group (A.6). Thus if $u(x, t)$ is any solution of the KdV equation in the (x, t, u) space, then $u^*(x^*, t^*)$ is also a solution of the KdV equation. It is noted here that there is a one-one correspondence between $u(x, t)$ and $u^*(x^*, t^*)$ under the group transformation (A.6).

The composition law is given by

$$x^{**} = f(x^*, t^*, u^*, \delta) = e^{-(\varepsilon+\delta)}x, \tag{A.7a}$$

$$t^{**} = g(x^*, t^*, u^*, \delta) = e^{-3(\varepsilon+\delta)}t, \tag{A.7b}$$

$$u^{**} = h(x^*, t^*, u^*, \delta) = e^{2(\varepsilon+\delta)}u, \tag{A.7c}$$

where $\varepsilon,\ \delta \in \mathbb{R}$. In this parameterization, the Lie group of point transformations has the parameter composition law of an Abelian group:

$$\phi(\varepsilon, \delta) = \varepsilon + \delta. \tag{A.8}$$

If we define $e^{\varepsilon} = A$ and $e^{\delta} = B$, then

$$x^* = A^{-1}x, \quad t^* = A^{-3}t, \quad u^* = A^2u, \tag{A.9}$$

and the composition of transformations yields

$$x^{**} = \frac{1}{AB}x, \tag{A.10a}$$

$$t^{**} = \frac{1}{(AB)^3}t, \tag{A.10b}$$

$$u^{**} = (AB)^2u. \tag{A.10c}$$

The group operation composition law is thus given by $\phi(A, B) = AB$.

Appendix B

Big O and Little o Notation

Big O notation [16] is a mathematical notation that describes the limiting behavior of a function when the argument tends to a particular value or infinity. Let f and g be two functions defined on some subset of the real numbers. Then, with big O notation, one writes

$$f(x) = O(g(x)) \quad \text{as} \quad x \to \infty \tag{B.1}$$

when there is a positive constant C such that for all sufficiently large values of x, the absolute value of $f(x)$ is at most C multiplied by the absolute value of $g(x)$. That is, $f(x) = O(g(x))$ if and only if there exists a positive real number C and a real number x_0 such that

$$|f(x)| \leq C\,|g(x)| \quad \text{for all} \quad x \geq x_0. \tag{B.2}$$

The notation can also be used to describe the behavior of f near some finite number a (often, $a = 0$): one says

$$f(x) = O(g(x)) \quad \text{as} \quad x \to a \tag{B.3}$$

when there exist positive numbers δ and C such that

$$|f(x)| \leq C\,|g(x)| \quad \text{for} \quad |x - a| < \delta. \tag{B.4}$$

Again, if $g(x)$ is non-zero for values of x sufficiently close to a, both of these definitions can be unified using the limit superior:

$$f(x) = O(g(x)) \quad \text{as} \quad x \to a \tag{B.5}$$

if and only if

$$\limsup_{x \to a} \left| \frac{f(x)}{g(x)} \right| < \infty. \tag{B.6}$$

Let f and h be two real valued functions. One says "f is little o of h as x approaches x_0" and writes

$$f(x) = o(h(x)) \quad \text{as} \quad x \to x_0 \tag{B.7}$$

to mean that

$$\lim_{x \to x_0} \frac{f(x)}{h(x)} = 0. \tag{B.8}$$

with $h(x) \neq 0$. Intuitively, this means that $f(x)$ is *much* smaller than $h(x)$ for x near x_0. As an example, $x - \sin(x) = o(x)$ as $x \to 0$.

Appendix C

MAPLE Code for Conservation Laws

(A) Here is the MAPLE programming code for zeorth order conservation laws under **GeM** package [4]:

```
> restart:
> read("//cabinet/work$/abm947/Desktop/Gem32/gem32_02.mpl");
```

Declare variables G_1, G_2.

```
> G1(x,t):=diff(U(x,t),t,x)+U(x,t)*diff(U(x,t),x,x)-diff(U(x,t),x)^2;
> G2(x,t):=diff(V(x,t),t,x)+V(x,t)*diff(V(x,t),x,x)-diff(V(x,t),x)^2;
```

Declare parameters, independent variables, dependent variables. We use Z instead of ζ, U instead of v_1, V instead of v_2 in the program.

```
> gem_decl_vars(freeconst=[g, h1, h2, rho1, rho2], indeps=[x, t], freefunc=[],
  deps=[Z(x,t), U(x,t), V(x,t), P(x,t)]);
```

Insert Choi-Camassa equations, and call a solved form.

```
> gem_decl_eqs(
[
diff(Z(x,t),t)-(h1-Z(x,t))*diff(U(x,t),x)+U(x,t)*diff(Z(x,t),x) = 0,

diff(Z(x,t),t)+(h2+Z(x,t))*diff(V(x,t),x)+V(x,t)*diff(Z(x,t),x) = 0,

diff(U(x,t),t)+U(x,t)*diff(U(x,t),x)+g*diff(Z(x,t),x)+(h1-Z(x,t))*G1(x,t)*diff(Z(x,t),x)
-1/3*(h1-Z(x,t))^2*diff(G1(x,t),x)+diff(P(x,t),x)/rho1 = 0,

diff(V(x,t),t)+V(x,t)*diff(V(x,t),x)+g*diff(Z(x,t),x)-(h2+Z(x,t))*G2(x,t)*diff(Z(x,t),x)
-1/3*(h2+Z(x,t))^2*diff(G2(x,t),x)+diff(P(x,t),x)/rho2 = 0
],
solve_for=
[
diff(Z(x,t),t), diff(Z(x,t),x),
diff(U(x,t),x,x,t), diff(V(x,t),x,x,t)
]
);
```

Produce the determining equations.

```
> det_eqs:=gem_conslaw_det_eqs(
[
 x, t, Z(x,t), U(x,t), V(x,t), P(x,t)
]):


> CL_multipliers:=gem_conslaw_multipliers();
```

Differential reduction is done by using **rifsimp** operation.

```
> simplified_eqs:=DEtools[rifsimp](
{det_eqs[]} union {rho1<>0, rho2<>0, rho1<>rho2},
CL_multipliers, mindim=1, casesplit);
```

Solve the reduced determining system by using **pdsolve**.

```
> multipliers_sol:=pdsolve(simplified_eqs[Solved], CL_multipliers);
```

Verify solutions of the determining equations.

```
> sim_multipliers_sol := subs(_F1(t, (h1-Z)*U+(h2+Z)*V)=0, multipliers_sol);
```

```
> subs(multipliers_sol, det_eqs): simplify(%);
```

Call the direct method to produce conserved quantity and flux.

```
> gem_get_CL_fluxes(sim_multipliers_sol, method="Direct");
```

Call the homotopy1 formula to produce conserved quantity and flux.

```
> gem_get_CL_fluxes(sim_multipliers_sol, method="Homotopy1"):
```

(B) Here is the MAPLE programming code for first and second order conservation laws:

```
> restart:
> read("//cabinet/work$/abm947/Desktop/Gem32/gem32_02.mpl");


> G1(x,t):=diff(U(x,t),t,x)+U(x,t)*diff(U(x,t),x,x)-diff(U(x,t),x)^2;
> G2(x,t):=diff(V(x,t),t,x)+V(x,t)*diff(V(x,t),x,x)-diff(V(x,t),x)^2;

> gem_decl_vars(freeconst=[g, h1, h2, rho1, rho2], indeps=[x, t],freefunc=[],
deps=[Z(x,t), U(x,t), V(x,t), P(x,t)]);


> gem_decl_eqs(
[
diff(Z(x,t),t)-(h1-Z(x,t))*diff(U(x,t),x)+U(x,t)*diff(Z(x,t),x) = 0,

diff(Z(x,t),t)+(h2+Z(x,t))*diff(V(x,t),x)+V(x,t)*diff(Z(x,t),x) = 0,

diff(U(x,t),t)+U(x,t)*diff(U(x,t),x)+g*diff(Z(x,t),x)+(h1-Z(x,t))*G1(x,t)*diff(Z(x,t),x)
 -1/3*(h1-Z(x,t))^2*diff(G1(x,t),x)+diff(P(x,t),x)/rho1 = 0,

diff(V(x,t),t)+V(x,t)*diff(V(x,t),x)+g*diff(Z(x,t),x)-(h2+Z(x,t))*G2(x,t)*diff(Z(x,t),x)
 -1/3*(h2+Z(x,t))^2*diff(G2(x,t),x)+diff(P(x,t),x)/rho2 = 0
],
solve_for=
[
diff(Z(x,t),t), diff(Z(x,t),x),
diff(U(x,t),t,x,x), diff(V(x,t),t,x,x)
]
):

> det_eqs:=gem_conslaw_det_eqs(
[
 x, t, Z(x,t), U(x,t), V(x,t), P(x,t), diff(U(x,t),x), diff(V(x,t),x),
 diff(U(x,t),x,x), diff(V(x,t),x,x)
]):


> CL_multipliers:=gem_conslaw_multipliers():

> simplified_eqs:=DEtools[rifsimp](
{det_eqs[]} union {rho1<>0, rho2<>0, rho1<>rho2},
CL_multipliers, mindim=1):

> OFF;
> multipliers_sol:=pdsolve(simplified_eqs[Solved], CL_multipliers):

> sim_multipliers_sol := subs(_F1(t, (h1-Z)*U+(h2+Z)*V)=0, multipliers_sol):
subs(sim_multipliers_sol, det_eqs): simplify(%):
```

1. Apply Direct method:

```
> gem_get_CL_fluxes(sim_multipliers_sol, method="Direct"):
```

2. Apply Homotopy1 formula:

```
> gem_get_CL_fluxes(sim_multipliers_sol, method="Homotopy1"):
```

Appendix D

MAPLE Code for Solitary Wave Solutions and Plotting Densities

```
> restart; with(plots):
> #Note: h_1,2=H_1,2, rho_1,2=R_1,2, X=xi=x-c*t, q_1,2=Q_1,2, zeta=u, u1=v1=U1, u2=v2=U2

> R2:=1000; H2:=1;
> R1:=600; H1:=5.00;
> g:=9.8;
> H1/H2>(R1/R2)^0.5;

> c0:=sqrt(g*H1*H2*(R2-R1)/(R1*H2+R2*H1));

> (R1*H1^2-R2*H2^2);

> Astar:=-H1*H2*(R1*H1+R2*H2)/(R1*H1^2-R2*H2^2);

> Q11:=subs(c=2,-c^2/g-H1+H2);
  Q12:=subs(c=2.2,-c^2/g-H1+H2);
  Q13:=subs(c=2.4,-c^2/g-H1+H2);

> Q21:=subs(c=2,H1*H2*(c^2/c0^2-1));
  Q22:=subs(c=2.2,H1*H2*(c^2/c0^2-1));
  Q23:=subs(c=2.4,H1*H2*(c^2/c0^2-1));

> eq_Apm1:=xi^2+Q11*xi+Q21=0;
  eq_Apm2:=xi^2+Q12*xi+Q22=0;
  eq_Apm3:=xi^2+Q13*xi+Q23=0;

> eqS1:=solve(eq_Apm1);
  eqS2:=solve(eq_Apm2);
  eqS3:=solve(eq_Apm3);

> Ap1:=max([eqS1]);Am1:=min([eqS1]);
  Ap2:=max([eqS2]);Am2:=min([eqS2]);
  Ap3:=max([eqS3]);Am3:=min([eqS3]);

> M:=(3*g*(R2-R1)/c^2/(R1*H1^2-R2*H2^2));
> M1:=subs(c=2,M); M2:=subs(c=2.2,M); M3:=subs(c=2.4,M);

> DEm1:=diff(u(xi),xi)=-sqrt(M1* u(xi)^2*(u(xi)-Am1)*(u(xi)-Ap1)/(u(xi)-Astar)):
  DEp1:=diff(u(xi),xi)=sqrt(M1* u(xi)^2*(u(xi)-Am1)*(u(xi)-Ap1)/(u(xi)-Astar)):
  DEm2:=diff(u(xi),xi)=-sqrt(M2* u(xi)^2*(u(xi)-Am2)*(u(xi)-Ap2)/(u(xi)-Astar)):
  DEp2:=diff(u(xi),xi)=sqrt(M2* u(xi)^2*(u(xi)-Am2)*(u(xi)-Ap2)/(u(xi)-Astar)):
  DEm3:=diff(u(xi),xi)=-sqrt(M3* u(xi)^2*(u(xi)-Am3)*(u(xi)-Ap3)/(u(xi)-Astar)):
```

```
  DEp3:=diff(u(xi),xi)=sqrt(M3* u(xi)^2*(u(xi)-Am3)*(u(xi)-Ap3)/(u(xi)-Astar)):

#***IC has to be less tha Ap and less tha Am also.***
> IC1:=u(0)=Am1-0.000001;IC2:=u(0)=Am2-0.000001;IC3:=u(0)=Am3-0.000001;

> DSm1:=dsolve({DEm1,IC1},type=numeric,range=-50..50);
  DSm2:=dsolve({DEm2,IC2},type=numeric,range=-50..50);
  DSm3:=dsolve({DEm3,IC3},type=numeric,range=-50..50);
  DSp1:=dsolve({DEp1,IC1},type=numeric,range=-50..50);
  DSp2:=dsolve({DEp2,IC2},type=numeric,range=-50..50);
  DSp3:=dsolve({DEp3,IC3},type=numeric,range=-50..50);

> DSm1(0);DSm1(1.2);

#odeplot(DSm);
> Rplot1:=odeplot(DSm1,xi=0..20,labels = ["xi",""]):
  Rplot2:=odeplot(DSm2,xi=0..20,labels = ["xi",""],linestyle = dash):
  Rplot3:=odeplot(DSm3,xi=0..20,labels = ["xi",""],style = point,symbol = circle,
  symbolsize = 5):

> Lplot1:=odeplot(DSp1,xi=-20..0,labels = ["xi",""]):
  Lplot2:=odeplot(DSp2,xi=-20..0,labels = ["xi",""],linestyle = dash):
  Lplot3:=odeplot(DSp3,xi=-20..0,labels = ["xi",""],style = point,symbol = circle,
  symbolsize = 5):

> display(Lplot1,Rplot1,Lplot2,Rplot2,Lplot3,Rplot3):

#Recall initial value to plot U1, U2 and all the densities:
> c:=2;

#U1_plot, here  we used  zeta(xi )= u(xi):
> U_1(xi):= -c*u(xi)/(H1-u(xi));
> soln := dsolve( { DEm, IC}, {u(xi)}, numeric):
  U := proc(t) subs( soln(t), U_1(xi) ) end:
  U1plotR:=plot( 'U(xi)', xi=0 .. 20,color=blue ):
> soln := dsolve( { DEp, IC}, {u(xi)}, numeric):
  U := proc(t) subs( soln(t), U_1(xi) ) end:
  U1plotL:=plot( 'U(xi)', xi=-20 .. 0,color=blue ):
> display(U1plotR,U1plotL):

#U2_plot
> U_2(xi):= c*u(xi)/(H2+u(xi));
> soln := dsolve( { DEm, IC}, {u(xi)}, numeric):
  V := proc(t) subs( soln(t), U_2(xi) ) end:
  U2plotR:=plot( 'V(xi)', xi=0 .. 20,color=blue ):
> soln := dsolve( { DEp, IC}, {u(xi)}, numeric):
  V := proc(t) subs( soln(t), U_2(xi) ) end:
  U2plotL:=plot( 'V(xi)', xi=-20..0, color=blue ):
> display(U2plotR,U2plotL):

#T1_plot (1st conserved density)
```

```
> T1(xi):= u(xi);
> soln := dsolve( { DEm, IC}, {u(xi)}, numeric):
  T := proc(t) subs( soln(t), T1(xi) ) end:
  T1plotR:=plot( 'T(xi)', xi=0 .. 20):
> soln := dsolve( { DEp, IC}, {u(xi)}, numeric):
  T := proc(t) subs( soln(t), T1(xi) ) end:
  T1plotL:=plot( 'T(xi)', xi=-20 .. 0):

> display(T1plotR,T1plotL);

#T2_plot (2nd conserved density)
> U1:=c*(1-H1/(H1-u(xi)));U2:=c*(1-H2/(H2+u(xi)));
> T2(xi):= R1*(H1-u(xi))*U1+R2*(H2+u(xi))*U2;
> soln := dsolve( { DEm, IC}, {u(xi)}, numeric):
  T := proc(t) subs( soln(t), T2(xi) ) end:
  T2plotR:=plot( 'T(xi)', xi=0 .. 20,linestyle = dash ):
> soln := dsolve( { DEp, IC}, {u(xi)}, numeric):
  T := proc(t) subs( soln(t), T2(xi) ) end:
  T2plotL:=plot( 'T(xi)', xi=-20 .. 0,linestyle = dash ):
> d2:=display(T2plotR,T2plotL):

#T3_plot (3rd conserved density)
> U1:=c*(1-H1/(H1-u(xi)));U2:=c*(1-H2/(H2+u(xi)));
> T3(xi):= (xi+c*t0)*(R2-R1)*u(xi)+t0*(R1*(H1-u(xi))*U1+R2*(H2+u(xi))*U2);

#We plot T3 for different times t (t  is denoted by t0 here):
> soln := dsolve( { DEm, IC}, {u(xi)}, numeric):
> P1:= proc(t) subs( t0=0,soln(t), T3(xi) ) end:
  T3plot1R:=plot( subs('P1(xi)'), xi=0 .. 20 ):
> P2:= proc(t) subs( t0=1,soln(t), T3(xi) ) end:
  T3plot2R:=plot( subs('P2(xi)'), xi=0 .. 20, linestyle = dash ):
> P3:= proc(t) subs( t0=2,soln(t), T3(xi) ) end:
  T3plot3R:=plot( subs('P3(xi)'), xi=0 .. 20, linestyle = longdash ):
  T3plot4R:=plot( subs('P4(xi)'), xi=0 .. 20,style = point , symbol = cross, symbolsize = 2 ):

> soln := dsolve( { DEp, IC}, {u(xi)}, numeric):
  T3plot1L:=plot( 'P1(xi)', xi=-20..0):
  T3plot2L:=plot( 'P2(xi)', xi=-20..0,linestyle = dash):
  T3plot3L:=plot( 'P3(xi)', xi=-20..0, linestyle = longdash ):
  T3plot4L:=plot( 'P4(xi)', xi=-20 .. 0, style=point, symbol = cross, symbolsize = 2 ):

>  display(T3plot1L,T3plot1R,T3plot2L,T3plot2R,T3plot3L,T3plot3R,T3plot4L,T3plot4R):


#T5_plot (5th conserved density)
> U1:=c*(1-H1/(H1-u(xi)));U2:=c*(1-H2/(H2+u(xi)));
> uxi:=sqrt(
(3*g*(R2-R1)/c^2/(R1*H1^2-R2*H2^2)) * u(xi)^2*(u(xi)-Am1)*(u(xi)-Ap1)/(u(xi)-Astar)
);
> T5:= 1/2*g*(R2-R1)*u(xi)^2+1/2*R1*(H1-u(xi))*U1^2+1/6*R1*(H1-
```

```
u(xi))^3*diff(U1,xi)^2+1/2*R2*(H2+u(xi))*U2^2+1/6*R2*(H2+u(xi))^3*diff(U2,xi)^2:
> T5:=subs( diff(u(xi),xi)=uxi,T5):
> soln := dsolve( { DEm, IC}, {u(xi)}, numeric):
  S:= proc(t) subs( soln(t), T5 ) end:
  T5plotR:=plot( 'S(xi)', xi= 0.. 20, linestyle = longdash):
> soln := dsolve( { DEp, IC}, {u(xi)}, numeric):
  S:= proc(t) subs( soln(t), T5 ) end:
  T5plotL:=plot( 'S(xi)', xi=-20 .. 0, linestyle = longdash ):
> d5:=display(T5plotL,T5plotR):

#T6_plot (6th conserved density):
> U1:=c*(1-H1/(H1-u(xi)));U2:=c*(1-H2/(H2+u(xi)));
> uxi:=sqrt(
(3*g*(R2-R1)/c^2/(R1*H1^2-R2*H2^2)) * u(xi)^2*(u(xi)-Am1)*(u(xi)-Ap1)/(u(xi)-Astar)
);
> diff(uxi,xi): uxixi:=subs(diff(u(xi),xi)=uxi,%):

#Note: We used T6:= -T6 here, which is allowed to do without loss of generality.
> T6:=-( R1*U1+1/6*R1*(H1-u(xi))^2*diff(U1,xi,xi) ):
> T6:=subs( {diff(u(xi),xi)=uxi,diff(u(xi),xi,xi)=uxixi},T6):

> soln := dsolve( { DEm, IC}, {u(xi)}, numeric):
  P := proc(t) subs( soln(t), T6 ) end:
  T6plotR:=plot( 'P(xi)', xi= 0.. 20, thickness=3):
> soln := dsolve( { DEp, IC}, {u(xi)}, numeric):
  P := proc(t) subs( soln(t), T6 ) end:
  T6plotL:=plot( 'P(xi)', xi=-20 .. 0, thickness=3):
> d6:=display(T6plotL,T6plotR):

#T7_plot(7th conserved density):
> U1:=c*(1-H1/(H1-u(xi)));U2:=c*(1-H2/(H2+u(xi)));
> uxi:=sqrt(
(3*g*(R2-R1)/c^2/(R1*H1^2-R2*H2^2)) * u(xi)^2*(u(xi)-Am1)*(u(xi)-Ap1)/(u(xi)-Astar)
);
> diff(uxi,xi):uxixi:=subs(diff(u(xi),xi)=uxi,%):
> T7:= R2*U2+1/6*R2*(H2+u(xi))^2*diff(U2,xi,xi):
> T7:=subs( {diff(u(xi),xi)=uxi,diff(u(xi),xi,xi)=uxixi},T7):

> soln := dsolve( { DEm, IC}, {u(xi)}, numeric):
  Q := proc(t) subs( soln(t), T7 ) end:
  T7plotR:=plot( 'Q(xi)', xi= 0.. 20, style = point, symbol = circle, symbolsize = 6 ):
> soln := dsolve( { DEp, IC}, {u(xi)}, numeric):
  Q := proc(t) subs( soln(t), T7 ) end:
  T7plotL:=plot( 'Q(xi)', xi=-20 .. 0, style = point, symbol = circle, symbolsize = 6 ):
> d7:=display(T7plotL,T7plotR):

#We plot four densities T2, T5, T6, and T7 together:

> display(d2,d5,d6,d7);
```

Appendix E

MAPLE Code for Kink Solutions and Plotting Densities

```
> restart;with(plots):
#Note: h_1,2=H_1,2,  rho_1,2=R_1,2,  X=xi=x-c*t,  q_1,2=Q_1,2,  eta=u, u1=v1=U1, u2=v2=U2
> R2:=1000;H2:=1;
> R1:=600;H1:=5.00;
> g:=9.8;
> H1/H2>(R1/R2)^0.5;

> c0:=sqrt(g*H1*H2*(R2-R1)/(R1*H2+R2*H1));

> (R1*H1^2-R2*H2^2);

> Astar:=-H1*H2*(R1*H1+R2*H2)/(R1*H1^2-R2*H2^2);

> Q11:=subs(c=2,-c^2/g-H1+H2);
  Q12:=subs(c=2.2,-c^2/g-H1+H2);
  Q13:=subs(c=2.4,-c^2/g-H1+H2);

> Q21:=subs(c=2,H1*H2*(c^2/c0^2-1));
  Q22:=subs(c=2.2,H1*H2*(c^2/c0^2-1));
  Q23:=subs(c=2.4,H1*H2*(c^2/c0^2-1));

> eq_Apm1:=xi^2+Q11*xi+Q21=0;
  eq_Apm2:=xi^2+Q12*xi+Q22=0;
  eq_Apm3:=xi^2+Q13*xi+Q23=0;
> eqS1:=solve(eq_Apm1);
  eqS2:=solve(eq_Apm2);
  eqS3:=solve(eq_Apm3);
> Ap1:=max([eqS1]);Am1:=min([eqS1]);
  Ap2:=max([eqS2]);Am2:=min([eqS2]);
  Ap3:=max([eqS3]);Am3:=min([eqS3]);

> M:=(3*g*(R2-R1)/c^2/(R1*H1^2-R2*H2^2));
> M1:=subs(c=2,M);M2:=subs(c=2.2,M);M3:=subs(c=2.4,M);
> DEm1:=diff(u(xi),xi)=-sqrt(M1* u(xi)^2*(u(xi)-Am1)*(u(xi)-Ap1)/(u(xi)-Astar)):
  DEp1:=diff(u(xi),xi)=sqrt(M1* u(xi)^2*(u(xi)-Am1)*(u(xi)-Ap1)/(u(xi)-Astar)):
  DEm2:=diff(u(xi),xi)=-sqrt(M2* u(xi)^2*(u(xi)-Am2)*(u(xi)-Ap2)/(u(xi)-Astar)):
  DEp2:=diff(u(xi),xi)=sqrt(M2* u(xi)^2*(u(xi)-Am2)*(u(xi)-Ap2)/(u(xi)-Astar)):
  DEm3:=diff(u(xi),xi)=-sqrt(M3* u(xi)^2*(u(xi)-Am3)*(u(xi)-Ap3)/(u(xi)-Astar)):
  DEp3:=diff(u(xi),xi)=sqrt(M3* u(xi)^2*(u(xi)-Am3)*(u(xi)-Ap3)/(u(xi)-Astar)):

#***IC has to be less tha Ap and less tha Am also.***
> IC1:=u(0)=Am1-0.000001;IC2:=u(0)=Am2-0.000001;IC3:=u(0)=Am3-0.000001;
```

```
> DSm1:=dsolve({DEm1,IC1},type=numeric,range=-50..50);
  DSm2:=dsolve({DEm2,IC2},type=numeric,range=-50..50);
  DSm3:=dsolve({DEm3,IC3},type=numeric,range=-50..50);
  DSp1:=dsolve({DEp1,IC1},type=numeric,range=-50..50);
  DSp2:=dsolve({DEp2,IC2},type=numeric,range=-50..50);
  DSp3:=dsolve({DEp3,IC3},type=numeric,range=-50..50);
> DSm1(0);DSm1(1.2);

#odeplot(DSm);
> KINK1:=odeplot(DSp1,xi=-20..20,labels = ["xi",""]);
  KINK2:=odeplot(DSp2,xi=-20..20,labels = ["xi",""],linestyle = dash);
  KINK3:=odeplot(DSp3,xi=-20..20,labels = ["xi",""],style = point,symbol = circle,
  symbolsize = 8 );
> AntKINK1:=odeplot(DSm1,xi=-20..20,labels = ["xi",""]);
  AntKINK2:=odeplot(DSm2,xi=-20..20,labels = ["xi",""],linestyle = dash);
  AntKINK3:=odeplot(DSm3,xi=-20..20,labels = ["xi",""],style = point,symbol = circle,
  symbolsize = 8 );

> display(KINK1,KINK2,KINK3);
> display(AntKINK1,AntKINK2,AntKINK3);

#U1_plot
> c:=2;DEm:=DEm1:DEp:=DEp1:IC:=IC1;

> U_1(xi):= -c*u(xi)/(H1-u(xi));
> soln := dsolve( { DEp, IC}, {u(xi)}, numeric);
  U := proc(t) subs( soln(t), U_1(xi) ) end;
  plot( 'U(xi)', xi=-20 .. 20,color=blue );
> soln := dsolve( { DEm, IC}, {u(xi)}, numeric):
  U := proc(t) subs( soln(t), U_1(xi) ) end:
  plot( 'U(xi)', xi=-20 .. 20,color=blue );

#U2_plot
> U_2(xi):= c*u(xi)/(H2+u(xi));
> soln := dsolve( { DEp, IC}, {u(xi)}, numeric):
  V := proc(t) subs( soln(t), U_2(xi) ) end:
  plot( 'V(xi)', xi=-20..20, color=blue );
> soln := dsolve( { DEm, IC}, {u(xi)}, numeric):
  V := proc(t) subs( soln(t), U_2(xi) ) end:
  plot( 'V(xi)', xi=-20 .. 20,color=blue );

#T1_plot (1st conserved density)
> T1(xi):= u(xi);
> soln := dsolve( { DEp, IC}, {u(xi)}, numeric):
  T := proc(t) subs( soln(t), T1(xi) ) end:
  T1KINK:=plot( 'T(xi)', xi=-20 .. 20);
> soln := dsolve( { DEm, IC}, {u(xi)}, numeric):
  T := proc(t) subs( soln(t), T1(xi) ) end:
  T1AntKINK:=plot( 'T(xi)', xi=-20 .. 20);
```

```
> display(T1KINK,T1AntKINK);

#T2_plot (2nd conserved density)
> U1:=c*(1-H1/(H1-u(xi)));U2:=c*(1-H2/(H2+u(xi)));
> T2(xi):= R1*(H1-u(xi))*U1+R2*(H2+u(xi))*U2;
> soln := dsolve( { DEp, IC}, {u(xi)}, numeric):
  T := proc(t) subs( soln(t), T2(xi) ) end:
  T2KINK:=plot( 'T(xi)', xi=-20 .. 20,linestyle = dash );
> soln := dsolve( { DEm, IC}, {u(xi)}, numeric):
  T := proc(t) subs( soln(t), T2(xi) ) end:
  T2AntKINK:=plot( 'T(xi)', xi=-20 .. 20,linestyle = dash );

#T3_plot (3rd conserved density)
> U1:=c*(1-H1/(H1-u(xi)));U2:=c*(1-H2/(H2+u(xi)));
> T3(xi):= (xi+c*t0)*(R2-R1)*u(xi)+t0*(R1*(H1-u(xi))*U1+R2*(H2+u(xi))*U2);

#We plot T3 for different times t (t  is denoted by t0 here):
> soln := dsolve( { DEp, IC}, {u(xi)}, numeric):
> P1:= proc(t) subs( t0=0,soln(t), T3(xi) ) end:
  T3KINK1:=plot( 'P1(xi)', xi=-20..20);
> P2:= proc(t) subs( t0=1,soln(t), T3(xi) ) end:
  T3KINK2:=plot( 'P2(xi)', xi=-20..20,linestyle = dash);
> P3:= proc(t) subs( t0=2,soln(t), T3(xi) ) end:
  T3KINK3:=plot( 'P3(xi)', xi=-20..20, linestyle = longdash );
> P4:= proc(t) subs( t0=3,soln(t), T3(xi) ) end:
  T3KINK4:=plot( 'P4(xi)', xi=-20 .. 20, style=point, symbol = cross, symbolsize = 2 );
  > display(T3KINK1,T3KINK2,T3KINK3,T3KINK4);

> soln := dsolve( { DEm, IC}, {u(xi)}, numeric):
> P1:= proc(t) subs( t0=0,soln(t), T3(xi) ) end:
  T3AntKINK1:=plot( subs('P1(xi)'), xi=-20 .. 20 );
> P2:= proc(t) subs( t0=1,soln(t), T3(xi) ) end:
  T3AntKINK2:=plot( subs('P2(xi)'), xi=-20 .. 20, linestyle = dash );
> P3:= proc(t) subs( t0=2,soln(t), T3(xi) ) end:
  T3AntKINK3:=plot( subs('P3(xi)'), xi=-20 .. 20, linestyle = longdash );
> P4:= proc(t) subs( t0=3,soln(t), T3(xi) ) end:
  T3AntKINK4:=plot( subs('P4(xi)'), xi=-20 .. 20,style = point , symbol = cross, symbolsize = 2 );
> display(T3AntKINK1,T3AntKINK2,T3AntKINK3,T3AntKINK4);


#T5_plot (5th conserved density)
> U1:=c*(1-H1/(H1-u(xi)));U2:=c*(1-H2/(H2+u(xi)));
> uxi:=sqrt(
(3*g*(R2-R1)/c^2/(R1*H1^2-R2*H2^2)) * u(xi)^2*(u(xi)-Am1)*(u(xi)-Ap1)/(u(xi)-Astar));
> T5:= 1/2*g*(R2-R1)*u(xi)^2+1/2*R1*(H1-u(xi))*U1^2+1/6*R1*(H1-u(xi))^3*diff(U1,xi)^2+
  1/2*R2*(H2+u(xi))*U2^2+1/6*R2*(H2+u(xi))^3*diff(U2,xi)^2:
> T5:=subs( diff(u(xi),xi)=uxi,T5);
> soln := dsolve( { DEp, IC}, {u(xi)}, numeric):
  S := proc(t) subs( soln(t), T5 ) end:
  T5KINK:=plot( 'S(xi)', xi=-20 .. 20, linestyle = longdash );
> soln := dsolve( { DEm, IC}, {u(xi)}, numeric):
```

```
  S := proc(t) subs( soln(t), T5 ) end:
  T5AntKINK:=plot( 'S(xi)', xi= -20.. 20, linestyle = longdash);


#T6_plot (6th conserved density):
> U1:=c*(1-H1/(H1-u(xi)));U2:=c*(1-H2/(H2+u(xi)));
> uxi:=sqrt(
(3*g*(R2-R1)/c^2/(R1*H1^2-R2*H2^2)) * u(xi)^2*(u(xi)-Am1)*(u(xi)-Ap1)/(u(xi)-Astar));
> diff(uxi,xi): uxixi:=subs(diff(u(xi),xi)=uxi,%):

#Note: We used T6:= -T6 here, which is allowed to do without loss of generality
> T6:=-( R1*U1+1/6*R1*(H1-u(xi))^2*diff(U1,xi,xi) ):
> T6:=subs( {diff(u(xi),xi)=uxi,diff(u(xi),xi,xi)=uxixi},T6):

> soln := dsolve( { DEp, IC}, {u(xi)}, numeric):
  P:= proc(t) subs( soln(t), T6 ) end:
  T6KINK:=plot( 'P(xi)', xi=-20 .. 20, style = point, symbol = circle, symbolsize = 6   );
> soln := dsolve( { DEm, IC}, {u(xi)}, numeric):
  P:= proc(t) subs( soln(t), T6 ) end:
  T6AntKINK:=plot( 'P(xi)', xi= -20.. 20, style = point, symbol = circle, symbolsize = 6  );

#T7_plot(7th conserved density):
> U1:=c*(1-H1/(H1-u(xi)));U2:=c*(1-H2/(H2+u(xi)));
> uxi:=sqrt(
(3*g*(R2-R1)/c^2/(R1*H1^2-R2*H2^2)) * u(xi)^2*(u(xi)-Am1)*(u(xi)-Ap1)/(u(xi)-Astar));
> diff(uxi,xi):uxixi:=subs(diff(u(xi),xi)=uxi,%):
> T7:= R2*U2+1/6*R2*(H2+u(xi))^2*diff(U2,xi,xi):
> T7:=subs( {diff(u(xi),xi)=uxi,diff(u(xi),xi,xi)=uxixi},T7):

> soln := dsolve( { DEp, IC}, {u(xi)}, numeric):
  Q := proc(t) subs( soln(t), T7 ) end:
  T7KINK:=plot( 'Q(xi)', xi=-20 .. 20, style = point, symbol = cross, symbolsize = 6  );
> soln := dsolve( { DEm, IC}, {u(xi)}, numeric):
  Q := proc(t) subs( soln(t), T7 ) end:
  T7AntKINK:=plot( 'Q(xi)', xi= -20.. 20, style = point, symbol = cross, symbolsize = 6   );


#Plot four densities T2, T5, T6, and T7 together on the kink solution:

> display(T2KINK,T5KINK,T6KINK,T7KINK);

#Plot four densities T2, T5, T6, and T7 together on the anti-kink solution:

> display(T2AntKINK,T5AntKINK,T6AntKINK,T7AntKINK);
```

Appendix F

MATLAB Code for KdV Soliton Solutions

(A) A complete MATLAB code for finding 1-soliton solution (see Figure 3.4) is written as under.

```
clear all
figure; tic;

N = 250; dt = 0.4/N^2; x = (2*pi/N)*(-N/2:N/2-1)';dx = x(2)-x(1);

clf, drawnow, set(gcf,'renderer','zbuffer')
A = 16; x0=-2;
u = 0.5*A^2*sech(.5*(A*(x-x0))).^2;
v = fft(u); k = [0:N/2-1 0 -N/2+1:-1]'; P = i*k.^3;

tmax = 0.015; nplt = floor((tmax/25)/dt); nmax = round(tmax/dt);
udata = u; tdata = 0;
e1all = dx*sum(u);
e2all = dx*sum(0.5*u.^2);
e3all=5/2*dx*sum(u.^3-0.5*(real(ifft(i*k.*v))).^2);
h = waitbar(0,'please wait...');

for n = 1:nmax
    t = n*dt; g = -3*i*dt*k;
    E = exp(dt*P/2); E2 = E.^2;
    a1 = g.*fft(real( ifft( v ) ).^2);
    a2 = g.*fft(real( ifft(E.*(v+a1/2)) ).^2);
    a3 = g.*fft(real( ifft(E.*v + a2/2) ).^2);
    a4 = g.*fft(real( ifft(E2.*v+E.*a3) ).^2);
    v = E2.*v + (E2.*a1 + 2*E.*(a2+a3) + a4)/6;
  if mod(n,nplt) == 0
    u = real(ifft(v)); waitbar(n/nmax)
    udata = [udata u]; tdata = [tdata t];
    e1 = dx*sum(u);e2 = dx*sum(0.5*u.^2);
    e3 = 5/2*dx*sum(u.^3-0.5*(real(ifft(i*k.*v))).^2);
    e1all = [e1all e1];e2all = [e2all e2];e3all = [e3all e3];
  end
end

toc
waterfall(x,tdata,udata'), colormap(1e-6*[1 1 1]); view(-20,25)
title('KdV 1-soliton solution','FontWeight','bold');
xlabel('x','FontSize',12,'FontWeight','bold'),
ylabel('t','FontSize',12,'FontWeight','bold'),
axis([-pi pi 0 tmax 0 max(max(udata))]), grid off
close(h), pbaspect([1.2 1 .25])
```

(B) MATLAB code for finding 2-soliton solution (see Figure 3.5) is written as under.

```
% KdV eq. u_t + uu_x + u_xxx = 0 on [-pi,pi] by
% FFT with integrating factor v = exp(-ik^3t)*u^hat.
% Set up grid and two-soliton initial data:

clear all
figure; tic;
N = 250; dt = .4/N^2; x = (2*pi/N)*(-N/2:N/2-1)';
dx = x(2)-x(1);
A1 = 18; A2 = 9;
x1_ 0=-2;x2_ 0=0;
clf, drawnow, set(gcf,'renderer','zbuffer')
u = 0.5*A1^2*sech (.5*(A1*(x-x1_ 0))).^2 + 0.5*A2^2*sech (.5*(A2*(x-x2_ 0))).^2;
v = fft(u); k = [0:N/2-1 0 -N/2+1:-1]'; P = i*k.^3;

% Solve PDE and plot results:

tmax = 0.015; nplt = floor((tmax/25)/dt); nmax = round(tmax/dt);
udata = u; tdata = 0;
h = waitbar(0,'please wait...');

for n = 1:nmax
    t = n*dt; g = -3*i*dt*k;
    E = exp(dt*P/2); E2 = E.^2;
    a1 = g.*fft(real ( ifft( v ) ).^2);
    a2 = g.*fft(real ( ifft(E.*(v+a1/2)) ).^2); % 4th-order
    a3 = g.*fft(real ( ifft(E.*v + a2/2) ).^2); % Runge-Kutta
    a4 = g.*fft(real ( ifft(E2.*v+E.*a3) ).^2);
   v = E2.*v + (E2.*a1 + 2*E.*(a2+a3) + a4)/6;
 if mod(n,nplt) == 0
   u = real(ifft(v)); waitbar(n/nmax)
   udata = [udata u]; tdata = [tdata t];
 end
end

toc
waterfall(x,tdata,udata'), colormap(1e-6*[1 1 1]); view(-20,25)
% title('KdV 2-soliton solution','FontWeight','bold');
xlabel('x','FontSize',12,'FontWeight','bold'),
ylabel('t','FontSize',12,'FontWeight','bold'),
axis([-pi pi 0 tmax 0 max(max(udata))]), grid off
close(h), pbaspect([1.4 1.2 .35])
```